

**Mechanism of Action of Group II Chaperonins:
Impact of the Built-in Lid on the Conformational Cycle**

Dissertation

Fakultät für Biologie

Ludwig-Maximilians-Universität München

carried out at the

Department of Biological Sciences

Stanford University

presented by

Stefanie Reißmann

May 2007

1. Reviewer: Prof. Dr. A. Böck

2. Reviewer: Prof. Dr. K. Jung

Date of the oral examination: July 24, 2007

PUBLICATIONS:

Research articles:

Reissmann S., Hochleitner E., Wang H., Paschos A., Lottspeich F., Glass R.S. and Böck A. (2003) Taming of a poison: Biosynthesis of the NiFe-Hydrogenase Cyanide Ligands. *Science* **299**, 1067-70

Blokesch M., Paschos A., Bauer A., Reissmann S., Drapal N., Böck A. (2004) Analysis of the transcarbamoylation-dehydration reaction catalysed by the hydrogenase maturation proteins HypF and HypE. *Eur J Biochem* **271**: 3428-3436

Reissmann S., Parnot C., Booth CR, Chiu W. and Frydman J. (2007) Essential function of the built-in lid in the allosteric regulation of eukaryotic and archaeal chaperonins. *Nat Struct Mol Biol* May;14(5):432-440

Reissmann S., Meyer A. and Frydman J. Positive cooperativity in group II chaperonins is a sequential event driven by a gradient of affinities for ATP. *Manuscript in preparation.*

Review articles:

Spiess C., Meyer S.A., Reissmann S. and Frydman J. (2004) Mechanism of the eukaryotic chaperonin: protein folding in the chamber of secrets. *Trends Cell Biol.* 2004 Nov; **14**(11): 598-604.

I. INTRODUCTION	1
I.1. PROTEIN FOLDING <i>IN VITRO</i> VERSUS <i>IN VIVO</i>	1
I.2. THE CYTOPLASMATIC CHAPERONE MACHINERY	2
<i>The Hsp70-Hsp40 chaperone system</i>	2
<i>The chaperonins are Hsp60 family members</i>	4
<i>Not all chaperones are heat shock proteins</i>	6
<i>Co-translational folding in the eukaryotic cytoplasm</i>	7
I.3. CHAPERONINS - A DISTINCT CLASS OF MOLECULAR CHAPERONES	8
<i>Chaperonin structure</i>	8
<i>Group I chaperonins: The GroEL-GroES machinery</i>	10
<i>Group II chaperonins from archae and eukarya</i>	12
I.4. AIMS OF THIS WORK	15
II. MATERIALS AND METHODS	16
II.1. PLASMIDS AND STRAINS	16
II.2. MEDIA AND SUPPLEMENTS	17
II.3. <i>Oligonucleotides</i>	18
II.4. CHEMICALS AND REAGENTS	18
II.5. MICROBIOLOGICAL METHODS	19
<i>Bacterial and yeast cultures</i>	19
<i>Pulse-chase of yeast cells with [³⁵S]-methionine</i>	19
<i>Overproduction of [³⁵S]-labeled rhodanese in E. coli</i>	19
II.6. MOLECULAR GENETIC METHODS	20
<i>Standard Methods</i>	20
<i>Construction of the bacterial expression vector pET21MmCpnWT</i>	20
<i>Site-directed mutagenesis</i>	20
<i>Sequencing of DNA</i>	20
II.7. <i>Electrophoresis</i>	21
<i>Electrophoresis of DNA</i>	21
<i>Denaturing and native polyacrylamide gel electrophoresis (PAGE)</i>	21

II.8. PROTEIN PURIFICATION	21
<i>Purification of TRiC</i>	21
<i>Purification Mm-Cpn wild type and mutant forms</i>	22
<i>Purification of rhodanese</i>	23
<i>Purification of [³⁵S]-labeled actin</i>	24
II.9. BIOCHEMICAL METHODS	24
<i>Determination of protein concentrations</i>	24
<i>Isolation of Mm-Cpn-substrate complexes</i>	25
<i>Generation of cTRiC</i>	25
<i>Proteinase K protection assay</i>	26
<i>Rhodanese folding assay</i>	26
<i>Actin folding assays</i>	27
<i>Rhodanese binding assay</i>	27
<i>Preparation of EL-trap</i>	28
<i>ATPase assay</i>	28
<i>Cross-link of α-[³²P]-8-N₃-ATP to TRiC and separation of subunits by RP-HPLC</i>	28
<i>Filter binding assays</i>	29
<i>DNaseI pull-down of native actin</i>	29
<i>TRiC Immunoprecipitation</i>	30
<i>Sample preparation for cryo-electron microscopy</i>	30
II.10. BIOINFORMATICAL METHODS	31
<i>Image analysis</i>	31
<i>Molecular modeling</i>	31
<i>Analysis of autoradiograms</i>	31
<i>Analysis of mathematical data</i>	31
III. RESULTS	33
III.1. THE GROUP II CHAPERONIN MM-CPN FROM <i>M. MARIPALUDIS</i>	33
<i>Cloning, purification and initial characterization of Mm-Cpn</i>	33
<i>The search for intrinsic substrate proteins of Mm-Cpn</i>	35
<i>Analysis of the conformational cycle in Mm-Cpn</i>	36

<i>ATP hydrolysis is required to generate the folding-active state of Mm-Cpn</i>	37
III.2. THE IRIS-LIKE LID STRUCTURE OF GROUP II CHAPERONINS PREVENTS PREMATURE RELEASE OF	
SUBSTRATE PROTEIN EJECTED INTO THE CENTRAL CAVITY.	40
<i>The apical protrusions are required for efficient substrate folding in Mm-Cpn</i>	40
<i>Mm-Cpn Δlid is unable to encapsulate substrate protein within the central cavity</i>	42
<i>ATP hydrolysis in Mm-Cpn results in the release of bound substrate protein</i>	44
<i>Substrate binding sites are hidden in the closed conformational state induced by ATP hydrolysis</i>	47
III.3. LID FORMATION TRIGGERS COOPERATIVITY IN GROUP II CHAPERONINS	50
<i>The built-in lid in TRiC couples ATP hydrolysis to substrate folding</i>	51
<i>The built-in lid establishes allosteric coupling between subunits in one ring</i>	52
<i>Negative allosteric coupling between rings affects ATP binding and hydrolysis</i>	56
<i>Negative allosteric coupling between rings drives a “two-stroke” motor cycle</i>	58
<i>The second allosteric transition is absent in lid-less group II chaperonins</i>	60
III.4. POSITIVE COOPERATIVITY IN THE EUKARYOTIC CHAPERONIN TRiC IS A SEQUENTIAL EVENT DRIVEN	
BY A GRADIENT OF AFFINITIES FOR ATP	63
<i>A gradient of affinities for ATP binding in TRiC</i>	64
<i>Not all subunits in TRiC cross-link to ATP at saturating conditions</i>	67
<i>Stoichiometry of TRiC-nucleotide complexes under equilibrium conditions</i>	69
<i>ATP binding to CCT6 is dispensable for TRiC’s catalytic cycle in vivo</i>	71
IV. DISCUSSION	74
IV.1. ALLOSTERIC REGULATION IN GROUP II CHAPERONINS	74
<i>Similar allosteric coupling within the subunits of a ring is achieved by different strategies in Group I</i>	
<i>and group II chaperonins</i>	74
<i>Influence of the built-in lid on inter-ring communication</i>	75
IV.2. POSITIVE COOPERATIVITY IN GROUP II CHAPERONINS PROPAGATES SEQUENTIALLY	77
<i>What is the structural feature common to all high affinity subunits?</i>	77
<i>The order of sequential ATP-induced allosteric transitions in one ring of TRiC</i>	79
<i>Do the low affinity subunits fulfill a regulatory function?</i>	80
IV.3. THE APICAL PROTRUSIONS AND THE CONFORMATIONAL CYCLE OF GROUP II CHAPERONINS	81
<i>Conformational changes in group II chaperonins upon binding of ATP</i>	81

ATP hydrolysis is the central step in the folding cycle of group II chaperonins 82

What is the signal for re-opening of the lid?..83

V. SUMMARY.....84

VI. REFERENCES.....86

ABBREVIATIONS:

AAA-ATPase	ATPases associated with diverse cellular activities
ADP	adenosine diphosphate
amp ^R	ampicillin resistance
ATP	adenosine triphosphate
BCA	bichinoic acid
bp	base pairs
BSA	bovine serum albumin
C-	carboxy-terminal
CDTA	1,2 cyclohexane-diaminetetra-acetic acid
CLIPs	chaperones linked to protein synthesis
DEAE-	diethylaminoethyl-
DTT	dithiothreitol
EDTA	ethylenediamine tetraacetic acid
IPTG	isopropyl- β -D-1-thiogalactopyranoside
N-	amino-terminal
HEPES	(4-(2-hydroxyethyl)-1-piperazineethanesulfonic acid)
HSPs	heat shock proteins
MOPS	3-(N-morpholino)propanesulfonic acid
PBS	phosphate buffered saline
PCR	polymerase chain reaction
PEI-cellulose	polyethyleneimine cellulose
psi	pounds per square inch
RAC	ribosome associated complex
RP-HPLC	reversed phase HPLC
rpm	rounds per minute
SDS	sodium dodecyl sulfate
SDS-PAGE	SDS-polyacrylamide gel electrophoresis
TAE	Tris-Acetate-EDTA
TBS	Tris-buffered saline
TBS-T	Tris-buffered saline plus 0.1 % Tween-20
TF	trigger factor

TFA	trifluoroacetic acid
TLC	thin layer chromatography
TRiC/ CCT	tailless complex polypeptide 1 (TCP1) ring complex/ chaperonin containing TCP1
Tris	tris-(hydroxymethyl)-aminomethan
WD repeats	tryptophan-aspartate repeats

COLLABORATIONS:

Cryo Electron Microscopy was performed in collaboration with the laboratory of Prof. Dr. Wah Chiu, National Center for Macromolecular Imaging, Baylor College of Medicine, Houston, TX, USA.

Mathematical analysis of kinetic data was performed in collaboration with Dr. Charles Parnot, Stanford University, CA, USA.

I. INTRODUCTION

A central theme of biology is the conversion of genetic information into functional proteins. The fact that virtually every biological process involves proteins can be attributed to the enormous functional spectrum of this class of macromolecules, ranging from simply providing structure to catalyzing chemical reactions. The ribosome catalyzes an important step during protein biosynthesis, namely translation of the one-dimensional genetic code into a linear polypeptide chain. However, to actually perform the destined biological function, every polypeptide subsequently has to adopt a defined native three-dimensional structure in a process referred to as protein folding. To assure a robust cellular environment, newly synthesized polypeptides have to reliably fold into the native state and the native state, once acquired, has to be maintained throughout the lifespan of a protein. Defects in both protein folding and quality control are associated with a variety of different diseases, such as cystic fibrosis and neurodegenerative disorders like Huntington and Alzheimer's^{1,2}. Understanding of the process of protein folding in molecular detail would lead to fundamental advances in many aspects of biology and medicine but would also benefit industrial production of insoluble proteins like insulin.

I.1. Protein folding *in vitro* versus *in vivo*

Landmark experiments for which Christian Anfinsen was awarded the Nobel Prize over three decades ago revealed that the three-dimensional structure of a native protein under physiological conditions is the one with the lowest Gibbs free energy and hence determined by the amino acid sequence³. Consequently, many small proteins are able to spontaneously fold into the corresponding native state after denaturing stresses *in vitro*. According to the current view, a polypeptide chain can follow multiple folding pathways towards the energetic minimum, driven by burying hydrophobic stretches inside the 3-D structure^{4,5}. However, those conclusions are derived from *in vitro* folding experiments, which are usually performed at low temperature and a high protein dilution, both conditions that prevent off-pathway reactions like aggregation.

In contrast, the cytosol is a concentrated broth containing 200–300 mg of protein per ml^{6,7}, resulting in a situation described as “excluded volume effect” or “molecular crowding”^{8,9}, where protein aggregation is favored and strongly competes with

refolding to the native state¹⁰. The situation is aggravated by the vectorial emergence of the linear polypeptide chain in the cytosol during synthesis on the ribosome. Since the information for the native state is encoded by the entire amino acid sequence, the nascent polypeptide chain is unable to fold stably until fully synthesized, but exposes hydrophobic sequences into the cytoplasm. Additionally, translation occurs on polysomes where many ribosomes move along the same mRNA and thereby produce a high local concentration of unfolded polypeptides with high propensity to aggregate. In order to cope with such unfavorable conditions, cells evolved a set of remarkable enzymes, called molecular chaperones, that assist folding of both newly synthesized and stress-denatured proteins¹¹⁻¹⁵. Chaperones can selectively detect unfolded proteins by specifically binding to exposed stretches of hydrophobic amino acids, since those residues are usually buried inside the three-dimensional structure of the native state. By shielding those hydrophobic patches from the cellular environment, they successfully prevent off-pathway reactions like aggregation thereby keeping the polypeptides in a soluble, folding competent state¹¹⁻¹⁵.

1.2. The cytoplasmatic chaperone machinery

Molecular chaperones, frequently also referred to as heat shock proteins (Hsp), comprise a family of structurally unrelated proteins^{11,12,14,16}. They are functionally coupled to a machinery and fulfill a key role in cellular protein folding under normal growth condition as well as under stresses. Furthermore, they are involved in a variety of cellular processes that require maintenance of proteins in specific conformational states, such as protein translocation¹⁷ and targeting for degradation^{18,19}. Prior to describing the cell biological aspect of chaperone networks in the cytoplasm, the mechanistic principles of the two major classes of ATP-dependent molecular chaperones, found in all three kingdoms of life, namely the Hsp70s and the chaperonins (Hsp60s) are introduced.

The Hsp70-Hsp40 chaperone system

Hsp70 chaperones are monomeric proteins with a molecular mass of approximately 70 kDa that bind to both newly translated and stress-denatured proteins^{16,20}. They are ubiquitously found in all kingdoms of life but seem to be absent in certain methanogenic archaea²¹. The functionally best characterized Hsp70 is the *E. coli* DnaK protein (**Fig. 1**)^{16,22,23}. ATP binding opens a peptide-binding cleft, resulting in a

conformational state where substrate binds with low affinity due to high on and off rates. The substrate binding cleft closes during ATP hydrolysis, facilitating stable association of substrate with DnaK in the ADP state. Hsp70 chaperones work hand in hand with co-chaperones from the Hsp40 family named DnaJ in *E. coli*^{16,22,23}. DnaJ binds denatured substrate proteins and its characteristic J-domain activates ATP hydrolysis in DnaK resulting in the transfer of the polypeptide chain to the Hsp70 protein. In *E. coli*, a second DnaK co-factor, GrpE, catalyzes the exchange of bound ADP for ATP, thereby promoting substrate release from DnaK^{16,22,23}. As a consequence, the DnaK-DnaJ-GrpE machinery reversibly binds hydrophobic patches exposed by unfolded proteins and thereby maintains unfolded polypeptides in a soluble, folding competent state (**Fig. 1**).

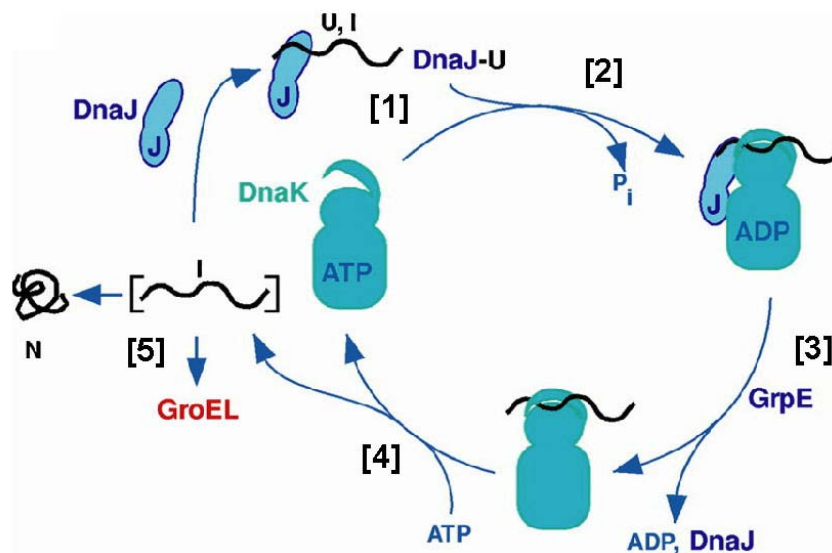


Figure 1. The well-studied bacterial DnaJ-DnaK-GrpE chaperone system exemplifies the Hsp70 reaction cycle. ATP binding to the bacterial Hsp70 homologue DnaK induces a conformational change that results in opening of a substrate-binding cleft (1). Interaction with the J-domain of its Hsp40 co-chaperone DnaJ stimulates ATP hydrolysis in DnaK and results in stable association of unfolded protein (U) or a folding intermediate (I) and DnaK (2). GrpE serves as a nucleotide exchange factor for DnaK (3) and subsequent ATP binding results in the release of bound substrate protein (4) in the unfolded state or an intermediate folding state. The protein can either fold spontaneously into the native state or alternatively is transferred to the Hsp60 chaperone system (GroEL) for further assistance (5). The figure is taken from Frydman J., 2001¹².

Due to their broad substrate spectrum and their property to “hold” a polypeptide in an unfolded state, chaperones from the Hsp70 family form a central intersection in the

pathway of cytoplasmatic protein folding. They bind to newly translated polypeptides as well as stress-denatured proteins and either support their folding to the native state or transfer them to a different chaperone machinery, like the chaperonins, where folding is completed, or to the degradation machinery^{18,19}. Moreover, chaperones from the Hsp70 family work hand in hand with the oligomeric AAA+ ATPase ClpB in *E. coli* (Hsp104 in yeast) during the recovery of proteins from protein aggregates.^{18,24} Intriguingly, a number of different Hsp70 proteins are found in the yeast cytosol. Ssb1 and Ssb2 as well as the Hsp70-related protein Ssz (Pdr13) and its Hsp40 cofactor zuotin are associated with the ribosome and therefore recruited for the folding of newly synthesized proteins²⁵⁻²⁷. The latter pair, Ssz/zuotin, forms a stable heterodimer, also termed RAC²⁷, and stimulates the ATPase activity of Ssb²⁸. The other four Hsp70 family members, Ssa1-4, as well as the closely related homologue Sse1 are free in the cytosol and cover the broad spectrum of Hsp70-function in this compartment.

The chaperonins are Hsp60 family members

Chaperonins on the other hand comprise a family of large (800–900 kDa) oligomeric assemblies composed of two rings that are stacked back to back giving rise to two central cavities^{29,39} (**Fig. 2** and **4A**). Substrate binding sites are exposed at the distal rim of each ring in the nucleotide-free state. During the ATP-dependent folding reaction²⁹ (**Fig. 2**) the bound substrate becomes encapsulated within the central cavity. Chaperonins therefore transiently provide a microenvironment protected from the unfavorable cytoplasmic conditions. In the case of the well-studied bacterial chaperonin GroEL, closure of the central cavity requires binding of the dome-shaped co-chaperonin GroES^{16,29} (**Fig. 2A**). GroES binding induces a structural conversion of the inner GroEL surface from a mainly hydrophobic to a hydrophilic environment and generates an enclosed space of approximately 80 Å in diameter and 85 Å in height spacious enough to accommodate a protein of up to 60 kDa in size³⁰. Whether the cavity simply resembles an “Anfinsen-cage”, this is an environment favorable for protein folding comparable to an *in vitro* situation, or if the cavity walls actively influence the folding pathway is currently under investigation³¹. Recent biochemical analysis of the GroEL-GroES “nano-cage”³² suggests that a combination of structural confinement together with repulsion from the hydrophilic wall and specific interactions with conserved C-terminal Gly-Gly-Met repeats may provide an optimal

environment to catalyze folding of certain proteins³². Additionally, it has been proposed that chaperonins apply pulling forces, thereby unfolding bound substrate proteins before ejection into the central cavity³³, but such a mechanism needs yet to be proven. The basic structure of archaeal and eukaryotic chaperonins is very similar to that of their bacterial counterparts^{34,35} (**Fig. 2B**). However, they can function independent of a GroES-like co-chaperone and achieve closure of their central cavity with the help of an integrated lid structure^{34,35} (**Fig. 2B**). This fundamental difference, which resulted in their classification as group II chaperonins, might be a result of an exclusive role in co-translational folding of polypeptides during protein synthesis^{36,37}. Consequently, expression of the eukaryotic chaperonin TRiC is not stress-induced but co-regulated with the expression of the translational machinery³⁶. However, the cell biological role of chaperonins in the cytoplasm of archaea has not been investigated yet.

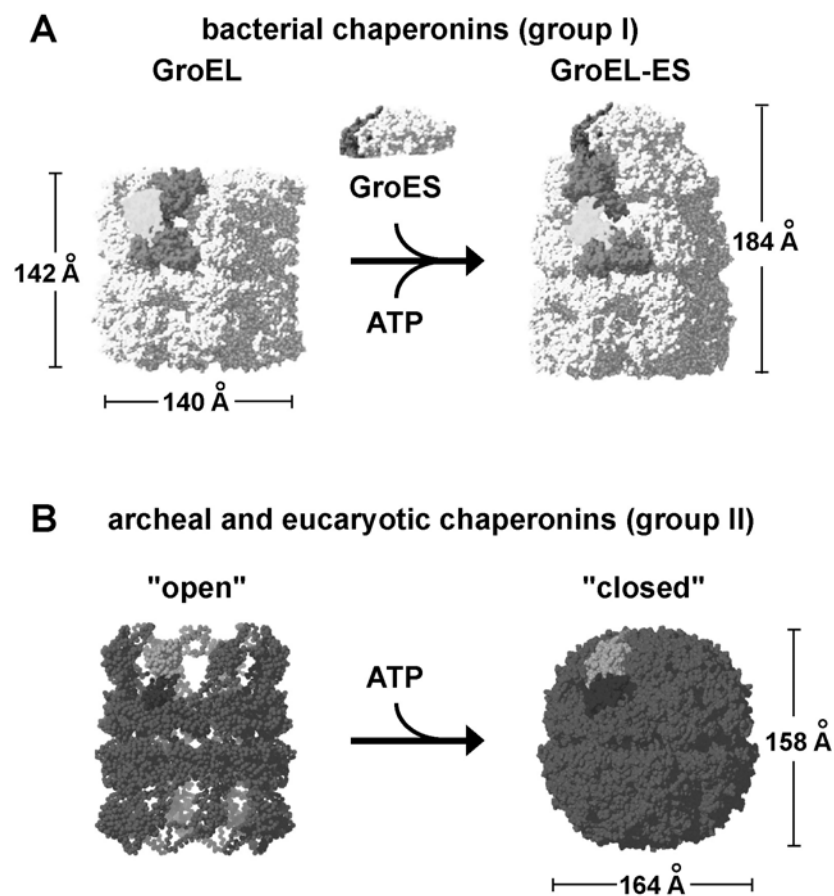


Figure 2. Chaperonins are oligomeric double ring structures that open and close their two central cavities in an ATP regulated manner. (A) The bacterial group I chaperonin GroEL interacts with the GroES co-chaperonin in a nucleotide dependent reaction resulting in closure of the central

chamber and encapsulation of substrate protein. **(B)** Group II chaperonins from eukaryotic and archaeal origin are independent of a GroES-like co-chaperonin but possess a built-in lid that assembles over the central chamber in an ATP dependent fashion. This figure is modified from Frydman, J., 2001¹² and from Spiess *et al.*, 2004⁵⁴.

Not all chaperones are heat shock proteins

Although the terms “heat shock protein” and “chaperone” are often used as synonyms recent genomic analysis in yeast³⁶ discovered the existence of a subset of molecular chaperones, the so-called CLIPS (chaperones linked to protein synthesis), which is transcriptionally co-regulated with the translational machinery and therefore actually down-regulated under stress conditions. Prominent members of the CLIP family in yeast are ribosome-associated chaperones namely the Hsp70-homologue Ssb1/2, a hetero-dimer composed of the DnaK-related Ssz/Pdr13 and the DnaJ-like protein zuotin (termed RAC, ribosome-associated complex), as well the eukaryotic chaperonin TRiC. Comprehensive functional analysis³⁶ revealed that the CLIP chaperones are exclusively involved in the folding of newly synthesized polypeptides as they emerge from the ribosome (**Fig. 3A**). On the other hand, the classical heat shock proteins (HSPs) comprise a class of stress-inducible eukaryotic chaperones that function either in re-folding or clearing of misfolded proteins³⁸.

A picture emerges where two different chaperone networks cope with the two distinct pathways of protein folding in the eukaryotic cytosol, namely co-translational folding^{37,39,40} of newly synthesized polypeptides and re-folding of denatured proteins during stress situations (**Fig. 3A**).

In contrast, the bacterial chaperone system comprises one global network of stress-inducible heat shock proteins (**Fig. 3B**)³⁸. The only ribosome associated chaperone in bacteria, trigger factor (TF), is located in proximity of the ribosomal exit tunnel⁴¹ and maintains the emerging polypeptides in a folding competent conformation⁴². Further downstream, the GroEL-ES and Hsp70 machinery collaborate during both post-translational folding of newly synthesized polypeptides and the re-folding of stress denatured proteins^{38,43,44}.

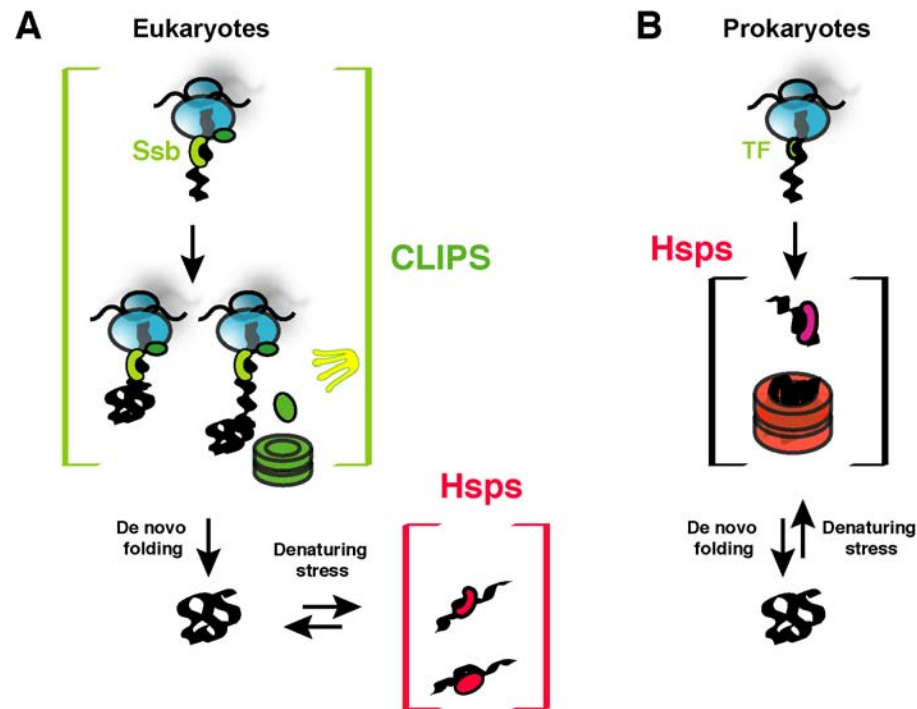


Figure 3. In contrast to bacterial cells two distinct chaperone networks divide forces in the eukaryotic cytosol. (A) Two distinct chaperone networks fulfill different functions in the eukaryotic cytosol: Chaperones of the CLIP (chaperones linked to protein synthesis)- family are transcriptionally co-regulated with the translational machinery and play an exclusive role in the co- and post-translational folding of newly synthesized polypeptides. The CLIP-family members are down regulated under stress-conditions and a second distinct chaperone network consisting of classical heat shock proteins (Hsps) takes over in the re-folding of stress-denatured proteins. (B) In bacteria one chaperone network covers the entire protein folding requirement in the cytoplasm, namely folding of newly synthesized polypeptides that is thought to occur mainly post-translational as well as re-folding of stress denatured proteins. With the exception of the ribosome associated trigger factor (TF) all bacterial chaperones are stress inducible and therefore classical heat shock proteins (Hsps). This figure was kindly provided by Veronique Albanese.

Co-translational folding in the eukaryotic cytoplasm

Cotranslational protein folding in the eukaryotic cytosol^{37,39,40} occurs in a sequestered environment that appears to be effectively shielded from disturbing cytoplasmic conditions by the close cooperation of the CLIP chaperone network⁴⁵⁻⁴⁸. Probably as a result of its prominent localization on the ribosome, Ssb1/2 interacts with most nascent chains whereas other members of the Hsp70 chaperone family, like Ssa1 and Sse1 as well as the eukaryotic chaperonin TRiC, interact with a smaller subset of nascent chains and therefore presumably function downstream of Ssb1/2⁴⁹. The

majority of polypeptides can be folded solely by the Hsp70 members, whereas only about 10 to 15 % of newly synthesized proteins require the chaperonin TRiC for further assistance⁴⁷. The most prominent substrates are the highly abundant components of the cytoskeleton, actin and tubulin, and it has been well established that TRiC cooperates with different CLIP family members in their folding⁴⁵⁻⁴⁷. During this process, the emerging polypeptide chain is transferred from the ribosome to TRiC with the help of the specialized GimC (prefoldin) chaperone complex^{46,50}. Other TRiC substrates, including the WD repeat protein Cdc20 or the von-Hippel-Lindau tumor suppressor are transferred from the ribosome with the help of Ssb^{51,52}. Most components of the yeast chaperone networks are present also in higher eukaryotes, suggesting a similar mechanism of protein biogenesis⁵³.

Intriguingly, many eukaryotic proteins such as actin, tubulin, and luciferase cannot fold after expression in bacteria^{39,40,48} suggesting a major difference in the chaperone networks. Comparison of the eukaryotic and bacterial proteome reveals that eukaryotes possess a higher portion of multi-domain proteins. The ability to co-translationally fold individual domains could therefore be of major advantage in eukaryotes.

1.3. Chaperonins - a distinct class of molecular chaperones

Chaperonins appear to be mechanistically very specialized members of the chaperone family that play a central role for the folding of a number of essential cytosolic proteins^{29,54}. No other chaperone system can substitute for their function *in vivo* and consequently deletion of the chaperonin subunits-encoding genes is lethal. What is the unique clue of those sophisticated molecular machines? The following section provides an overview of the current mechanistic understanding of the structurally related chaperonin groups in all three kingdoms of life.

Chaperonin structure

Chaperonins are ATP-driven molecular machines composed of two cylinders stacked back to back^{30,34} (**Fig. 4A**). The resulting internal cavities can enclose unfolded polypeptides in an ATP-dependent manner and provide a protected microenvironment for protein folding to occur. All chaperonins subunits share a similar architecture^{30,34} (**Fig. 4B**), consisting of three distinct domains: an equatorial domain connected via a hinge-like intermediate to the distal apical domain. The equatorial domain provides

the interaction surface between the two rings and harbors the major sites of ATP binding. The adjacent intermediate domain closes over bound ATP, thereby generating the nucleotide binding pocket. This ATP-induced conformational change in the intermediate domain is transferred to the apical domain, where the substrate binding sites are located. Despite overall structural similarities, there are significant differences between the eubacterial chaperonins, such as GroEL from *E. coli*^{16,29,55}, and the chaperonins from archaea and eukaryotes^{54,56}.

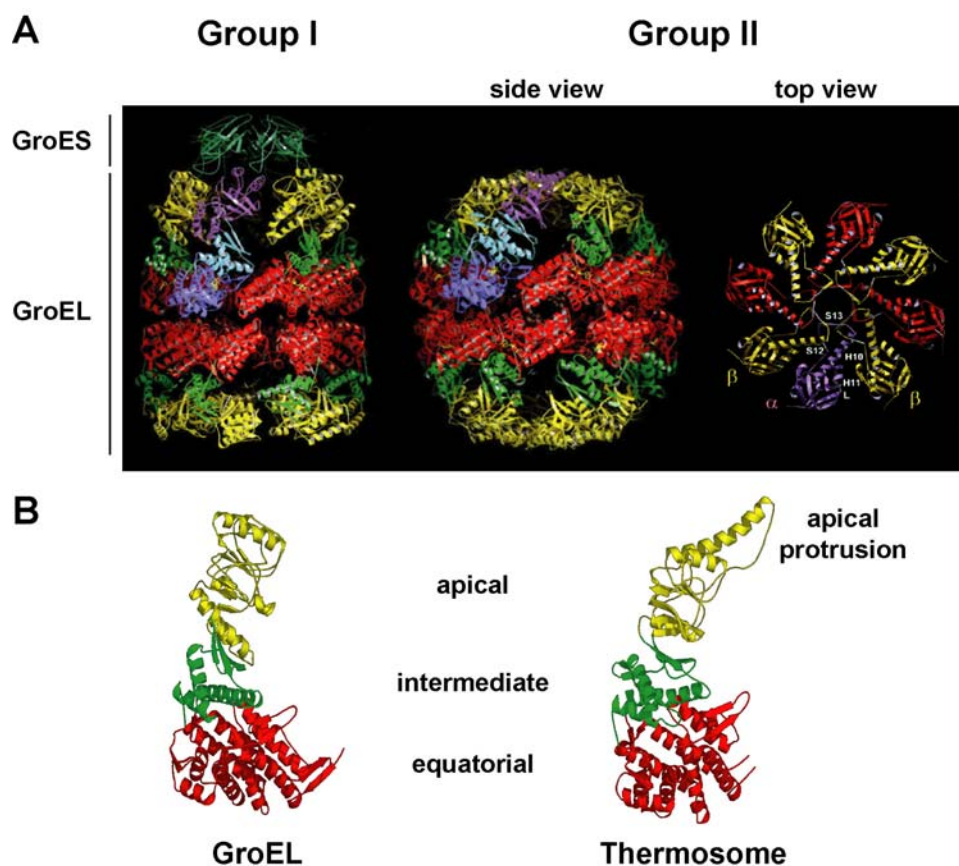


Figure 4. Architecture of group I and group II chaperonins. (A) Crystal structures of the GroEL-GroES-(ADP)₇ complex³⁰ (left) and the thermosome³⁴ (middle), respectively. The image on the right side corresponds to the top view of the crystal structure of the thermosome³⁴ and shows assembly of the apical protrusions in the iris-like lid structure characteristic for all group II chaperonins. (B) Crystal structures of a single subunit of GroEL (left) and the thermosome (right), respectively. The equatorial domain (red) is linked via the hinge-like intermediate domain (green) to the apical domain (yellow). In contrast to the group I chaperonin GroEL group II chaperonins contain apical protrusions extending from the tip of the apical domain.

While the, so-called group I chaperonins from bacteria are homo-oligomeric and each cylinder is made up of seven subunits, eukaryotic and archaeal group II chaperonins are with a few exceptions hetero-oligomeric⁵⁴ and composed of eight or nine subunits per ring. The eukaryotic group II chaperonin TRiC is the most complex group II chaperonin as it is composed of eight different subunits, CCT1-8, which share only 25-36 % sequence identity among each other⁵⁷. The most dramatic difference between group I and group II chaperonins resides in their distinct strategies to mediate closure of their central folding chamber. Group I chaperonins use a ring-shaped co-chaperone GroES as a detachable lid. In the presence of ATP, GroES binds to the apical domains of the GroEL subunits and thereby generates the central cavity⁵⁵ (**Fig. 3A** and **4A**).

One long-standing mystery in the chaperonin field involved the apparent lack of a cofactor for type II chaperonins, which appeared to be fully functional without such an accessory protein. The answer to this puzzle was found in the crystal structure of the group II chaperonin from the archaeum *Thermoplasma acidophilum*³⁴. The structure revealed that each subunit of the thermosome complex can be superimposed onto a GroEL subunit with the exception of an additional loop protruding from the tip of the thermosome apical domain. This so-called apical protrusion (**Fig. 4B**) from neighboring subunits forms a β -sheet and creates an iris-like lid structure (**Fig 4A**, right) that may restrict access to the cavity³⁴. Clearly, group II chaperonins require a highly coordinated ATPase cycle to reversibly open and close a central cavity without the help of an external co-factor. Since basic structural features are conserved between chaperonins from different groups, it is helpful to consider the molecular details of the well-studied group I chaperonin GroEL in order to investigate the adaptations of archaeal and eukaryotic chaperonins necessary to maintain a built-in lid.

Group I chaperonins: The GroEL-GroES machinery

The ATPase cycle of the group I chaperonin GroEL has been studied in detail and high-resolution structures of several conformational states along the reaction cycle, obtained by both cryo-electron microscopy and crystallography, are available^{29,30,58-60}. Each individual ring in GroEL represents a functional unit, whose individual subunits have to act fully synchronized. Accordingly, chaperonins are highly allosteric protein machines⁶¹⁻⁶³. Subunits within each ring are coupled via positive cooperativity in ATP binding^{61,64,65}, which allows them to act in a concerted fashion to create the closed

folding chamber. In addition, negative communication between the rings causes ATP binding to one ring to inhibit ATP binding to the adjacent ring^{64,65}. This feature ensures that only one ring, the so called *cis*-ring, is folding-active at a given time, allowing GroEL to function as a "two-stroke" motor where the two rings alternate during the reaction cycle. This unique allosteric behavior is described as nested cooperativity, since the positive cooperative transitions within each ring are nested into the overall negative cooperativity between them⁶⁴.

Substrate binds to hydrophobic sites located at the inner rim of the central cavity⁶⁶ (**Fig. 5**). Binding of ATP to the substrate-bound *cis*-ring initiates the attachment of the heptameric GroES lid⁶⁷, resulting in encapsulation of the substrate within the cavity (**Fig. 5**). Association of GroES induces dramatic conformational changes in the GroEL apical domains, discharging the substrate into the GroES-capped chamber, where it commences folding^{29,68,31}. Surprisingly, ATP hydrolysis is not required for quantitative substrate folding within the central chamber as shown for the ATPase deficient GroEL mutant form D398A⁶⁹. However, ATP hydrolysis to ADP in the *cis*-ring has to occur in order to facilitate ATP binding to the *trans*-ring, which in turn results in release of ADP, GroES, and the native substrate protein from the *cis*-ring^{29,69}. GroES then binds to the "new" *cis*-ring, and a new round of folding starts⁷⁰ (**Fig. 5**).

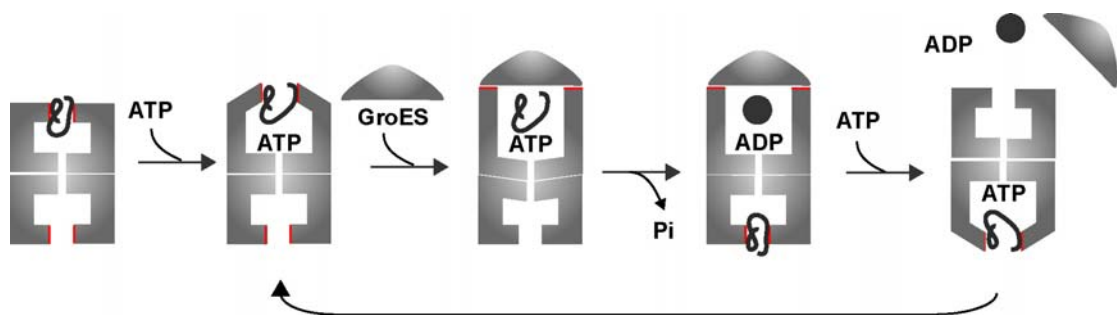


Figure 5. The folding cycle of the bacterial chaperonin system GroEL-ES. Cooperative binding of ATP to the substrate bound GroEL *cis*-ring induces slight conformational changes that result in increased affinity for GroES. GroES binding induces large conformational changes in the apical domains of GroEL, which move the hydrophobic substrate binding sites (red) away from the central chamber and permit GroES to bind on top of GroES thereby encapsulating substrate protein and forming the the asymmetric *cis*-folding active complex. Hydrolysis of ATP to ADP occurs with a half time of 8-10 sec and serves as a timer mechanism since the association of GroEL and GroES in the ADP bound post hydrolysis complex is less stable. Binding of ATP to the *trans*-ring finally discharges

ADP, GroES and the encapsulated substrate from the *cis*-ring and the next folding cycle starts in the new *cis*-ring.

Group II chaperonins from archaea and eukarya

Despite intensive studies on the biochemistry and function of the bacterial chaperonin GroEL along with its co-chaperonin GroES, little is known on the mechanistic and biological significance underlying the unique structural features of eukaryotic and archaeal chaperonins. Central objects of current studies are the eukaryotic chaperonin TRiC purified from bovine tissue⁵⁴ and two crystallized homologues from hyperthermophilic archaeobacteria, namely the thermosome from *Thermoplasma acidophilum*^{34,56} and KS-1 from *Methanococcus spec.*³⁵.

In the absence of nucleotide, all group II chaperonins adopt a symmetrically open conformation and can bind unfolded substrate protein (**Fig. 6 [1]**)^{71,38,44,45,46,43}. Unfortunately, high-resolution structural information of this conformation is not available, as irrespective of the nucleotide state, group II chaperonins have only been crystallized in a symmetrically closed state so far^{34,35}.

Upon binding of non-hydrolysable nucleotide analogs, the lid structures in TRiC and the thermosome remain in an open conformation⁷²⁻⁷⁴ (**Fig. 6 [2]**). Intriguingly, incubation of the thermosome with ATP at low temperatures, where ATP is not hydrolyzed, cannot trigger lid assembly either^{73,75}. Contradicting results are reported for the group II chaperonin KS-1, where nucleotide binding seems to be sufficient to induce lid closure⁷⁶. In TRiC and the thermosome, ATP hydrolysis is required to induce a conformational change during which the apical protrusions of neighboring subunits assemble into an iris-like β -sheet and that leads to a conformational state that supports substrate folding^{72,77} (**Fig. 6 [3]**). Group II chaperonins trapped in the transition state of ATP hydrolysis by incubation with ATP and AlF_x adopt a symmetrically closed conformation^{72,78} (**Fig. 6 [4]**). In the presence of ADP, by contrast, all group II chaperonins are rendered in the open conformation (**Fig. 6 [5]**), suggesting that gamma-phosphate release triggers re-opening of the lid structure^{72,73,75,76}. Investigation of the allosteric properties of TRiC revealed a nested cooperative mechanism similar to that of GroEL, suggesting the existence of positive *intra*-ring and negative *inter*-ring cooperativity^{79,80}. Consistently, asymmetric conformations have been reported for the thermosome^{81,82} and TRiC in the presence

of ATP⁸³ and ADP-AlF_x⁷² as well as for KS-1 in the presence of ADP-BeF_x⁷⁸. Our current interpretation of the ATPase cycle in group II chaperonins relies on a collection of isolated conformational states that need to be interconnected. Detailed analysis of the allosteric regulation in group II chaperonins as well as further structural analysis will provide insight into the relevance of the different conformations for the nucleotide cycle and might elucidate whether group II chaperonins function as two-stroked molecular machines comparable to the GroEL-ES chaperonin system. Remarkably, GroEL, although able to bind several TRiC substrates, cannot assist in the folding reaction^{71,84,85}. Better understanding of the folding cycle of TRiC might help to explain its unique ability to fold a variety of essential eukaryotic proteins⁵⁴.

It is becoming increasingly clear that TRiC's essential function in the co-translational folding of a variety of proteins is connected to several disease phenotypes. Tumor-causing mutations in the tumor suppressor protein VHL are found to be located in the TRiC-binding sites⁸⁶ and lead to severe misfolding of VHL *in vivo* explaining the lack of function of the mutant protein^{51,87}. More recently, TRiC was attributed an essential role in protecting cells against the formation of cytotoxic conformations of proteins with extended polyglutamine repeats, which underlie Huntington's disease and other neurodegenerative disorders⁸⁸⁻⁹⁰. In order to understand the contribution of TRiC to these processes and to be able to counteract cellular imbalances that lead to disease states, it is necessary to obtain a defined structural view in synergy with a molecular understanding of the ATP driven motions in TRiC during the folding cycle.

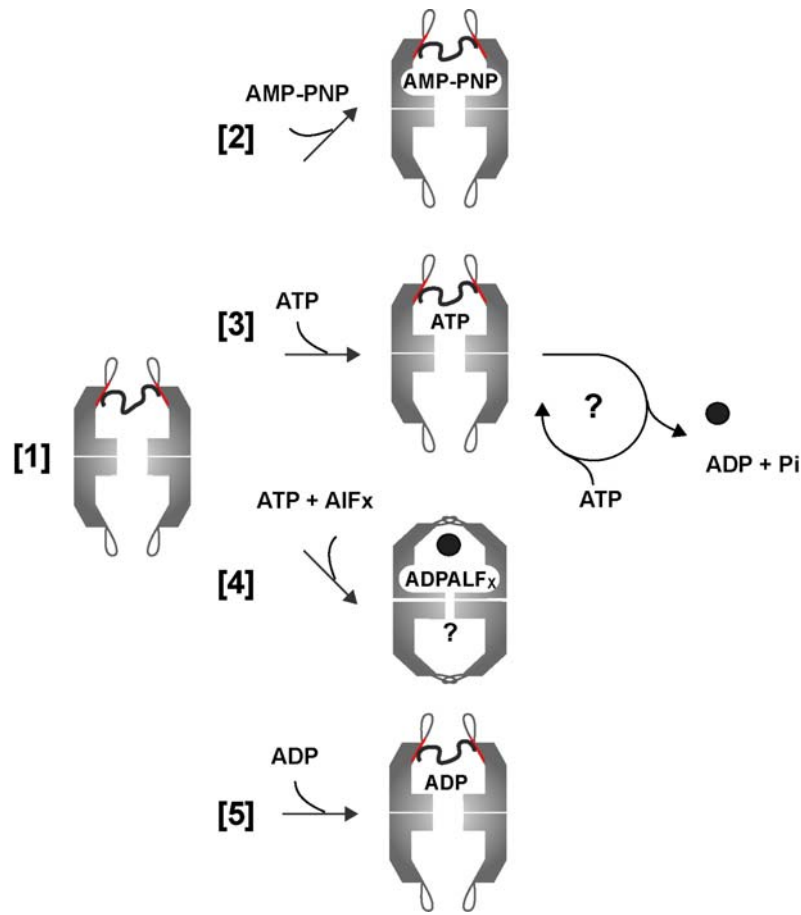


Figure 6. Current understanding of the conformational states in group II chaperonins. (1) In the absence of nucleotide group II chaperonins are in an open conformation and bind to substrate protein. (2) Binding of non-hydrolysable nucleotide analogues does not induce lid closure in the eukaryotic chaperonin TRiC and the thermosome (3) The folding-active closed state is only sampled in the presence of hydrolysable ATP but a detailed view of the ATPase cycle of group II chaperonins especially in respect of their possible function as a two-stroke motor remains to be established. (4) Incubation with ATP and AIF_x traps group II chaperonins in a conformation with both rings in the closed state. (5) In the ADP bound state group II chaperonins are found to be in the open conformation with exposed substrate binding sites.

1.4. Aims of this work

The aim of this work was to understand how group II chaperonins maintain a productive folding cycle without the help of an external GroES-like lid co-factor and to identify the molecular adjustments necessary to use a built-in lid. To this end, it was planned to investigate the role of the lid-forming segments in the catalytic cycle and to determine the molecular basis of cooperative conformational changes that result in lid closure in group II chaperonins. Intrigued by the subunit heterogeneity in TRiC it was furthermore intended to investigate whether the eight different subunits contribute equally to the ATPase cycle.

Although the study mainly focused on the eukaryotic chaperonin TRiC it was planned to investigate the homo-oligomeric chaperonin Mm-Cpn from the mesophilic methanogenic archaeon *Methanococcus maripaludis* in parallel. Development of biochemical techniques to study the folding cycle of this distantly related group II chaperonin would on the one hand provide the possibility to generate genetically modified mutant forms of a group II chaperonin and on the other hand allow to base the biochemical analysis of group II chaperonins on two distinct model systems of different origin and complexity.

II. MATERIALS AND METHODS

II.1. Plasmids and Strains

All bacterial and yeast strains used in this study are listed in **Table 1**. All plasmids generated during this study or used from different sources are listed in **Table 2**.

Table 1: Bacterial and Yeast strains

Strain	Genotype	Reference
Bacterial strains:		
Rosetta2 (DE3)pLysS	<i>E. coli</i> B, F ⁻ , <i>ompT</i> , <i>hds</i> _B (r _B ⁻ m _B ⁻), <i>gal</i> , <i>dcm</i> , λDE3, pLysSRARE (Cam ^R)	Invitrogen
DH5α	<i>E. coli</i> K12, F ⁻ , <i>gyrA96</i> , <i>recA1</i> , <i>relA1</i> , <i>endA1</i> , <i>thi-1</i> , <i>hdsR17</i> , <i>glnV44</i> , <i>deoR</i> , Δ(<i>lacZYA-argF</i>)U169, [Φ80dΔ(<i>lacZ</i>)M15]	Invitrogen
Yeast strains:		
B-9018	<i>cct6-Δ1::TRP1</i> , <i>MATa</i> , <i>ura3-52</i> , <i>trp1-Δ63</i> , <i>leu2-Δ1</i> , <i>GAL2</i> , pAB990, pAB1058	Lin <i>et al.</i> , 1997 ⁹¹
B-10301	<i>cct6-Δ1::TRP1</i> , <i>MATa</i> , <i>ura3-52</i> , <i>trp1-Δ63</i> , <i>leu2-Δ1</i> , <i>GAL2</i> , pAB990, pAB1852	Lin <i>et al.</i> , 1997 ⁹¹

Table 2: Plasmids

Plasmid	Genotype	Reference
Bacterial plasmids:		
pET21a ⁺	pBR322 <i>ori</i> , amp ^R , T ₇ promotor	Novagen
pET11d	pBR322 <i>ori</i> , amp ^R , T ₇ promotor	Novagen
pETMm-CpnWT	pET21a ⁺ -derivate, carrying the <i>mm-cpn</i> -gene (amp ^R)	this study
pETMm-CpnΔlid	pETMm-CpnWT-derivative	this study
pETMm-CpnD386A	pETMm-CpnWT-derivative	this study
pETMm-CpnΔlid/ D386A	pETMm-CpnWT-derivative	this study
pBROD	pET11d-derivative, carrying bovine adrenal rhodanese cDNA (amp ^R)	Miller <i>et al.</i> , 1991 ⁹²

<i>Yeast plasmids:</i>		
pAB990	<i>CCT6, URA3, CEN4, ARS1</i>	Lin <i>et al.</i> , 1997 ⁹¹
pAB1058	<i>CCT6, LEU2, CEN6, ARSH4</i>	Lin <i>et al.</i> , 1997 ⁹¹
pAB1852	PAB1058 derivative, <i>CCT6-24</i>	Lin <i>et al.</i> , 1997 ⁹¹

II.2. Media and Supplements

The media listed in **Table 3** were used to cultivate bacterial and yeast cells.

Table 3: Media

Medium	Composition
LB-medium	1 % pepton, 0.5 % yeast extract, 0.5 % NaCl
LB-agar	1 % pepton, 0.5 % yeast extract, 0.5 % NaCl, 1.5 % agar
M9-medium	0.6 % Na ₂ HPO ₄ , 0.3 % KH ₂ PO ₄ , 0.05 % NaCl, 0.1% NH ₄ Cl, 0.3 % CaCl ₂ , 1 mM MgSO ₄ , 0.8 % glucose, 0.00005 % thiamine
YPD-medium	2 % peptone, 1 % yeast extract, 1 % glucose
Complete synthetic yeast medium	0.17 % Yeast nitrogen base (Difco 0335-15), 2 % glucose, 0.5 % (NH ₄) ₂ SO ₄ , 2 g/L of dropout mix (see below) lacking either uracil (-Ura), leucine (-Leu), or methionine (-Met).
dropout powder-mix	0.5 g adenine, 2 g alanine, 2 g arginine, 2 g asparagine, 2 g aspartic acid, 2 g cysteine, 2 g glutamic acid, 2 g glutamine, 2 g glycine, 2 g histidine, 2 g myo-inositol, 2 g isoleucine, 4 g leucine, 2 g lysine, 2 g methionine, 0.2 g para-aminobenzoic acid, 2 g phenylalanine, 2 g proline, 2 g serine, 2 g threonine, 2 g tryptophane, 2 g tyrosine, 2 g uracil, 2 g valine

Supplements were used at the final concentration listed in **Table 4**.

Table 4: Supplements

Supplements	
Ampicillin	100 µg/ml
Chloramphenicol	50 µg/ml
IPTG	100 µM

II.3. Oligonucleotides

The oligonucleotides used in this study are listed in **Table 5**.

Table 5: Oligonucleotides

Name	Sequence
Mm-Cpn-fw	5'-ggaattccatattgtcacaacaaccaggagtttacc-3'
Mm-Cpn-rev	5'-cgcgatccttacatcattctggcattccgccattcc-3'
Mm-Cpn-midfw	5'-atcgcaatgacctcaatcaccgaaaagg-3'
Mm-Cpn Δ lid(link)-fw	5'-ctagctagcgaaatgttaaagacatggttgctgaaatcaaagcaagcgg-3'
Mm-Cpn Δ lid(link)-rev	5'-ctagctagctgattcttcgattgcacagtttaaagtcaattttgcgtcag-3'
Mm-CpnD386A-fw	5'-gaagaagtgcaagagcagtagacgctgctgttggtgtagttggatgtac-3'
Mm-CpnD386A-rev	5'-gtacatccaactacaccaacagcagcgtctactgctcttgcaacttcttc-3'

II.4. Chemicals and Reagents

8-N₃-ATP and α -[³²P]-8N₃-ATP were obtained from ALT Inc. (KY, USA). α -[³²P]-ATP and [³⁵S]-methionine was purchased from Perkin-Elmer Life and Analytical Sciences (Boston, MA, USA). ATP of highest purity was purchased from Sigma-Aldrich (Mo, USA). All other chemicals were either obtained from Sigma-Aldrich or from J.T. Baker (NJ, USA) unless mentioned otherwise. Restriction enzymes and other DNA-modifying enzymes were obtained from MBI Fermentas (MD, USA), Stratagene (CA, USA), and Invitrogen (CA, USA). Genomic DNA from *M. maripaludis* strain LL was kindly provided by Dr. John Leigh (Department of Microbiology, University of Washington, Seattle, WA, USA). *Methanococcus mariplaudis* cells were kindly provided by Prof. Dr. A. Böck (Department of Biology I, LMU München, Germany). HELA cells used to purify radiolabeled actin were generously provided by Dr. John Christianson (laboratory of Prof. R. Kopito, Stanford, CA, USA) and Ron Geller (laboratory of Prof. J. Frydman, Stanford, CA, USA). Purified GroEL and GroES proteins were kindly provided by Dr. Sheila Jaswal (laboratory of Prof. J. Frydman, Stanford, CA, USA) and Dr. Anne Meyer (laboratory of Prof. J. Frydman, Stanford, CA, USA) respectively.

II.5. Microbiological Methods

Bacterial and yeast cultures

Bacteria and yeast cultures were cultivated in either reaction tubes or Erlenmeyer flasks filled with 1/10th of their assigned volume and incubated on a shaker in order to ensure sufficient aeration. Bacterial cultures were incubated at 37°C, yeast cultures were grown at 30°C. To overproduce chaperonin proteins, the *E. coli* strain Rosetta (DE3) pLysS (EMD Biosciences, USA) harboring the corresponding pET21-derived expression plasmid was grown to an OD₆₀₀ of 0.8 in the presence of ampicillin. Protein production was induced by addition of 100 µM IPTG and the cells were cultivated for additional 4 hours. Subsequently, they were harvested by centrifugation at 15 000 g, washed in PBS and flash-frozen in liquid nitrogen.

Pulse-chase of yeast cells with [³⁵S]-methionine

Yeast strains B-1098 (*Δcct6/ LEU2cct6*)⁹³ and B-10301 (*Δcct6/ LEU2cct6-24*)⁹³ were grown to log phase and starved for 30 min in complete synthetic medium without methionine. The cells were then labeled with 100 µCi/ml [³⁵S]-methionine for 1 min, followed by a chase with 20 mM unlabeled methionine. At the indicated time points, aliquots were withdrawn, quickly chilled, and supplemented with 250 mM cold azide to deplete ATP and 0.5 mg/ml cycloheximide to stop protein synthesis. Cells were harvested and lysates were prepared in lysis buffer (10 mM HEPES [pH 7.5], 50 mM Tris/HCl [pH 8], 100 mM KCl, 10 mM MgCl₂, 10 % glycerol, 0.1 % triton-X-100, 1 mM DTT) supplemented with protease inhibitor cocktail by bead beating for 10 min at 4°C. The lysates were clarified by centrifugation for 15 min at 16,000 g and 4°C and used to isolate TRiC-substrate complexes by immunoprecipitation as well as native actin by a DNaseI pull-down experiment as described below.

Overproduction of [³⁵S]-labeled rhodanese in *E. coli*

Heterologous overproduction of [³⁵S]-labeled bovine rhodanese in *E. coli* was performed as described⁹⁴. *E. coli* strain Rosetta (DE3) pLysS (EMD Biosciences, USA) harboring the plasmid pBROD⁹² was grown at 37°C in 10 ml of LB-medium to OD₆₀₀ = 0.8, and synthesis of T₇-polymerase was induced by addition of IPTG to a final concentration of 0.1 mM. After 30 min of induction, the cells were harvested, washed in 5 ml sterile PBS, and resuspended in 10 ml of M-9 minimal medium

supplemented with all amino acids except methionine. After addition of rifampicin (200 $\mu\text{g/ml}$) and further incubation for 12 min, 300 μCi of S^{35} -methionine were added and the cells were cultivated for 2 hours at 37°C. Cells were harvested, washed in PBS and flash-frozen in liquid nitrogen.

II.6. Molecular Genetic Methods

Standard Methods

Molecular genetic standard methods like restriction, phosphorylation, dephosphorylation, and ligation were performed according to the instructions provided by the company the respective enzymes were obtained from. In order to extract DNA fragments from agarose gels, the QIAquick gel extraction kit (Qiagen) was used. Plasmids were isolated from 5ml of a bacterial culture grown to stationary phase in LB-medium. Plasmid preparation was achieved using the QIAprep Spin miniprep kit (Qiagen, USA) according to the manufacturer's instructions.

Construction of the bacterial expression vector pET21MmCpnWT

Genomic DNA from *M. maripaludis* strain LL was used as a template to amplify the *mm-cpn* gene by polymerase chain reaction (PCR). The PCR fragment was inserted into the vector pET21a⁺ (EMD Chemicals Inc., USA) using the *NdeI* and *BamHI* restriction sites, resulting in the vector pET21MmCpnWT.

Site-directed mutagenesis

To replace the helical protrusion region (amino acids I241-K267) by a short linker (ETASE), the plasmid pET21MmCpnWT was PCR-amplified using Pfu-Turbo DNA polymerase (Stratagene, USA) and primers (Mm-Cpn Δ lid(link)-fw and Mm-Cpn Δ lid(link)-rev) that were oriented divergently but overlapped at their 5' ends. Single amino acid changes in Mm-Cpn were performed by site-directed mutagenesis using plasmid pET21MmCpnWT as a template according to the QuikChange kit (Stratagene) protocol.

Sequencing of DNA

In order to obtain DNA sequences, 10 μl of a standard plasmid preparation were submitted to the company ElimBio Biopharmaceuticals Inc. (Hayward, CA, USA). To

sequence the entire *mm-cpn*-gene we used the primers T7-fw and T7-rev, provided by the company, as well as the primer Mm-Cpn-midfw.

II.7. Electrophoresis

Electrophoresis of DNA

Separation of DNA fragments was performed using horizontal 1% agarose gels in TAE-buffer⁹⁵.

Denaturing and native polyacrylamide gel electrophoresis (PAGE)

In order to separate proteins under denaturing conditions discontinuous polyacrylamide gel electrophoresis was applied⁹⁶. Protein solutions were mixed with SDS sample buffer⁹⁵, heated for 5 min at 95°C, and loaded on the gel. Fixation and detection of separated protein was achieved by Coomassie staining of the gel. To this end, the gel was incubated for 5 min in a staining solution (0.1% Coomassie-G, 50% Methanol, 10% acetic acid), followed by incubation in de-staining solution (10% acetic acid).

To analyze chaperonin and chaperonin-substrate complexes under native conditions, MOPS-based native gel electrophoresis was performed as described⁴⁸. To this end, 4% acrylamide gels were prepared in MOPS buffer (80 mM MOPS [pH 7.0], 5 mM MgCl₂, 50 mM KCl). Samples, in reaction buffer containing 10 % glycerol, were supplemented with 1 µl 1 % bromphenolblue solution, and directly loaded on the gel. Gels were run at 4°C in MOPS buffer containing 0.1% L-cysteine and 1 mM DTT for 2 hours at 120 V. Detection of protein was achieved by Coomassie staining and autoradiography.

II.8. Protein Purification

Purification of TRiC

TRiC was purified from bovine testis essentially as described⁸⁷. In brief, the tubules of bovine testis (500 g) separated from the tunica albuginea by dissection were homogenized in buffer H (20 mM HEPES/KOH [pH 7.4], 5 mM MgCl₂, 0.1 mM EDTA, 50 mM NaCl, 1 mM DTT) containing the protease inhibitors leupeptine (2 µg/ml), aprotinin (0.5 µg/ml), pepstatin (0.5 µg/ml) and PMSF (0.2 mM), and the lysate was clarified by centrifugation for 30 min at 20 000 g followed by a 1 hr centrifugation step at 100,000 g. The lysate was subjected to a 35% ammonium

sulfate cut, and the resulting supernatant was precipitated with a final concentration of 50% ammonium sulfate. The pellet was resuspended in a small volume MQ-A buffer (20 mM HEPES/KOH [pH 7.4], 5 mM MgCl₂, 0.1 mM EDTA, 50 mM NaCl, 10% glycerol, 1 mM DTT) and 30 ml aliquots, respectively, were loaded on sucrose cushions (lower layer: 2 ml 60% sucrose in MQ-A buffer; upper layer 5 ml 20% sucrose in MQ-A buffer). After 20 hr ultracentrifugation in a SW-28 rotor at 26 000 rpm and 4°C, the sucrose cushions together with all sedimented material were pooled, dialyzed against MQ-A buffer, and loaded on a Q Sepharose FF column (60 ml, GE Healthcare, USA) equilibrated in MQ-A buffer. Bound proteins were eluted with 0.4 M NaCl in MQ-A buffer. Fractions containing protein were pooled and diluted 1:1 in MQ-A buffer before they were loaded on a High-Trap Heparin column (20 ml, GE Healthcare, USA) equilibrated in MQ-A buffer containing 0.2 M NaCl. Bound proteins were eluted by a NaCl gradient ranging from 0.2 to 1 M NaCl. Fractions containing TRiC were pooled, concentrated using an Amicon Ultra-15 10K concentrator (Millipore Corporation, USA), and loaded on a Superose 6 10/300 GL column (GE Healthcare, USA). Fractions containing the oligomeric chaperonin were pooled, and aliquots were flash-frozen in liquid nitrogen.

Purification Mm-Cpn wild type and mutant forms

Purification of Mm-Cpn^{WT}, Mm-Cpn^{Δlid}, Mm-Cpn^{D386A} and Mm-Cpn^{Δlid/D386A} was achieved using the following procedure: chaperonin proteins were overproduced in *E. coli* strain Rosetta (DE3) pLysS (EMD Biosciences, USA) harboring plasmid pET21MmCpnWT, pET21MmcpnΔlid, pET21aMmCpnD386A, or pET21MmcpnΔlid/D386A respectively. The cells were harvested by centrifugation, resuspended in MQ-A buffer (20 mM HEPES/KOH [pH 7.4], 50 mM KCl, 5 mM MgCl₂, 0.1 mM EDTA, 10% glycerol, 1 mM DTT, 0.1 mM PMSF) and disrupted using a French Press at a pressure of 16,000 psi. The lysate was centrifuged at 15 000 g for 30 min to pellet cell debris. The supernatant of a 55% ammonium sulfate cut was dialyzed against MQ-A buffer and loaded on a Q Sepharose FF column (60 ml, GE Healthcare, USA) equilibrated in MQ-A buffer. Bound proteins were eluted by a NaCl gradient ranging from 0–1 M NaCl. Fractions containing Mm-Cpn were pooled and diluted 1:1 in MQ-A buffer before they were loaded on a High-Trap Heparin column (20 ml, GE Healthcare, USA) equilibrated in MQ-A buffer containing 0.2 M NaCl. Bound proteins were eluted by a NaCl gradient ranging from 0.2 to 1 M NaCl.

Fractions containing Mm-Cpn were pooled, concentrated using an Amicon Ultra-15 10K concentrator (Millipore Corporation, USA), and loaded on a Superose 6 10/300 GL column (GE Healthcare, USA). Fractions containing the oligomeric chaperonin were pooled, and aliquots were flash-frozen in liquid nitrogen. The protein concentration was determined using the BCA-Assay (Pierce, USA) with BSA as a standard.

Purification of rhodanese

Bovine rhodanese (type II highly purified) was purchased from Sigma-Aldrich (USA) and further purified as described⁹⁷. To this end, the lyophilized protein was dissolved in buffer A (50 mM Na-acetate pH 5.0, 20 mM Na-thiosulfate) at a concentration of 10 mg/ml and loaded onto a Mono-S HR 5/5 column (GE Healthcare, USA) equilibrated in buffer A. Bound proteins were eluted by a salt gradient from 0-500 mM NaCl in buffer A. Fractions containing rhodanese were pooled and concentrated using Amicon Ultra-15 10K concentrator (Millipore Corporation, USA) and loaded on a Superdex 75 HR 10/30 column (GE Healthcare, USA) equilibrated in buffer A. Fractions containing rhodanese were pooled and concentrated as before. The protein concentration was determined spectroscopically ($\epsilon_{280}=60890 \text{ M}^{-1}/\text{cm}$).

[³⁵S]-labeled bovine rhodanese was purified from inclusion bodies after heterologous overexpression of the protein in *E. coli* strain Rosetta (DE3) pLysS (EMD Biosciences, USA) harboring the plasmid pBROD⁹². The cells were lysed in 1 ml lysis buffer (10 mM HEPES [pH 7.5], 50 mM Tris/HCl [pH 8], 10 mM MgCl₂, 100 mM KCl, 10 % glycerol, 0.1 % Triton X-100, 1 mM DTT and 0.2 mM PMSF) by three freeze-thawing cycles in liquid nitrogen. Inclusion bodies were sedimented by centrifugation for 30 min at 16,000 g, washed in lysis buffer and subsequently solubilized in 1 ml 8 M urea/ 50 mM Na-acetate (pH 5.0). After addition of 100 μ l of a 1:1 slurry of SP-Sepharose (GE Healthcare) in 6 M urea/ 50 mM Na-acetate (pH 5.0) and incubation for 15 min at 4°C, the mixture was transferred into a 1 ml empty gravity column and washed with 2 x 200 μ l of 6 M urea/50 mM Na-acetate (pH 5) containing 100 mM, 500 mM and 1M NaCl, respectively. [³⁵S]- labeled rhodanese, eluting in the fractions containing 500 mM NaCl, was concentrated using a Amicon Ultra-0.5 10K concentrator (Millipore Corporation, USA) and subjected to a buffer change into 6 M urea/ 50 mM Na-acetate (pH 5) and 1 mM DTT using a P(30) spin

column (BioRad). The protein concentration was determined spectroscopically ($\epsilon_{280}=60890 \text{ M}^{-1}/\text{cm}$).

Purification of [^{35}S]-labeled actin

[^{35}S]-labeled actin was purified from HELA cells essentially as described⁴⁸. 4 x 150 mm plates to 40 % confluence and labeled overnight in medium lacking methionine using 30 μCi ^{35}S -methionine per plate. The cells were washed in ice-cold PBS, harvested in 2 ml cold PBS/ plate, sedimented by centrifugation at 4°C for 10 min at 1000 g, washed in PBS, and resuspended in a total of 1.5 – 3 ml G_{10} buffer (10 mM Tris/HCl [pH 7.4], 1 mM CaCl_2 , 10 % formamide, 1 mM DTT, 1 mM ATP) supplemented with 1 mM PMSF and protease inhibitor cocktail.

Cells were lysed by 50 douncing cycles and the cell debris was removed by centrifugation at 4°C for 20 min at 14,000 g. The supernatant was loaded on a column containing 0.5 ml bed volumes of DNase I covalently attached to Sepharose 4B (GE Healthcare) equilibrated in buffer G_{10} -buffer supplemented with 10 % glycerol (G_{10} '-buffer). The lysate was incubated with the DNaseI-sepharose beads for 1 h at 4°C while gently shaking. Subsequently unbound proteins were removed by two 1 ml washes G_{10} '-buffer, followed by a 0.5 ml wash in G_{10} '-buffer supplemented with 0.4 M KCl and two further 0.5 ml washes in buffer G_{10} '-buffer. To obtain native [^{35}S]-labeled actin, 0.5 ml of G_{40} '-buffer (as G_{10} '-buffer but 40 % formamide) were added to the column and the eluate was collected after a 5 min incubation at 4°C. After 1:10 dilution in G_{10} -buffer, the native [^{35}S]-actin was concentrated to a final volume of 100 μl , supplemented with 0.002 % NaN_3 , and stored at 4°C. The majority of the DNase I-bound [^{35}S]-actin was recovered as denatured protein following incubation of the beads with 1 ml of 6 M guanidinium/ HCl for 1 h at 4°C. The column was subjected to a low speed centrifugation step in order to recover the sample quantitatively. Denatured [^{35}S]-actin was flash-frozen in liquid nitrogen and stored at -80°C.

II.9. Biochemical Methods

Determination of protein concentrations

The GroEL concentration was determined spectrometrically by measuring the absorption at 280 nm (Gill and Hippel, 1989). The protein concentration of TRiC was determined by the BCA Assay (Pierce, IL, USA), using BSA (Pierce) as a standard.

By submission of a TRiC sample of known concentration (by BCA Assay) to Amino Acid Sequencing facility of the Molecular Structure Facility (UC Davis, CA, USA) we obtained a correction factor to determine the actual protein concentration.

Isolation of Mm-Cpn-substrate complexes

To isolate Mm-Cpn-substrate complexes, we prepared lysates from anaerobically grown *M. maripaludis* cells. Cells were lysed by incubation of 5 g frozen cell pellet in 4 ml Mm-Cpn lysis buffer (25 mM PIPES [pH 6.8], 1 mM DTT, 5 mM PMSF) by an 30 min incubation at 30°C in the presence of 50 µg/ml DNaseI. Lysates were clarified by 20 min centrifugation at 13 000 g and 4 °C followed by a 1 hr ultracentrifugation step (100 000 g) at 4°C. *M. maripaludis* lysates were supplemented with 20 mg/ml BSA, 5 mM EDTA, and 6 µl of affinity-purified anti-Mm-Cpn antibodies, and then incubated on ice for 40 minutes. The samples were centrifuged at 16 000g for 15 min to remove protein aggregates and 10 µl 1:1 slurry of Protein G Sepharose in TBS were added. The assays were gently rotated for 30 min at 4°C. Sepharose beads were sedimented by low speed centrifugation and washed twice with TBS + 0.05%Tween and then three times with TBS + 1% Tween, as described ⁴⁷. Samples were resuspended in SDS-sample buffer, and proteins were separated by 12% SDS-PAGE gel electrophoresis and detected by Coomassie staining. Protein bands of interest were excised from the gel and submitted to mass spectrometric analysis by the SU Mass Spectrometry facility (Stanford, CA, USA). In an alternative approach, proteins from a *M. maripaludis* lysate, prepared as described above, were denatured by addition of solid Guanidin/ HCl to a final concentration of 6 M and incubation at 30 °C for 1 hr. Aggregated proteins were removed by centrifugation at 4°C at 16 000 g for 30 min. The lysate in 6 M Guanidin/ HCL was diluted 1:100 into a reaction mix containing 0.25 µM purified Mm-Cpn protein in MQ-A buffer and incubated for 30 min at 30°C. Potential Mm-Cpn-substrate complexes were isolated by size exclusion chromatography on a Superose 6 10/300 GL column (GE Healthcare, USA). Fractions containing the oligomeric chaperonin were pooled and analyzed by 12% SDS-PAGE.

Generation of cTRiC

cTRiC was generated essentially as described⁷². Briefly, 0.25 µM purified TRiC protein was pre-incubated in TRiC-ATPase buffer I (50 mM Tris/HCl [pH 7.4], 50 mM KCl, 5 mM MgCl₂, 1 mM EGTA) for 5 min at 25°C. After addition of 20 µg/ ml

Proteinase K and further incubation for 10 min at 25°C, protease activity was inhibited by supplementing the reaction with PMSF to a final concentration of 5 mM. After incubation on ice for approximately 10 min, the quantitative conversion of TRiC to cTRiC was confirmed by SDS-PAGE analysis. Reactions containing cTRiC were kept on ice for maximally 2 hours before they were used for further biochemical analysis.

Proteinase K protection assay

0.25 μ M purified TRiC or 0.25 μ M purified Mm-Cpn^{WT} or Mm-CpnD^{386A}, respectively, were pre-incubated in the respective ATPase buffer (Cpn-buffer: 20 mM Tris/ HCl [pH 7.5], 100 mM KCl, 5 mM MgCl₂, 10 % glycerol), which was supplemented with EDTA (5 mM), ADP (1 mM), or ATP (0.2 or 1 mM). To generate AlF_x, Al(NO₃)₃ (5 mM) and NaF (30 mM) were included in the reaction. The reactions were incubated for 10 min (30 min for reactions containing AlF_x) at 30°C for Mm-Cpn and 25°C for TRiC. After addition of 20 μ g/ ml proteinase K and further incubation for 10 min at 25°C, PMSF was supplemented to a final concentration of 5 mM to inhibit protease activity. Subsequently the reaction was incubated on ice for 10 min and analyzed by SDS-PAGE. For N-terminal sequencing, the protein fragments were transferred on a PVDF-membrane and visualized by amido-black stain. The protein bands were cut from the membrane and submitted to the Stanford PAN facility.

Rhodanese folding assay

Rhodanese folding by Mm-Cpn^{WT} and Mm-Cpn ^{Δ lid} was assayed as described⁹⁷. In brief, 0.25 μ M protein was incubated in Cpn-buffer supplemented with 20 mM sodium thiosulfate. Purified rhodanese was denatured in 6 M guanidinium/HCl containing 5 mM DTT and rapidly diluted 1:100 to a final concentration of 30 μ M into the reaction mix. After incubation for 5 min at 37°C, the reaction was started by addition of 2 mM ATP and allowed to proceed for 50 min at 37°C. In order to detect the presence of re-folded rhodanese, 10 μ l of the reaction were withdrawn and applied to a rhodanese activity assay performed as described⁹⁷.

Actin folding assays

The standard actin-folding assay was carried out as described⁴⁸. In brief, 0.25 μM TRiC or cTRiC, respectively, were incubated in buffer A (20 mM Hepes-KOH [pH 7.5], 100 mM potassium acetate, 5 mM MgCl_2 , 1 mM DTT, 10 % glycerol, and 1% PEG 8000). Subsequently, [³⁵S]-actin denatured in 6 M guanidin/ HCl⁴⁸ was rapidly diluted 1:100 to a final concentration of 30 μM into the reaction mix. After incubation for 10 min at 4°C, the assay was supplemented with 1 mM ATP and incubated for 40 minutes at 30°C. Generation of native [³⁵S]-actin was determined by native gel electrophoresis using folded [³⁵S]-actin as a control as described previously⁴⁸. The gel was exposed on a phosphor storage screen (Kodak, USA), which was scanned in a Typhoon 9410 imager (GE Healthcare, USA). The radioactive signal was quantified using Image Quant 5.2 (Molecular Dynamics). The amount of actin migrating with native mobility is expressed as percent of total radioactivity per lane.

To determine actin-folding rates at different ATP concentrations, generation of native [³⁵S]-actin was determined by a protease protection assay as described⁷². To this end, TRiC and actin were incubated as described above. After addition of 5 mM EDTA, 0.2 mM ATP, and 1 mM ATP, respectively, samples were withdrawn at the indicated time points and the folding reaction was stopped by incubation on ice and supplementation of the reactions with 10 mM CDTA. Subsequently, the samples were incubated with 20 $\mu\text{g/ml}$ Proteinase K for exactly 5 min at 25°C, before protease activity was inhibited by adding PMSF to a final concentration of 5 mM. After incubation on ice for 10 min, the samples were analyzed by SDS-PAGE. The gel was exposed on a phosphor storage screen (Kodak, USA), which was scanned in a Typhoon 9410 imager (GE Healthcare, USA). The radioactive signal corresponding to native actin⁷² was quantified using Image Quant 5.2 (Molecular Dynamics).

Rhodanese binding assay

0.25 μM Mm-Cpn^{WT} and Mm-Cpn^{Alid}, respectively, were incubated in Cpn-buffer. Purified [³⁵S]-rhodanese, denatured in 6 M urea⁹⁴ was rapidly diluted 1:100 to a final concentration of 26 μM into the assay. After incubation for 15 min at 4°C, chaperonin-bound rhodanese was detected by native gel electrophoresis as described for TRiC⁴⁸. The migration behavior of the chaperonin proteins was analyzed by Coomassie staining of the gel. To visualize co-migration of [³⁵S]-rhodanese, the gel

was exposed on a phosphor storage screen (Kodak, USA), which was scanned in a Typhoon 9410 imager (GE Healthcare, USA).

Preparation of EL-trap

The GroEL-trap was prepared essentially as described⁹⁸. 0.4 μM purified GroEL protein was incubated in a buffer composed of 25 mM MOPS pH [7.2], 75 mM KCl, 5 mM MgCl_2 , 1 mM DTT with 1.5% glutaraldehyde at 25°C for 45 min. The reaction was applied to a P(30) gel-filtration spin-column (Bio-Rad, Hercules, CA, USA) equilibrated in buffer A in order to achieve buffer exchange. Aliquots of the resulting EL-trap were frozen in liquid nitrogen.

ATPase assay

ATP hydrolysis by wild-type chaperonins and chaperonin variants was measured at 25 °C for TRiC and cTRiC and at 37°C for Mm-Cpn^{WT}, Mm-Cpn^{Alid}, and Mm-Cpn^{D386A} in the respective ATPase buffer in the presence of 1 – 1000 μM α - [³²P]-ATP. After 5 minutes of pre-incubation, the reaction was started by mixing 5 μl of α - [³²P]-ATP (0.01 $\mu\text{Ci}/\mu\text{l}$) solution with 20 μl of 1.25-fold concentrated reaction mix. At the indicated time points, 2 μl samples were taken and transferred onto PEI-cellulose F TLC plastic sheets (EMD Chemicals Inc.). The plates were developed in a solvent system containing 1 M LiCl and 0.5 M formic acid in H₂O, air-dried, and exposed to a phosphor screen (Kodak). After scanning the screen in a Typhoon 9410 imager, the amount of α - [³²P]-ADP was quantified using Image Quant 5.2.

ATPase assays of TRiC in the presence of denatured actin were performed in the same way with the following modification: to generate TRiC-actin complexes, 300 μM actin (Sigma) denatured either in 6M guanidin/HCl or 8 M urea was diluted 1:100 to a reaction mix containing 0.25 μM purified TRiC. After 15 min incubation at 4°C, samples were shifted to 30°C and the ATPase reaction was started as described above. Additionally, 10 μl of the reaction mix was analyzed by 12 % SDS-PAGE.

Cross-link of α -[³²P]-8-N₃-ATP to TRiC and separation of subunits by RP-HPLC

To generate TRiC 8-N₃-ATP complexes, 2 μM TRiC in buffer A (50 mM Tris-HCl [pH 7.4], 50 mM KCl, 10 mM MgCl_2 , 10% glycerol) were pre-incubated with 10 μM α -[³²P]-8N₃-ATP (8 mCi/ μmol) or 0.2, 0.5, 1 and 2 mM α -[³²P]-8-N₃-ATP (0.8 mCi/ μmol), respectively. To trap TRiC in the closed conformation, the transition state

analog ADP-AlF_x was generated by supplementing the reaction with 1 mM α -[³²P]-8-N₃-ATP (8 mCi/ μ mol), 5 mM Al(NO₃)₃, 30 mM NaF, 10 mM MgCl₂ and incubation at 25°C for 30 min. Since the α -[³²P]-8-N₃-ATP was dissolved in methanol, the required volume was initially pipetted on parafilm and allowed to evaporate for 20 min at 25°C before it was resuspended in the TRiC-buffer mix. Activation of the azido group was achieved by exposing the reaction mix to UV light from a hand-held UVGL-25 lamp (UVP Inc., USA) on the short wavelength setting for 2 min from a distance of 1 inch with the sample placed on chilled parafilm. Subsequently, the activated azido group was quenched with 10 mM DTT for 10 min on ice and the free α -[³²P]-8-N₃-ATP was separated from the cross-linked fraction using a P (30) gel filtration spin column (Bio-Rad, Hercules, CA, USA) equilibrated in buffer A. To separate the eight different TRiC subunits, TFA was added to a final concentration of 0.1%, and the sample was loaded on a RP-HPLC C4-column (214TP54, Grace Vydac, USA). TRiC subunits elute at 50 % to 60% acetonitril/ 0.1% TFA as described⁸⁶. Elution of the TRiC subunits was monitored by measuring the absorption at 214 nm, and collected fractions were subjected to scintillation counting in order to detect co-eluting α -[³²P]-labeled nucleotides.

Filter binding assays

0.25 μ M TRiC or 0.25 μ M GroEL in the presence of 0.5 μ M GroES, were pre-incubated in buffer A in the presence of 1 mM DTT and 1 mM α -[³²P]-ATP (0.1 μ Ci/ μ mol) for 5 min at 30°C in case of TRiC and 37°C in case of GroEL/ES. Subsequently, 10 μ l of the reaction mix were applied to a protran-nitrocellulose membrane (Schleicher & Schuell, USA) placed on a vacuum system. After two brief washes with 1 ml of chilled buffer A supplemented with 1 mM DTT, the filter was dried at room temperature and subjected to scintillation counting. This filter-binding procedure was repeated four times for each reaction and the average number was calculated.

DNaseI pull-down of native actin

Selective pull-down of native actin using DNaseI covalently attached to beads was performed as described by Thulasiraman *et al.*, (2000)⁹⁹ with some minor modifications. Highly purified DNase I was covalently attached to cyanogen-bromide-activated Sepharose 4B (GE-Healthcare, USA) as described⁹⁹. Yeast lysates

from puls-chase experiments were diluted into buffer G10' (20 mM Tris/HCl [pH7.4], 2 mM CaCl₂, 1mM DTT, 10 % glycerol, 10 % formamide, and 0.2 mM ATP), and aggregated proteins were removed by centrifugation at 16,000 g for 30 min at 4°C. After addition of a 1:1 slurry of DNase I sepharose equilibrated in buffer G10' the samples were rotated at 4°C for 30 min. Subsequently, the DNaseI-coupled beads were sedimented by low-speed centrifugation and washed two times in buffer G10' followed by one wash in buffer G10', containing 40% formamide and two more washes in buffer G10'. The beads were resuspended in SDS-sample buffer and heated for 5 min at 95°C. The supernatant of a subsequent low-speed centrifugation was loaded on a 15% SDS-PAGE gel, which was exposed on a phosphor storage screen (Kodak, USA).

TRiC Immunoprecipitation

Yeast lysates from the puls-chase experiment were supplemented with 20 mg/ml BSA and 2 µl of anti-CCT polyclonal antibody and incubated on ice for 40 minutes. The reactions were further clarified to remove protein aggregates before addition of 10 µl of a 1:1 slurry of Protein G Sepharose in TBS. The reactions were rotated for 30 minutes at 4°C. Sepharose beads were sedimented by low-speed centrifugation and washed twice with TBS + 0.05% Tween and then three times with TBS + 1% Tween. Proteins were eluted from the beads by incubation with SDS-sample buffer, separated by 12% SDS-PAGE gel, and detected on a phosphor storage screen (Kodak, USA), which was scanned in a Typhoon 9410 imager (GE Healthcare, USA).

Sample preparation for cryo-electron microscopy

Chaperonin samples were prepared in Cpn-buffer without the addition of glycerol for Mm-Cpn and in buffer A without glycerol and PEG 8000 for TRiC/CCT. Samples were embedded in vitreous ice as follows: 3 µl of TRiC and cTRiC sample, respectively, were placed onto a washed, glow-discharged 200 mesh R2-1 Quantifoil continuous carbon grid (Quantifoil Micro Tools GmbH, Jena Germany). The grid was blotted and flash-frozen in liquid ethane using a Vitrobot (FEI, USA). Grids were stored in liquid nitrogen until imaging.

II.10. Bioinformatical Methods

Image analysis

SDS-PAGE gels were scanned in a regular document scanner at a resolution of 200 dpi and further analyzed using the program Photoshop 7.0 (Adobe Systems, San Jose, USA).

Molecular modeling

The homology model for Mm-Cpn was obtained by submitting the protein sequence to the SWISS-Model server¹⁰⁰ (<http://www.swissmodel.expasy.org>). The figures were prepared using MacPyMOL (<http://www.pymol.org>).

Analysis of autoradiograms

Phosphor storage screens (Kodak, USA) were scanned in a Typhoon 9410 imager (GE Healthcare, USA). The radioactive signals were quantified using Image Quant 5.2 (Molecular Dynamics).

Analysis of mathematical data

Analysis of the allosteric properties of TRiC, cTRiC, Mm-Cpn^{WT} and MmCpn^{Alid} with respect to ATP was performed by directly fitting the data points to equation (1) or (2) as indicated in the corresponding figure legends using Kaleidagraph Version 4.0 (Synergy Software).

$$(1) \quad v_0 = (v_{\max(1)} + v_{\max(2)} ([S]/K_2)^m) / (1 + (K_1/[S])^n + ([S]/K_2)^m)$$

v_0 is the observed initial rate of ATP hydrolysis, $[S]$ is the ATP concentration, $v_{\max(1)}$ and $v_{\max(2)}$ are the respective maximal initial rates of ATP hydrolysis by a single ring and by both rings of group II chaperonins, n and m are the Hill coefficients for the first and second allosteric transition respectively, and K_1 and K_2 are the respective apparent binding constants of ATP to the first and second ring⁸⁰.

$$(2) \quad v_0 = v_{\max} / 1 + (K_1/[S])^n$$

v_0 is the observed initial rate of ATP hydrolysis, $[S]$ is the ATP concentration, v_{\max} is the maximal initial rate of ATP hydrolysis, n is the Hill coefficient, and K_1 is the respective apparent binding constant for ATP.

To determine whether the allosteric parameters derived above using the Hill equation explained the experimental data more accurately than a simple non-allosteric

Michaelis-Menten model, the statistical significance of both fits was compared in collaboration with Dr. Charles Parnot (Stanford, CA) using an F-test, as implemented in the Prism statistical analysis package (GraphPad Software, Inc.). Briefly, for each chaperonin, the fit obtained using equation (2) with a free Hill coefficient (n) value was compared with a fit done using equation (2) but the Hill coefficient (n) value arbitrarily fixed at 1 (i.e. no allosteric regulation, Michaelis-Menten equation). This analysis indicated that the Hill equation shown in Table 1 was significantly better at explaining the experimental data than a Michaelis-Menten model (p values of 0.0004 and <0.0001 for TRiC and Mm-Cpn respectively). A similar approach was used to assess the significance of the loss of cooperativity observed upon removal of the lid segments in TRiC or Mm-Cpn. Briefly, for both TRiC and Mm-Cpn an F-test was used to compare the global fits obtained for the intact and lid-less versions of the chaperonin using either two independently fitted n values, or an identical n value for both curves. This test indicated that the loss of positive cooperativity measured in the fits is statistically significant as the experimental data are best explained by two different n values for intact and lidless versions (p values of 0.01 for TRiC vs cTRiC and 0.004 for Mm-Cpn^{WT} vs Mm-Cpn^{Δlid}).

III. RESULTS

III.1. The group II chaperonin Mm-Cpn from *M. maripaludis*

Biochemical characterization of the cytosolic chaperonin TRiC is compromised by methodological limitations, since the protein is purified from bovine tissue. Archaeal group II chaperonins like the thermosome from *T. thermolittotrophus* and the chaperonin KS-1 from *Thermococcus spec.* have proven to be useful model systems for structural analyses and both complexes have been crystallized^{34,35}. However, both chaperonins are hetero-oligomeric versions and, due to their hyperthermophilic origin they depend on high temperatures (55-60°C) for optimal enzymatic activity^{75,76}. Therefore it is complicated to reproduce physiological conditions *in vitro*.

We planned to establish the recently introduced chaperonin (Mm-Cpn) from the archaeon *Methanococcus maripaludis*¹⁰¹ as a model system to study group II chaperonins in molecular detail. Mm-Cpn consists of eight identical subunits per ring, and the protein complex can be heterologously expressed and purified in an active form from *E. coli*¹⁰¹. In contrast to TRiC, Mm-Cpn is therefore amenable for mutational analysis. Importantly, Mm-Cpn originates from a mesophilic organism, which implies optimal enzyme activity at 37°C.

Cloning, purification and initial characterization of Mm-Cpn

The *mm-cpn* gene was amplified using *M. maripaludis* genomic DNA as a template and cloned in a bacterial expression vector. After heterologous overproduction in *E. coli*, the wild-type Mm-Cpn protein (Mm-Cpn^{WT}, WT) was purified as an oligomeric complex to apparent homogeneity.

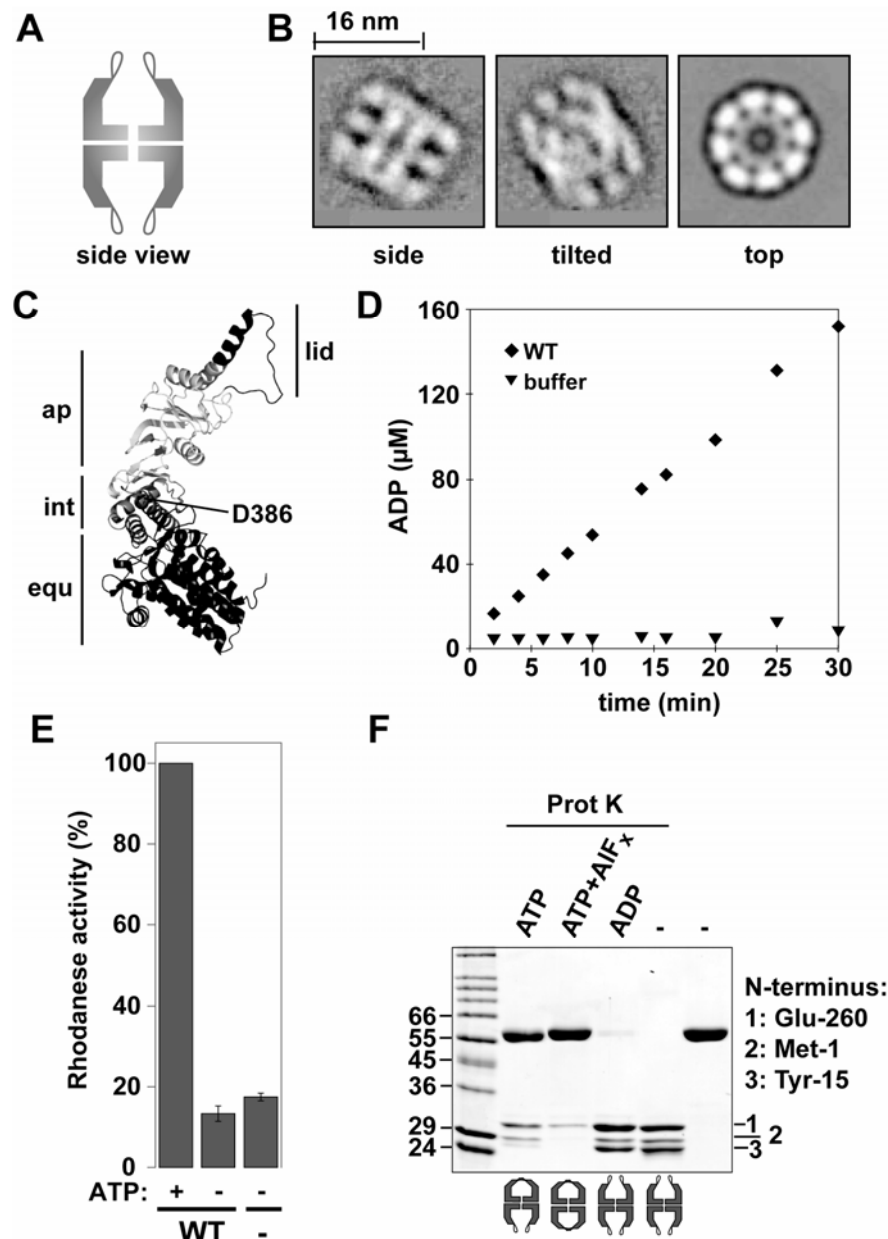


Figure 7. The archaeal group II chaperonin Mm-Cpn is purified from *E. coli* in a correctly assembled and enzymatic active form. (A) Schematic illustration of the group II chaperonin architecture. (B) Cryo-EM analysis reveals preservation of the chaperonin-like oligomeric assembly in Mm-Cpn. Three representative reference-free class averages of a side, tilted, and top view of Mm-Cpn are shown. (C) Homology model of a single subunit of Mm-Cpn. The equatorial domain (equ, black) is linked to the apical domain (ap, light grey) via the flexible intermediate domain (int, grey). The position of D386 is indicated. (D) ATP hydrolysis rate of Mm-Cpn measured at 0.5 mM α - ^{32}P -ATP. (E) Mm-Cpn is able to promote rhodanese folding in the presence of ATP. (F) Mm-Cpn closes its lid in the presence of ATP. Different conformational states in the presence or absence of nucleotides were detected by a protease sensitivity assay. N-terminal sequencing of bands 1, 2 and 3 revealed the respective site of protease cleavage.

Cryo-EM analysis confirmed the chaperonin-like oligomeric assembly of 16 subunits arranged into two stacked rings (**Fig. 1A and B**), and confirms that Mm-Cpn^{WT} displays the same eight-fold symmetry as TRiC. The homology model derived for one subunit of Mm-Cpn (**Fig. 1C**) suggests a three-domain arrangement typical for all chaperonin subunits^{30,34}. The equatorial domains (**Fig. 1C**, eq, black) provide the *inter*-ring contacts and contribute predominantly to the ATP binding pocket. The hinge-like intermediate domains (**Fig. 1C**, int, grey) cover the ATP binding pocket from the top and communicate ATP-induced conformational changes to the distal apical domain (**Fig. 1C**, ap, light grey), where the substrate binding sites are located. Protrusions (**Fig. 1C**, ap, black) extend from the very tip of the apical domains in every single subunit.

Apart of its unique structural features, Mm-Cpn exhibited enzymatic activities typically observed for chaperonin proteins. As shown in **Figure 1D** and **E** respectively, Mm-Cpn was able to hydrolyze ATP and to promote ATP-dependent folding of denatured rhodanese *in vitro*.

The search for intrinsic substrate proteins of Mm-Cpn

Rhodanese is a 33 kDa mitochondrial protein and has been used for decades as an artificial substrate protein to study GroEL activity^{94,102}. Therefore, it appears to be an appropriate substrate to investigate the basic folding cycle of Mm-Cpn. However, it would be of considerable advantage to identify native substrate proteins of Mm-Cpn and develop suitable folding assays. We have undertaken two approaches to detect Mm-Cpn-interacting proteins in *M. maripaludis* lysates prepared from an anaerobically grown culture. On one hand, we isolated potential chaperonin-substrate complexes by immunoprecipitation of endogenous Mm-Cpn using Mm-Cpn specific antibodies (**Fig. 8A**). In a second approach, we diluted *M. maripaludis* lysate prepared in 6 M guanidine/HCl into a reaction mix containing purified Mm-Cpn protein and isolated putative MmCpn-substrate complexes by gel filtration (**Fig. 8B**). Gel electrophoretic analysis of the isolated protein complexes indicated the presence of interacting proteins (**Fig. 8**). We were able to identify the 46 kDa and 50 kDa band from the co-immunoprecipitation experiment (**Fig. 8A**) by mass spectrometry. The 46 kDa band corresponds to elongation factor 1a (Mm-EIF1a) from *M. maripaludis*. EIF1a promotes the GTP-dependent binding of aminoacyl-tRNA to the A-site of the

ribosome during protein biosynthesis and would be a suitable substrate protein since proper folding could be monitored using a GTPase activity assay. The 50 kDa band corresponds to a yet uncharacterized open reading frame (ORF) named MMP0044, which is annotated as a predicted hydrolase of the metallo-beta-lactamase superfamily (COG0595)¹⁰³. Both genes were cloned in a bacterial expression vector and the proteins are subject to current analysis.

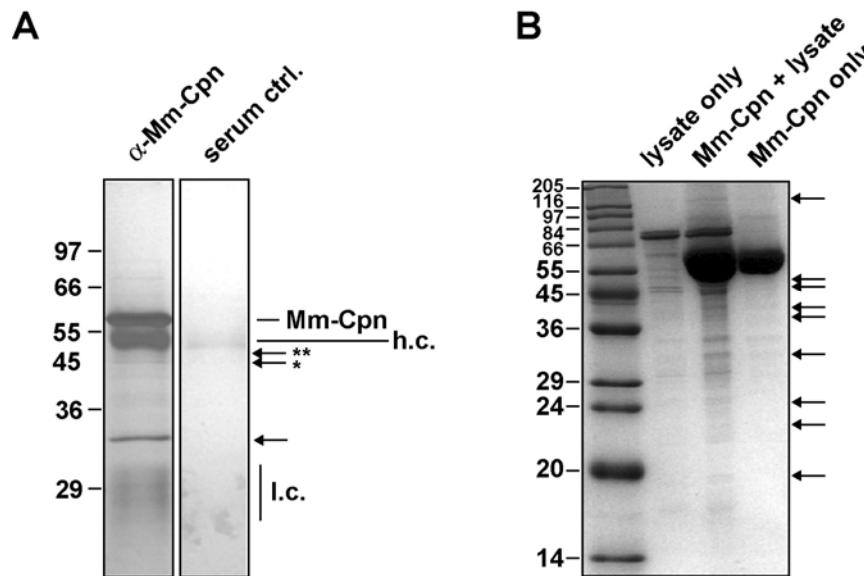


Figure 8. Isolation of Mm-Cpn-interacting proteins from *M. maripaludis* cell lysates. (A) Immunoprecipitation of endogenous Mm-Cpn allows detection of interacting proteins. Arrows indicate co-precipitated proteins. Single and double asterisks indicate the bands that were cut from the gel to determine protein identity by mass spectrometry. *46 kDa: Mm-EIF1a, **50 kDa: MMP0044 (uncharacterized *M. maripaludis* protein), L.c.= antibody light chain, H.c. = antibody heavy chain. (B) Interacting proteins from denatured *M. maripaludis* lysates co-elute with purified Mm-Cpn protein during size exclusion chromatography. Displayed is the Coomassie stain of an SDS-PAGE analysis of the high molecular weight fractions corresponding to oligomeric Mm-Cpn protein. Arrows indicate interacting proteins.

Analysis of the conformational cycle in Mm-Cpn

In order to define the nucleotide requirements for lid closure in Mm-Cpn, we exploited the differential protease susceptibility of the lid segments in the open and closed states^{72,104} (Fig. 7F). Mild proteolytic treatment of wild-type Mm-Cpn in the open, nucleotide-free state led to specific cleavage within the lid segments (Fig. 7F). N-terminal sequencing of the 30 kDa fragment revealed that the cleavage site located at the tip of the helical protrusion is analogous to the one in TRiC¹⁰⁴. The 29 kDa

fragment contains the original N-terminus whereas the third, slightly smaller fragment (24 kDa) results from the truncation of the first 15 N-terminal amino acids.

Incubation with ATP but not ADP triggers lid closure resulting in protection of the lid segments (**Fig. 7F**). Of note, incubation of Mm-Cpn with ATP and AlF_x results in a conformation whereby the apical protrusions in both rings are protected from protease digestion (**Fig. 7F**), as observed for TRiC⁷². AlF_x is thought to replace phosphate in the nucleotide-binding pocket after ATP hydrolysis has occurred. The resulting ADP- AlF_x is a transition state analog that mimics the pentagonal pyramidal state of ATP during the hydrolysis reaction^{105,106}. Although the exact nucleotide state of the symmetrically closed conformations in both Mm-Cpn and TRiC remains to be investigated, this property of group II chaperonins provides a biochemical tool to irreversibly lock the folding chambers in the folding-active state.

ATP hydrolysis is required to generate the folding-active state of Mm-Cpn

As an attempt to investigate whether ATP binding or ATP hydrolysis induces lid closure and to define the ATP-bound conformational state of Mm-Cpn in greater detail, we generated an ATPase-deficient version of Mm-Cpn. To this end, the conserved Asp-386 residue (**Fig. 7C**) was replaced by alanine, since the corresponding mutation has been shown to interfere with ATP hydrolysis in GroEL⁶⁹. This aspartate residue is located in the intermediate domain and, as apparent from the crystal structure of the thermosome³⁴, it interacts with the gamma-phosphate of bound ATP. Mm-Cpn^{D386A} (D386A) was purified as an oligomeric complex from *E. coli*. Biochemical analysis confirmed that Mm-Cpn^{D386A}, although it bound to ATP (**Fig. 9A**), was unable to hydrolyze ATP (**Fig. 9B**). Of note, Mm-Cpn^{D386A} binds two times more ATP than the wild type chaperonin as determined by the filter binding experiment displayed in **Figure 9A**. This finding awaits a more detailed analysis but it can be hypothesized that ADP generated only in the ATPase-active wild type chaperonin binds with lower affinity than ATP and can therefore not be detected in the assay applied. Mm-Cpn^{D386A} was not able to promote folding of denatured rhodanese *in vitro* (**Fig. 9C**), although it bound denatured rhodanese to the same extent as the wild-type protein (**Fig. 9C, inset**), suggesting that ATP hydrolysis is required for chaperonin activity. Analysis of the conformational state of Mm-Cpn^{D386A} in the presence and absence of ATP by the protease protection assay described above (**Fig. 1F**) revealed that ATP binding does not suffice for lid closure

(Fig. 9D) as Mm-Cpn^{D386A} is not protected from protease cleavage in any of the nucleotide states tested. Three-dimensional reconstruction of cryo-EM images obtained for Mm-Cpn^{D386A} in the presence of ATP (Fig. 9E) confirms that the chaperonin resides in the open state upon ATP binding. Accordingly, lid closure in Mm-Cpn is mediated by ATP hydrolysis, as observed for the eukaryotic chaperonin TRiC⁷² and the thermosome⁷⁵. Since Mm-Cpn^{D386A} is unable to promote rhodanese folding, we propose that the closed conformation corresponds to the folding active state in Mm-Cpn.

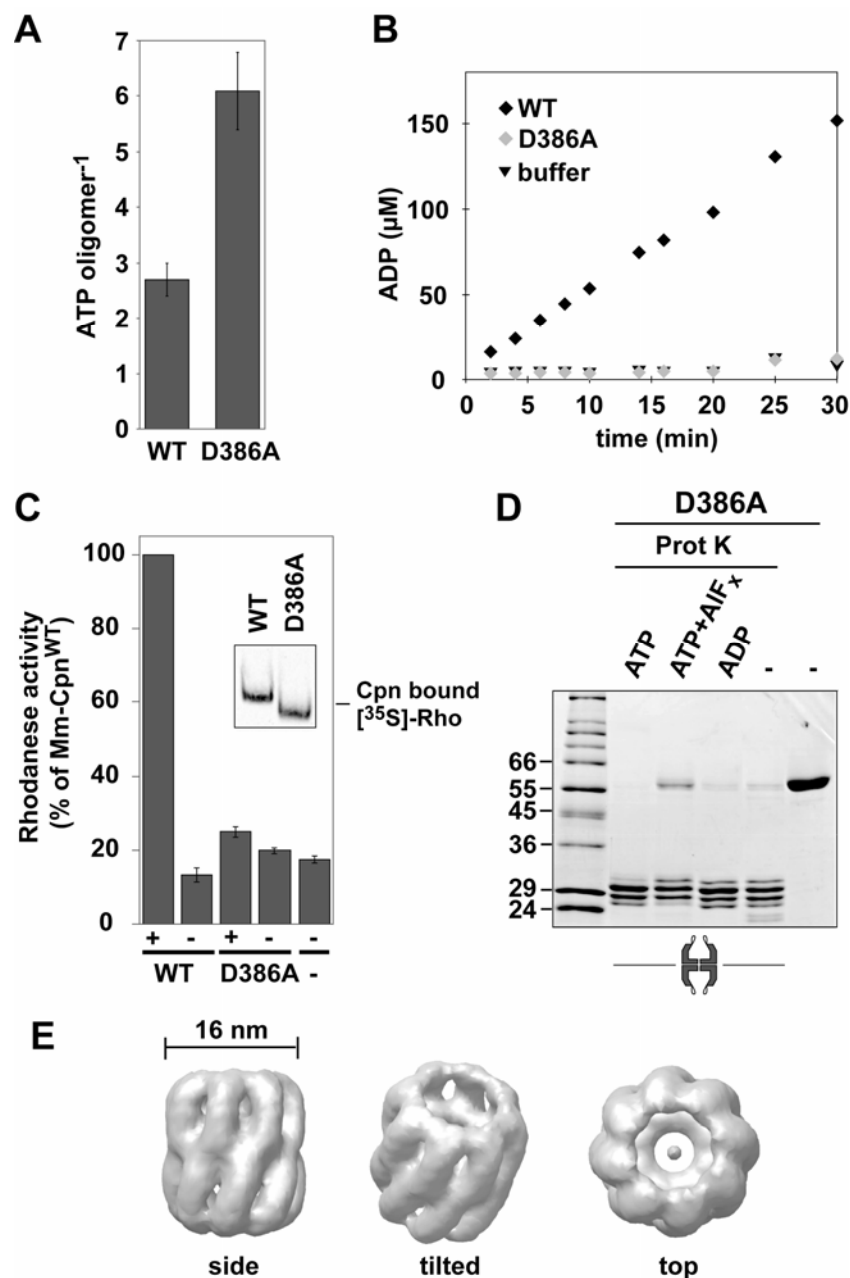


Figure 9. ATP binding to Mm-Cpn does not induce lid closure and is not sufficient to promote substrate folding. (A) The Mm-Cpn mutant version Mm-Cpn^{D386A} still binds to ATP. Binding of α -[³²P]-ATP to Mm-Cpn^{WT} and Mm-Cpn^{D386A} respectively in the presence of 2 mM ATP was detected by a filter-binding assay. (B) Mm-Cpn^{D386A} is unable to hydrolyze ATP. The ATP hydrolysis rate was measured at 0.5 mM α -[³²P]-ATP. (C) ATP binding is not sufficient to promote rhodanese folding by Mm-Cpn. Folding of denatured rhodanese was measured for Mm-Cpn^{WT} and Mm-Cpn^{D386A} in the presence and absence of ATP by a coupled enzyme assay. The inset shows an autoradiogram of [³⁵S]-rhodanese-chaperonin complexes formed in the presence of EDTA analyzed by 4 % native gel electrophoresis. (D) ATP hydrolysis but not ATP binding induces lid closure in Mm-Cpn. Conformational changes of Mm-Cpn^{D386A} upon incubation with ATP were detected by a protease sensitivity assay. Compare to Figure 1 for conformational changes in the wild type version of Mm-Cpn. (E) Three dimensional structure of Mm-Cpn^{D386A} incubated with 1 mM ATP obtained by cryo-EM.

III.2. The iris-like lid structure of group II chaperonins prevents premature release of substrate protein ejected into the central cavity.

The apical protrusions extending from every single subunit in group II chaperonins assemble into an iris-like lid structure upon ATP hydrolysis in the equatorial domain⁷². This distinct structural feature, which is exclusively found in archaeal and eukaryotic chaperonins, is absent in the bacterial chaperonin GroEL, in which this built-in lid is functionally replaced by the co-chaperonin GroES. In the GroEL-ES system, substrate proteins remain bound to the substrate binding sites upon initial association of GroES^{107,108}. Substrate release into the central cavity occurs in a conformational transition that follows immediately afterwards and is most likely accompanied by tight binding of GroES to GroEL. This sophisticated timing mechanism¹⁰⁷ ensures successful encapsulation of released substrate protein within the cavity. It seems challenging for group II chaperonins to achieve a similar type of timed substrate release without the help of an external co-factor. It was proposed that group II chaperonins might never completely release substrate protein from the substrate binding sites during the folding reaction¹⁰⁹. Based on our findings that the ATPase cycle in Mm-Cpn is very similar to the one in TRiC, the archaeal chaperonin appears to be a suitable model system to investigate molecular and mechanistic adjustments necessary to use a built-in lid. To this end, we used biochemical approaches to address the following three major questions. First: Are the apical protrusions required for chaperonin function? Second: Are substrate proteins ejected into the central cavity during the folding reaction or do they remain bound to the binding sites throughout the ATPase cycle of Mm-Cpn? And in case the substrate is released: Does the iris-like lid provide a functional barrier required to encapsulate substrate protein.

The apical protrusions are required for efficient substrate folding in Mm-Cpn

To study the role of the lid segments, we generated the mutant version Mm-Cpn^{Δlid} by replacing the apical protrusions (I241-K267) with a short linker (**Fig. 10**). As shown in **Figure 10B**, Mm-Cpn^{Δlid} hydrolyzes ATP with a rate comparable to that of the wild-type chaperonin. However, we cannot observe potential conformational changes by the protease protection assay employed for the wild-type protein (**Fig. 7F**) and the

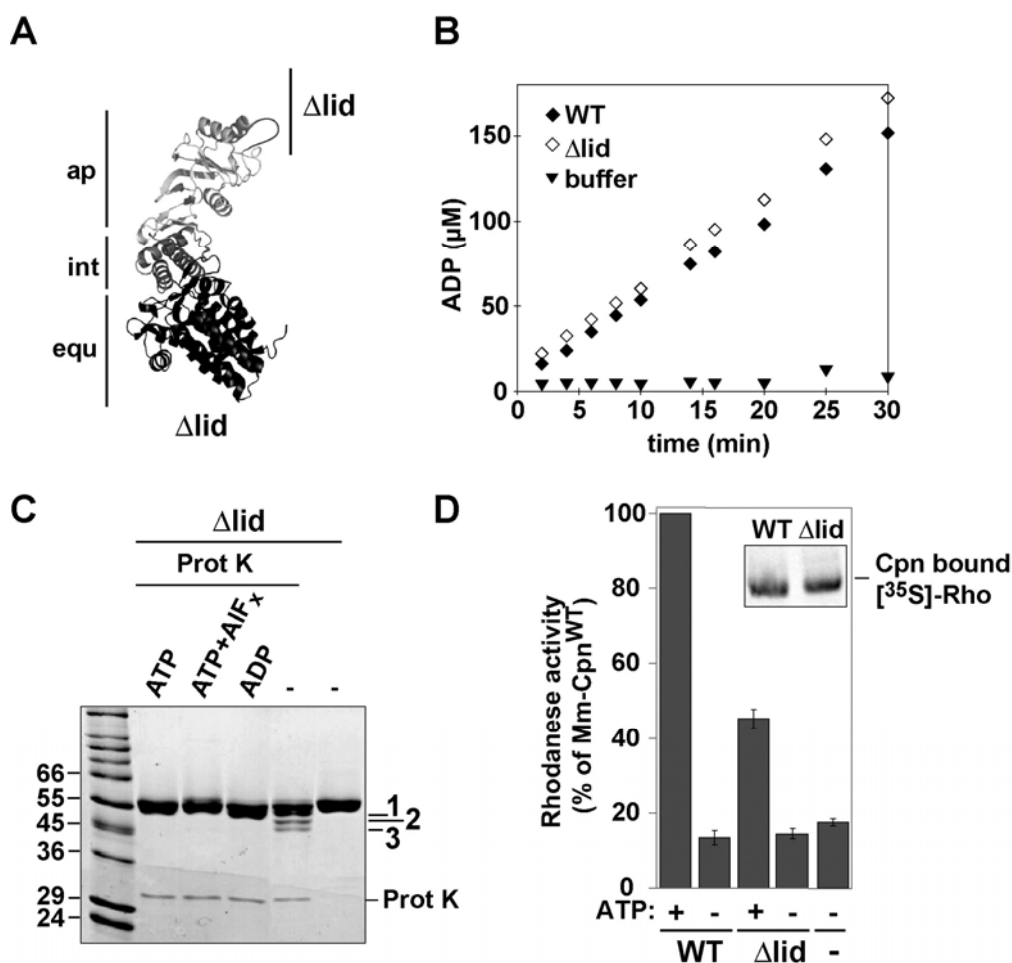


Figure 10. The built-in lid couples ATP hydrolysis to substrate folding in archaeal group II chaperonins. (A) Homology model of a single subunit of Mm-Cpn ^{Δ lid}. The equatorial domain (equ, black) is linked to the apical domain (ap, light grey) via the flexible intermediate domain (int, grey). A short linker replaces the apical protrusions. (B) Deletion of the lid structure does not affect ATPase activity in Mm-Cpn. ATP hydrolysis by Mm-Cpn ^{Δ lid} in comparison to Mm-Cpn^{WT} was measured at 0.5 mM α -[³²P]-ATP. (C) Mm-Cpn ^{Δ lid} is protected against proteolysis in agreement with deletion of the protease target sequence in the apical protrusions. The new occurring fragments between 55 and 45 kDa in the reaction of Δ lid with protease are the result of N- and C-terminal cleavage events. All three fragments (1, 2, and 3) share the same N-terminus starting with tyrosine-15 as determined by N-terminal sequencing. The 29 kDa band in the lane with Δ lid in the presence of protease corresponds to proteinase K (Prot K) (D) Mm-Cpn ^{Δ lid} cannot efficiently promote rhodanese folding in the presence of ATP. The inset shows an autoradiograph of [³⁵S]-rhodanese-chaperonin complexes formed in the presence of EDTA analyzed by 4 % native gel electrophoresis.

ATPase-deficient mutant since (**Fig. 9D**) the cleavage site is absent in Mm-Cpn^{Δlid}. Therefore, no internal digestion is observable even in the absence of nucleotide (**Fig. 10C**). Instead cleavage events occurring in the C- and N-terminal regions are unmasked in this mutant form (**Fig. 10C**). Those regions located in the equatorial domain (**Fig. 10A**) extend into the cavity and are thought to constitute the septum between the two rings^{34,35}. Intriguingly, nucleotide binding to Mm-Cpn seems to induce a conformational change in those regions, since no proteolytic fragments are detectable in the presence of ATP, ATPAlF_x, and ADP (**Fig. 10C**). N-terminal sequencing of the three 45 to 55 kDa fragments occurring in the absence of nucleotide revealed that they all contain the same N-terminal 15 amino acids, starting with methionine-1 and, therefore, differ in the length of their C-terminal regions. Interestingly, the lid-less version of Mm-Cpn, although it still binds to substrate protein (**Fig. 10D**, inset), is unable to promote rhodanese folding in the presence of ATP to the same extent as the wild-type protein (**Fig. 10D**). We therefore conclude that the apical protrusions are required for an efficient catalytic cycle in Mm-Cpn.

Mm-Cpn Δlid is unable to encapsulate substrate protein within the central cavity

A fraction of denatured rhodanese is capable to re-fold spontaneously under conditions where aggregation is minimized (e.g. high dilution)¹¹⁰. The residual 50% of folded rhodanese in the experiment described above (**Fig. 10C**) could indicate that Mm-Cpn^{Δlid} releases unfolded rhodanese in the presence of ATP to some extent and therefore supports spontaneous rhodanese re-folding. If this assumption proves to be correct it would indicate that the lid-less version of Mm-Cpn is not able to encapsulate substrate protein.

To test this possibility we performed a rhodanese binding experiment (**Fig. 11**). Wild-type and lid-less chaperonin proteins were incubated with radioactively labeled denatured rhodanese in the absence of nucleotide to achieve stable complex formation. The complex was purified by anion-exchange chromatography using a Mono-Q column (1 ml, Pharmacia) in order to remove unbound substrate protein (**Fig. 11A**). Subsequently the purified complex was incubated in the presence or absence of nucleotide, and rhodanese binding was analyzed by native gel electrophoresis (**Fig. 11B**, left panel). **Figure 11B** shows the autoradiograph of the corresponding native gel. Although Mm-Cpn^{WT} remains stably associated with [³⁵S]-

rhodanese even in the presence of ATP the rhodanese-chaperonin complex is destabilized in case of the lid-less chaperonin version.

To analyze the fraction of released rhodanese quantitatively, we included the protein GroEL-Trap (EL-trap) into the reaction (**Fig. 11B**, right panel). EL-trap is an internally cross-linked and thus inactive version of the bacterial chaperonin GroEL, generated by incubation of the purified protein with glutaraldehyde⁹⁸. It has proven to be a useful tool to distinguish natively folded substrates (e.g. rhodanese) from unfolded conformational states by irreversibly capturing exclusively denatured substrate in the reaction mix⁹⁸. Conveniently, EL-trap can be separated from Mm-Cpn by native gel electrophoresis allowing a comparative analysis of both [³⁵S]-rhodanese complexes (**Fig. 11B**, right panel). As apparent from **Figure 11B**, [³⁵S]-rhodanese is quantitatively transferred from Mm-Cpn^{Δlid} to EL-trap in the presence of nucleotide, indicating that Mm-Cpn^{Δlid} releases rhodanese in an unfolded state during the ATPase cycle. In the case of the wild-type chaperonin, only 50% of [³⁵S]-rhodanese is released as non-folded protein during the folding cycle and accessible for the EL-trap, whereas the other fraction remains associated with Mm-Cpn and is protected from EL-trap by encapsulation. It cannot be accounted for the fraction of folded rhodanese in this assay as native rhodanese does not enter the native gel under the chromatographic conditions required to analyse Mm-Cpn.

We conclude from those results that the helical protrusions of group II chaperonins assemble into an iris-like structure that indeed functions as a lid on top of the cavity and is necessary to encapsulate substrate proteins. Furthermore, it appears that rhodanese gets released from the binding sites during the ATP-induced conformational cycle of Mm-Cpn, arguing against a folding mechanism where the substrate remains associated with the binding sites during the folding cycle.

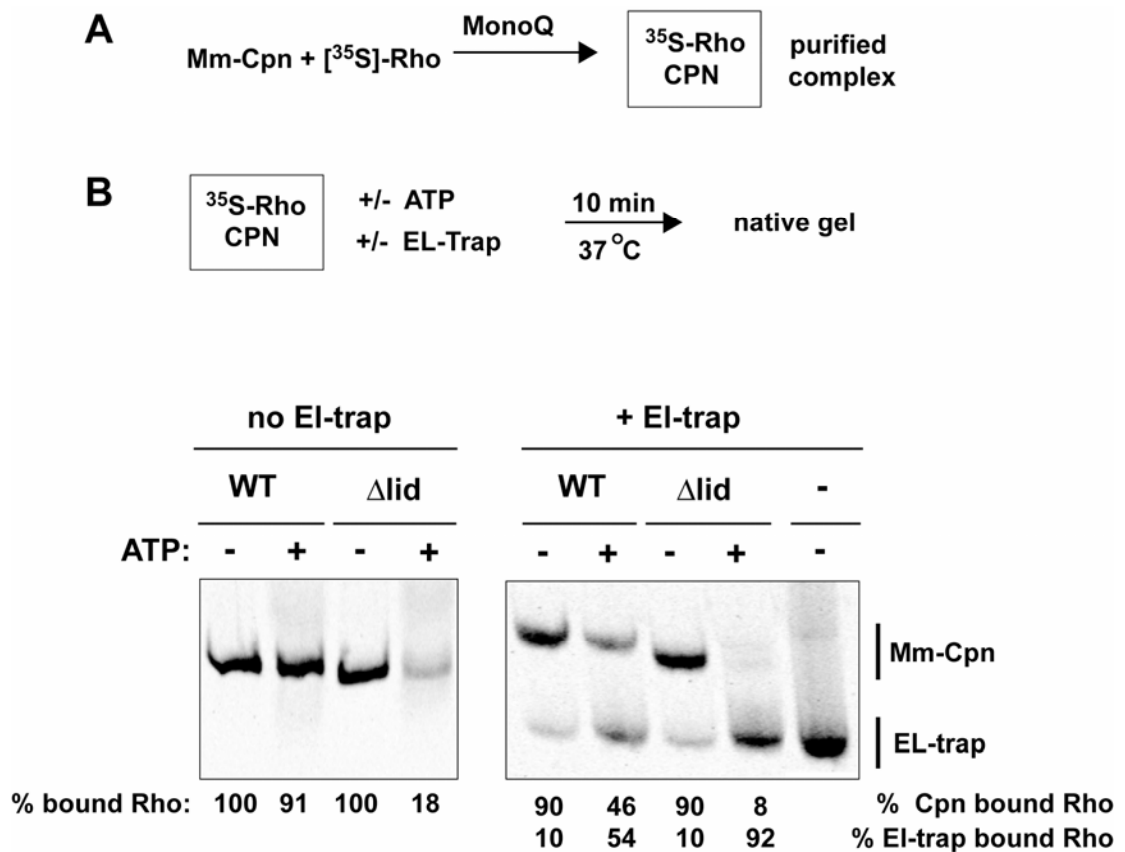


Figure 11. Mm-Cpn ^{Δ lid} is unable to encapsulate substrate protein in the central chamber. (A) To study chaperonin-rhodanese complexes at different nucleotide conditions the complex was formed and purified by anion-exchange chromatography to remove all unbound rhodanese. (B) Mm-Cpn ^{Δ lid} releases bound substrate in an unfolded conformational state upon incubation with ATP. Purified complexes of Mm-Cpn^{WT} and Mm-Cpn ^{Δ lid} respectively and [³⁵S]-rhodanese were incubated with ATP or EDTA in the absence (left panel) or presence of an inactivated GroEL version (EL-trap) that irreversibly binds to denatured substrate proteins and functions as a trap for denatured rhodanese. The reactions were analyzed by native gel electrophoresis and subsequent autoradiography.

ATP hydrolysis in Mm-Cpn results in the release of bound substrate protein

We next investigated during which step in the ATPase cycle Mm-Cpn releases substrate protein from the binding sites. To this end, we constructed a double-mutant version of Mm-Cpn, namely Mm-Cpn ^{Δ lid/D386A} (Fig. 12A), deficient in ATP hydrolysis and unable to form an iris-like lid structure. Accordingly, this mutant was not able to hydrolyze ATP (Figure 12B) and behaved like Mm-Cpn ^{Δ lid} in the protease protection assay (Fig. 12C).

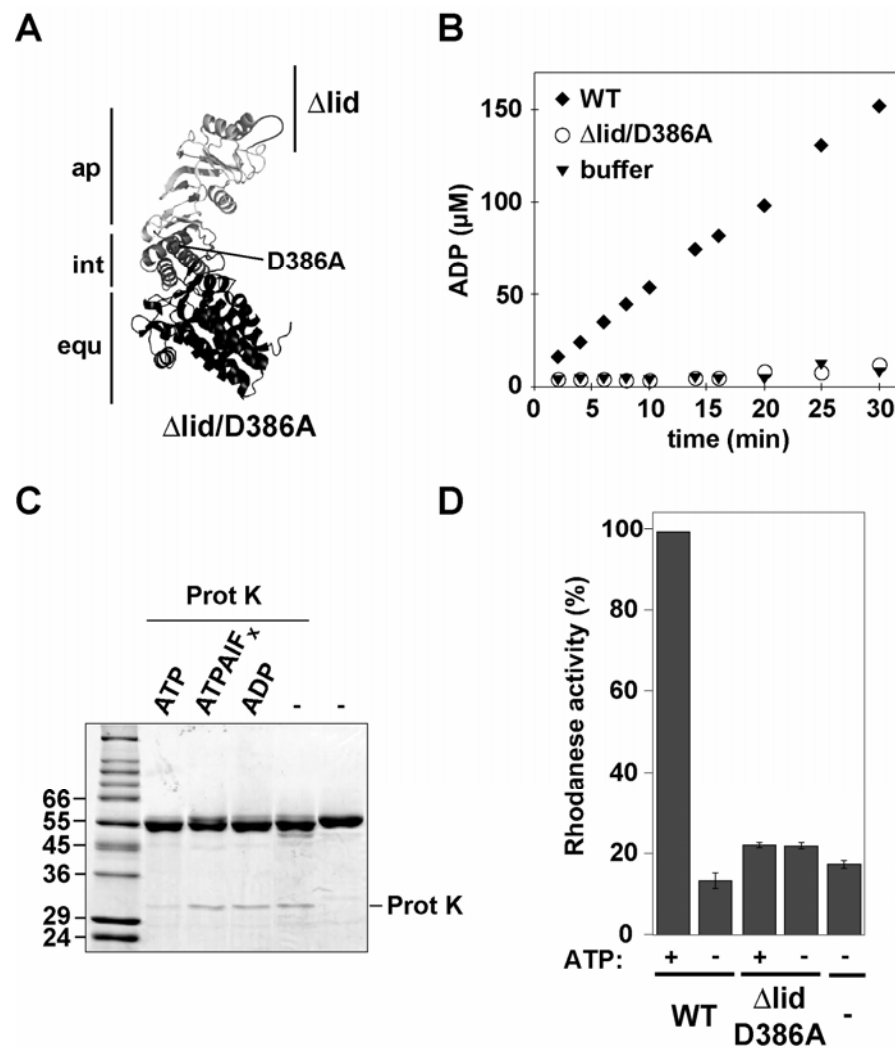


Figure 12. In the double mutant Mm-Cpn^{Δlid/D386A} the biochemical properties of both single mutant versions are combined. (A) Homology model of a single subunit of Mm-Cpn^{Δlid/D386A} (Δlid/D386A). The equatorial domain (equ, black) is linked to the apical domain (ap, light grey) via the flexible intermediate domain (int, grey). A short linker replaces the apical protrusions. Aspartate-386 is replaced by alanine. (B) The Mm-Cpn mutant version Mm-Cpn^{Δlid/D386A} is unable to hydrolyze ATP. The ATP hydrolysis rate was measured at 0.5 mM α-[³²P]-ATP. (C) Mm-Cpn^{Δlid/D386A} is protected against protease digestion comparable to Mm-Cpn^{Δlid} (Fig. 10C). The 29 kDa band in the lane with Δlid in the presence of protease corresponds to proteinase K (Prot K). (D) ATP hydrolysis by Mm-Cpn is required to promote rhodanese folding. Mm-Cpn^{Δlid/D386A} cannot catalyze refolding of denatured rhodanese *in vitro*.

Interestingly, Mm-Cpn^{Δlid/D386A} did not support folding of denatured rhodanese (Fig. 12D) indicating that the ATP hydrolysis activity is required for the residual folding activity in Mm-Cpn^{Δlid} (Fig. 10D). In agreement with this observation, Mm-

Cpn^{Δlid/D386A} did not release rhodanese upon incubation with nucleotide (**Fig. 13**, left panel). Consequently, no denatured rhodanese was captured by the GroEL-trap in levels above background (**Fig. 13**, right panel). As a control experiment, we carried out the same rhodanese binding analysis with the ATPase-deficient mutant Mm-Cpn^{D386A} (**Fig. 13**).

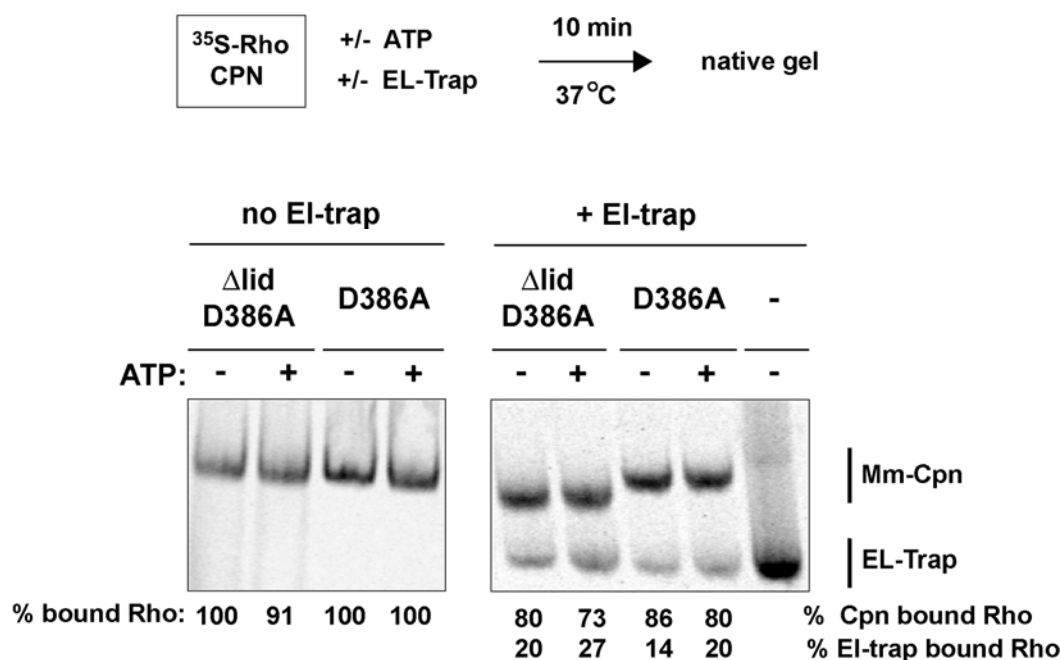


Figure 13. ATP binding to Mm-Cpn is not sufficient to trigger substrate release. The experimental setup is identical to the one described in **Figure 11** but the two mutant versions Mm-Cpn^{Δlid/D386A} and Mm-Cpn^{D386A} were analyzed. Purified complexes of Mm-Cpn^{Δlid/D386A} and Mm-Cpn^{D386A} respectively and [³⁵S]-rhodanese were incubated with ATP or EDTA in the absence (left panel) or presence of GroEL-trap (EL-trap) that irreversibly binds to denatured substrate proteins and functions as a trap for denatured rhodanese. The reactions were analyzed by native gel electrophoresis and subsequent autoradiography.

Taken together, the data strongly suggest that ATP hydrolysis presents a critical step during the ATPase cycle in group II chaperonins, resulting not only in lid closure but also in ejection of substrate protein into the central folding chamber. Of note, the corresponding conformational changes of the apical protrusions and substrate binding sites can occur independently of each other, since substrate release is still observed in the lid-less chaperonin version Mm-Cpn^{Δlid}.

Substrate binding sites are hidden in the closed conformational state induced by ATP hydrolysis

The substrate binding sites in TRiC have been mapped recently⁸⁶ and were found to locate to a position similar to that in GroEL within the groove between the two distal helices in the apical domain. It has been shown that the substrate binding sites in the double-closed conformation of TRiC⁸⁶ are not accessible from the outside.

In order to confirm those results for the wild-type chaperonin Mm-Cpn and to prove that the substrate binding sites are completely distorted in the folding-active state and neither available from the outside of the complex nor within the central chamber, we trapped MmCpn^{WT} and Mm-Cpn^{Δlid} in a conformation in which both rings are closed by incubation with ATP and AIF_x. Interestingly, the apical protrusions are not required to achieve the double-closed conformation since Mm-Cpn^{Δlid} migrates, comparable to the wild-type protein, as a more compact conformational species in a native gel upon incubation with ATP and AIF_x (**Fig. 14**, lane 2 and 5). However, in agreement with the observation that ATP hydrolysis is required for lid closure, we are not able to generate the fast-migrating species with the double mutant Mm-Cpn^{Δlid/D386A} (**Fig. 14**, lanes 3 and 6).

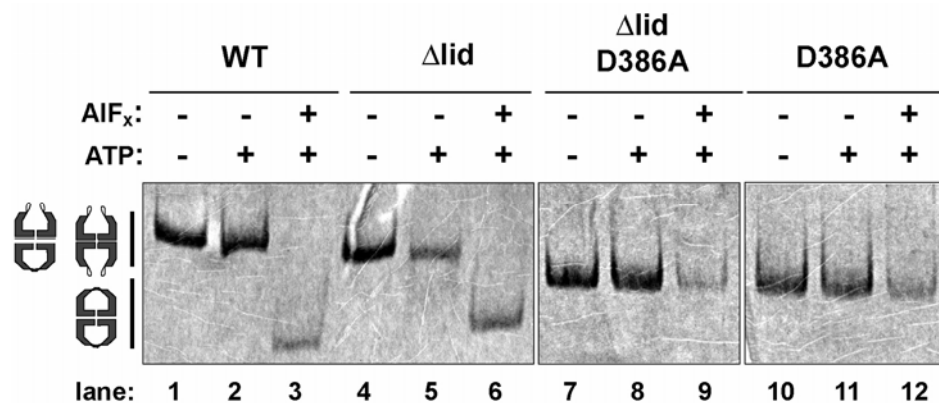


Figure 14. Mm-Cpn^{WT} and Mm-Cpn^{Δlid} but not ATPase deficient mutant versions can be trapped with ATP and AIF_x in a closed conformation that migrates faster on a non-denaturing gel. Wild-type and mutant chaperonin versions were incubated with EDTA, ATP or ATP plus AIF_x respectively and subsequently analyzed by native gel electrophoresis followed by Coomassie staining. The proposed conformational state of the differently migrating chaperonin species is indicated on the left.

To investigate the availability of the substrate binding sites in the state that mimics the folding-active conformation, we included [³⁵S]-rhodanese at two different steps

within the experimental procedure (**Fig. 15A**). First, we generated the chaperonin-substrate complex prior to addition of the nucleotide analog (**Fig. 15A**, left panel). In the second case, we first incubated with ATP and AlF_x and subsequently incubated the closed complexes with denatured [^{35}S]-rhodanese (**Fig. 15A**, right panel). In both cases, we analyzed formation of a chaperonin-rhodanese complex by native gel electrophoresis (**Fig. 15**).

Intriguingly, incubation of the Mm-Cpn-rhodanese complex with ATP and AlF_x results in co-migration of [^{35}S]-rhodanese with the fast-migrating species of Mm-Cpn^{WT} (**Fig. 15A**, lane 1). This proves that the wild-type chaperonin encapsulates rhodanese within its central cavity. However, no rhodanese is associated with the fast-migrating species of Mm-Cpn^{Alid}, although the majority of Mm-Cpn^{Alid} protein adopts the more compact double-closed conformation (**Fig. 15A**, lane 2) after incubation with ATP and AlF_x . [^{35}S]-rhodanese exclusively co-migrates with the small fraction of Mm-Cpn^{Alid} in the open, slower migrating conformation, which is hardly detectable in the Coomassie-stained gel (**Fig. 15A**, lane 2). The double mutant Mm-Cpn^{Alid/D386A} remains tightly associated with [^{35}S]-rhodanese even in the presence of ATP and AlF_x (**Fig. 15A**, lane 3), corroborating the finding that ATP hydrolysis is required for substrate release. We can thus provide further evidence that the apical protrusions indeed present a structural barrier comparable to a lid on top of the central cavity. Furthermore, as apparent from **Figure 15A** (lanes 4-6) denatured rhodanese can neither bind to wild-type chaperonin nor to the lid-less chaperonin version trapped in the double closed conformational state by incubation with ATP and AlF_x . However, rhodanese associates with Mm-Cpn^{Alid/D386A}. This observation strongly suggests that ATP hydrolysis induces a conformational change in the substrate binding sites that makes them unavailable from both the outside and the inside of the complex.

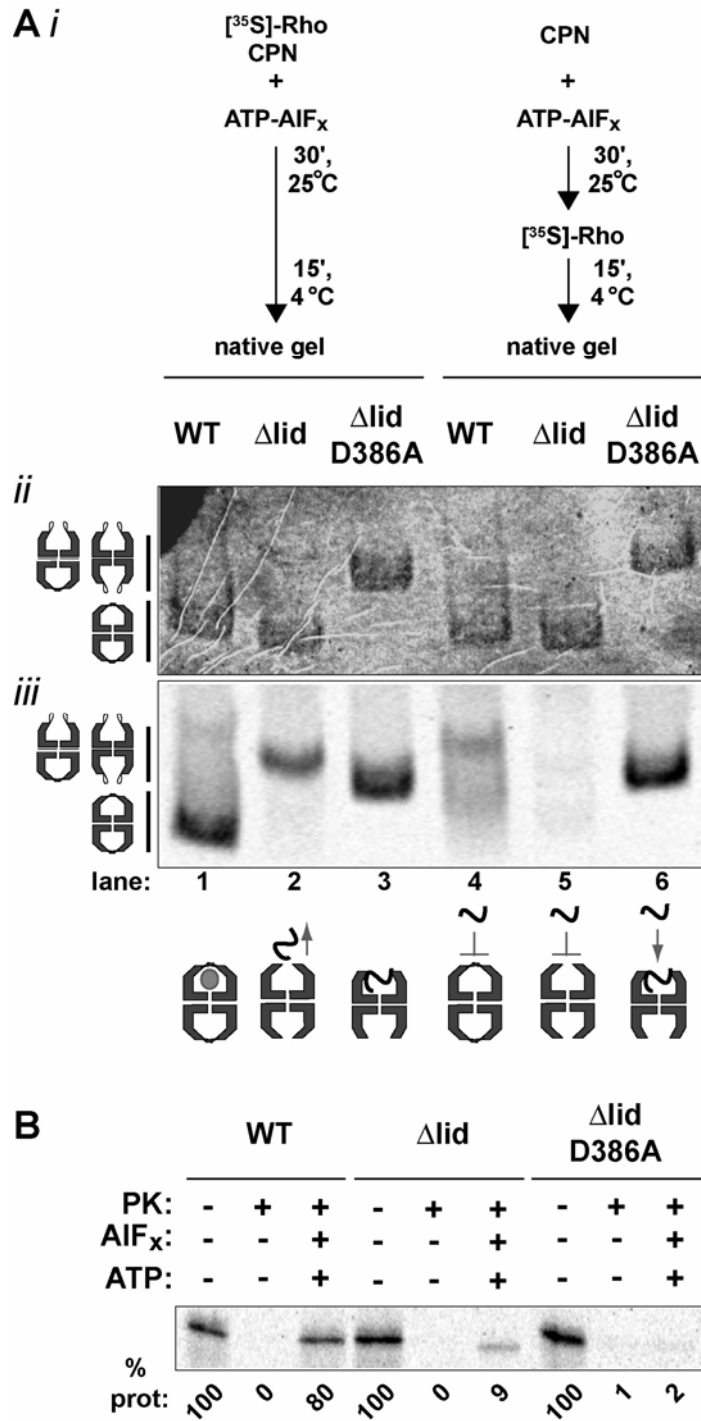


Figure 15. The substrate binding sites are occluded in the folding active, closed state of Mm-Cpn. (A) (i) Experimental approach. (ii) Coomassie stained native gel. In contrast to Mm-Cpn ^{$\Delta\text{lid/D386A}$} (lane 3 and 6) Mm-Cpn^{WT} (lane 1 and 4) and Mm-Cpn ^{Δlid} (lane 2 and 5) can be trapped in the double closed conformational state that migrates faster on a native gel (compare to Fig.14). (iii) Autoradiography of the native gel. (B) Formation of a functional lid-structure is required to encapsulate rhodanese in the presence of ATP and AIF_x. Encapsulation of rhodanese was determined by a protease protection assay. PK = proteinase K.

III.3. Lid formation triggers cooperativity in group II chaperonins

The chaperonin folding cycle is critically dependent on the synchronized action of individual subunits⁶¹⁻⁶³. The unique allosteric behavior observed in both group I and group II chaperonins^{61,64,65,79,80} is described as nested cooperativity, since positive cooperative transitions within each ring are nested into overall negative cooperativity between them. In the absence of ATP, both chaperonin rings are predominantly in the so-called T (“tense”)-state, which is characterized by low affinity for ATP. Binding of ATP to one subunit induces the transition of the corresponding ring, the so-called *cis*-ring, from the T- to the R (“relaxed”)-state, resulting in an increased affinity for ATP and cooperative binding of ATP within this *cis*-ring⁶¹. Despite this positive cooperativity between subunits of each individual ring, there is a negative cooperativity observed between the two rings⁶¹. As a consequence binding of ATP to the *cis*-ring has an inhibitory effect on ATP binding to the opposite *trans*-ring. Therefore, chaperonins undergo two allosteric transitions upon increasing ATP concentrations. The first allosteric transition occurs at a relatively low ATP concentration and corresponds to ATP binding and hydrolysis in the *cis*-ring. The second allosteric transition, by contrast, has its midpoint at a much higher ATP concentration, reflecting the lower affinity of the second ring for ATP. At high ATP concentrations, the negative cooperativity can be overcome and both rings are in the R-state with high affinity for ATP⁶¹.

The molecular basis of allosteric regulation in group I chaperonins has been extensively studied. Positive and negative cooperativity in GroEL is established independently of the GroES lid^{60,64}, although GroES profoundly influences the conformational changes of GroEL^{58-60,62,111}. In contrast, little is known about the molecular basis of allostery in eukaryotic and archaeal chaperonins. In group II chaperonins, all eight apical protrusions within a ring must interact tightly to form the iris-like lid³⁴. Given the overall conservation of the chaperonin structure, communication between subunits could be independent of the lid segments, as observed in GroEL⁶⁴. Alternatively, the apical protrusions themselves could synchronize the subunits within one ring, thus coordinating lid formation. To examine the role of the built-in lid in the folding cycle of group II chaperonins, we assessed the

effect of eliminating the lid from the eukaryotic chaperonin TRiC and the archaeal chaperonin Mm-Cpn (chapter III.2.)^{101,112}.

The built-in lid in TRiC couples ATP hydrolysis to substrate folding

As presented in chapter III.2 (**Fig. 10**) of the present study, the built-in lid of Mm-Cpn was dispensable for both ATP hydrolysis and substrate binding. However, deletion of the lid impaired the ability of Mm-Cpn to fold rhodanese in the presence of ATP.

Clipped TRiC (cTRiC) is a version of TRiC generated by mild Proteinase K treatment in the absence of nucleotide^{72,104} (**Fig. 16A,B**). Since the cleavage occurs within the helical protrusions¹⁰⁴, every single subunit gets cut in two halves of similar size, which can be separated under denaturing conditions (**Fig. 16B**). Cryo-EM analysis revealed that the double-ring architecture characteristic of chaperonins is preserved in cTRiC (**Fig. 16C**), consistent with previous findings⁷². Furthermore, both the substrate-binding and the ATPase domains retain their integrity in cTRiC, since it binds non-native substrates such as [³⁵S]-actin with an efficiency comparable to that of TRiC (**Fig. 16D** compare lanes 2 and 4), and can also effectively hydrolyze ATP (**Fig. 16E**). Strikingly, cTRiC is not able to promote actin folding upon incubation with ATP (**Fig. 16D**, compare lanes 3 and 5). We conclude that an intact lid is required to couple ATP hydrolysis with productive substrate folding in the eukaryotic chaperonin.

Taken together, our data suggest that, despite their evolutionary distance, the mechanism of closure and the function of the lid are conserved among all group II chaperonins. In both archaeal and eukaryotic chaperonins, lid closure is triggered by ATP hydrolysis. Furthermore, in both cases the lid is required to fold a bound substrate upon ATP hydrolysis (**Fig. 10D** and **Fig. 16D**). The characterization of lid-less variants of TRiC and Mm-Cpn provided a unique opportunity to define how the built-in lid regulated the ATP-driven conformational cycle of group II chaperonins.

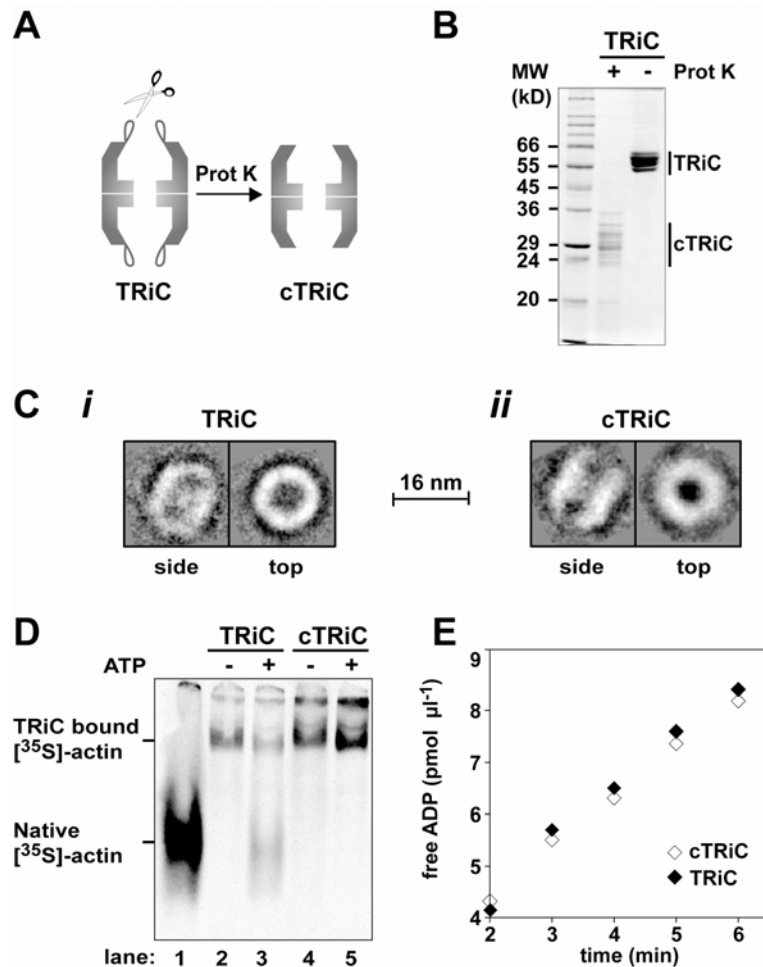


Figure 16. The built-in lid couples ATP hydrolysis to substrate folding in the eukaryotic chaperonin TRiC. (A and B) cTRiC is a lid-less version of TRiC generated by a selective cleavage within the apical protrusions. Prot K: Proteinase K (B) SDS-PAGE analysis followed by Coomassie staining of TRiC and cTRiC. Note that cleavage in the apical protrusion of each of the eight different 55–60 kDa subunits of TRiC results in sixteen 24–36 kDa fragments under denaturing conditions. (C) Cryo-EM analysis reveals preservation of the chaperonin-like oligomeric assembly in cTRiC. Two representative reference free class averages of TRiC (*i*) and cTRiC (*ii*) in top and a side view are shown. (D) cTRiC is able to bind denatured [^{35}S]-actin but cannot promote [^{35}S]-actin folding in the presence of ATP. Lane 1: native [^{35}S]-actin migration standard. (E) ATP hydrolysis by TRiC and cTRiC measured at 0.6 mM α -[^{32}P]-ATP.

The built-in lid establishes allosteric coupling between subunits within one ring

In group II chaperonins, all eight apical protrusions within a ring must interact tightly to form the iris-like lid³⁴. Accordingly, ATP should produce a concerted conformational change in all subunits of one ring. Given the overall conservation of the chaperonin structure, communication between subunits could be independent of

the lid segments, as observed in GroEL, where positive *intra*-ring cooperativity is independent of GroES⁶⁴ (**Fig. 17A**, Model 1). Alternatively, the apical protrusions themselves could synchronize the subunits within one ring, thus coordinating lid formation (**Fig. 17A**, Model 2). These models make distinct predictions for the contribution of the built-in lid to positive *intra*-ring cooperativity. While coupling between subunits would be retained in lid-less chaperonin variants according to the first model, it would be lost according to the second one. To distinguish between these possibilities, we compared the *intra*-ring cooperativity in wild-type (**Fig. 17B, C**) and lid-less (**Fig. 17E, F**) variants of both TRiC and Mm-Cpn. The allosteric properties of these chaperonins were determined by measuring the initial rates of ATP hydrolysis as a function of ATP concentration (**Fig. 17**). The first allosteric transition of TRiC and Mm-Cpn results from *intra*-ring communication^{80,112}. Accordingly we assessed coupling between subunits in one ring by comparing the kinetics of these chaperonins at ATP concentrations below 100 μM ^{80,112}. The kinetics obtained for both intact TRiC and Mm-Cpn^{WT} (**Fig. 17B, 17C**) were sigmoidal indicating positive cooperativity between the subunits of one ring ($p < 0.001$ for both proteins). The apparent ATP binding constant (K_1) and the Hill coefficient (n) for this first allosteric transition as well as the maximal turnover rate (v_{max}), were calculated by fitting the data points to the Hill equation (equation 1 and **Table 6**). For TRiC, the values for K_1 and n are $10.1 (\pm 0.5) \mu\text{M}$ and $2.0 (\pm 0.2)$ respectively, in very good agreement with previous observations⁸⁰. Comparison of the respective values for the catalytic rate (k_{cat} , calculated to be 0.04 sec^{-1} for TRiC and 0.7 sec^{-1} for Mm-Cpn^{WT}) reveals that the archaeal chaperonin is a much more efficient ATPase than TRiC - a property Mm-Cpn shares with its bacterial counterpart GroEL⁶⁴. Notably, although Mm-Cpn hydrolyzes ATP much more rapidly than TRiC, the affinity of the archaeal chaperonin for ATP ($K_1 = 5.8 \pm 0.3 \mu\text{M}$) as well as its degree of allosteric coupling ($n = 1.9 \pm 0.1$) were very similar to those of TRiC (**Table 6**). Thus, for both chaperonins, positive *intra*-ring cooperativity drives a concerted conformational change within all subunits of one ring that results in lid closure (**Fig. 17D**). This allosteric switch converts the subunits of one ring from a "tense" T state, with low affinity for ATP, to a "relaxed" R state with high affinity for ATP⁶¹ (**Fig. 17D**).

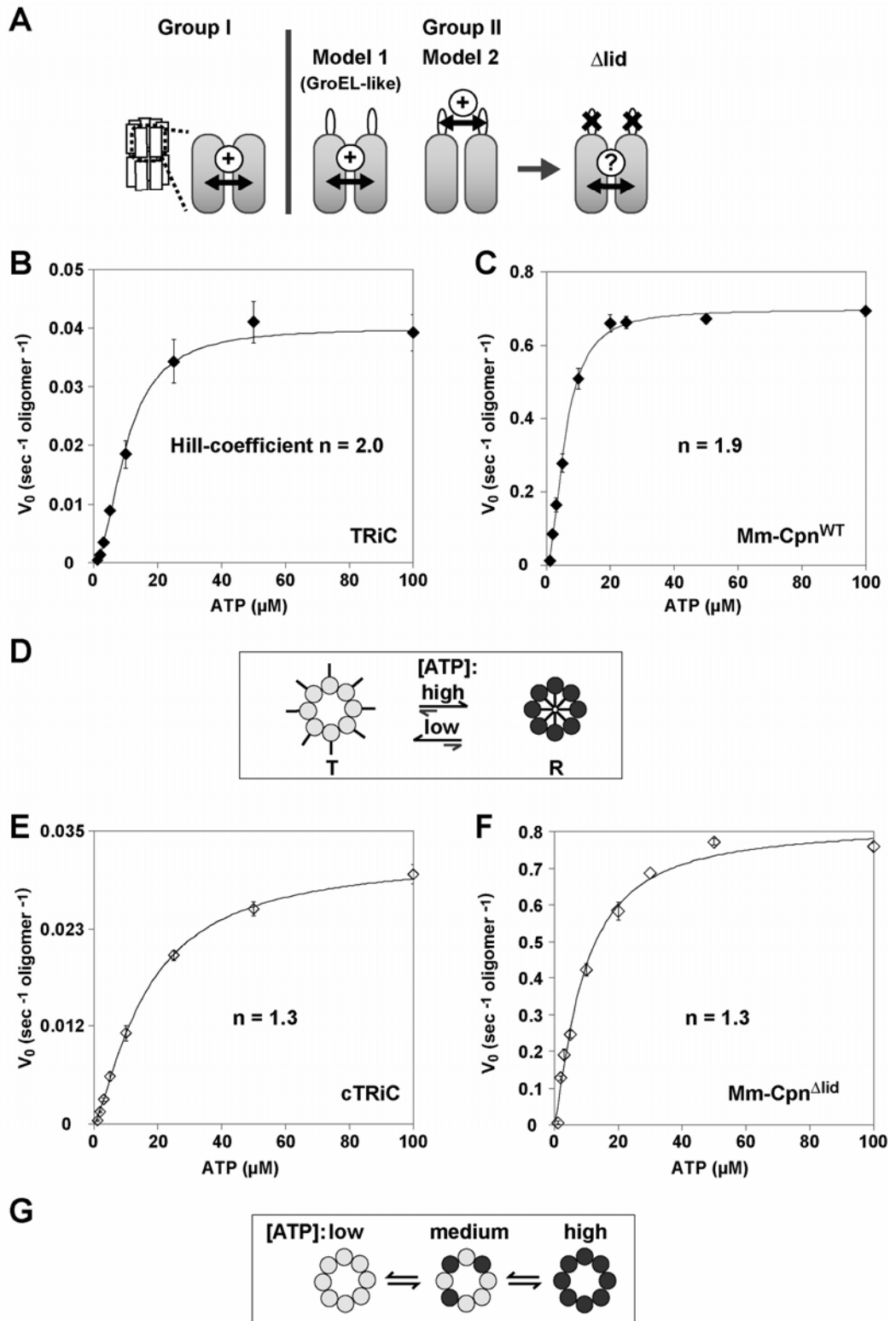


Figure 17. The built-in lid is required for positive cooperativity between the subunits of one ring. (A) Two different models could account for positive cooperativity in group II chaperonins. On the one hand *intra*-ring coupling could be similar to GroEL (Model 1). On the other hand the lid segments could be required to orchestrate synchronized action between subunits in one ring (Model 2). To distinguish between the two possibilities we investigate *intra*-ring coupling in the lid-less versions of group II chaperonins. (B and C) Wild-type eukaryotic and archaeal chaperonins display positive cooperativity within the subunits of one ring. Initial velocities of ATP hydrolysis by TRiC (B) and Mm-Cpn^{WT} (C) were plotted against the corresponding ATP concentrations (1 – 100 μ M ATP). The data were fitted to the Hill equation (equation 2, see methods). Each data point corresponds to the average of at least three independent experiments. The error bars represent the standard error of measurements (SEM). (D) Model of the ATP-induced conformational change of one ring of TRiC and Mm-Cpn^{WT}. Positive cooperativity causes subunits in one ring to undergo a concerted conformational change leading to lid closure. (E and F) Allosteric coupling of subunits within one ring is impaired in a lid-less chaperonin. Initial velocities of ATP hydrolysis by cTRiC (E) and Mm-Cpn^{Δlid} (F), plotted against the corresponding ATP concentrations (1 – 100 μ M ATP) and fitted to equation 2 as above. Each data point corresponds to the average of at least three independent experiments. The error bars represent the standard error of measurement (SEM). (G) Model of the ATP-induced conformational changes in lid-less cTRiC and Mm-Cpn^{Δlid}. No allosteric coupling between the subunits can be observed, indicating that the subunits bind to ATP independently of each other.

The allosteric coupling of lid-less variants of TRiC and Mm-Cpn was examined next (Fig. 17E, F). Loss of the lid segments did not affect the overall affinity for ATP, K_1 , and the maximal hydrolysis rate, v_{max} , of either chaperonin (Table 6). However, there was a dramatic loss in positive cooperativity between the subunits (Fig. 17E, F and Fig. 18), as indicated by significantly reduced values for the Hill coefficients (n) (Table 6; $p=0.01$ for n_{TRiC} vs n_{cTRiC} , $p=0.005$ for $n_{Mm-CpnWT}$ vs $n_{Mm-Cpn\Delta lid}$). Of note, deletion of the entire apical protrusion in Mm-Cpn (Fig. 17F) has a similar effect on the positive cooperativity as cleaving the lid-forming segments in TRiC (Fig. 17E). These lid-less chaperonins hydrolyze ATP with Michaelis-Menten kinetics typical of enzymes without allosteric regulation, indicating that the subunits within one ring bind ATP independently of each other (Fig. 17G).

These experiments indicate that the presence of intact lid segments is important to establish positive cooperativity within the subunits of one ring. Thus, the built-in lid is required to synchronize the ATP-induced conformational change of subunits within one ring.

Table 6. Parameters defining kinetic properties of Type II chaperonins.

	TRiC	cTRiC	Mm-Cpn ^{WT}	Mm-Cpn ^{Δlid}
K₁ (μM):	10.1 (+/- 0.5)	16.5 (+/- 1.0)	5.8 (+/- 0.3)	9.0 (+/- 0.6)
K₂ (μM):	593 (+/- 23)	na ^a	562 (+/- 175)	na
n^b:	2.0 (+/- 0.2)	1.3 (+/- 0.2)	1.9 (+/- 0.1)	1.3 (+/- 0.1)
m^c	10.8 (+/- 4.2)	na	2.9 (+/- 1.8)	na
k_{cat} R/T'				
(oligomer⁻¹ sec⁻¹):	0.04	0.03	0.7	0.8
k_{cat} R'/R'				
(oligomer⁻¹ sec⁻¹):	0.028	na	0.54	na

^a na: not applicable; ^b n: Hill coefficient of first allosteric transition; ^c m: Hill coefficient of second allosteric transition.

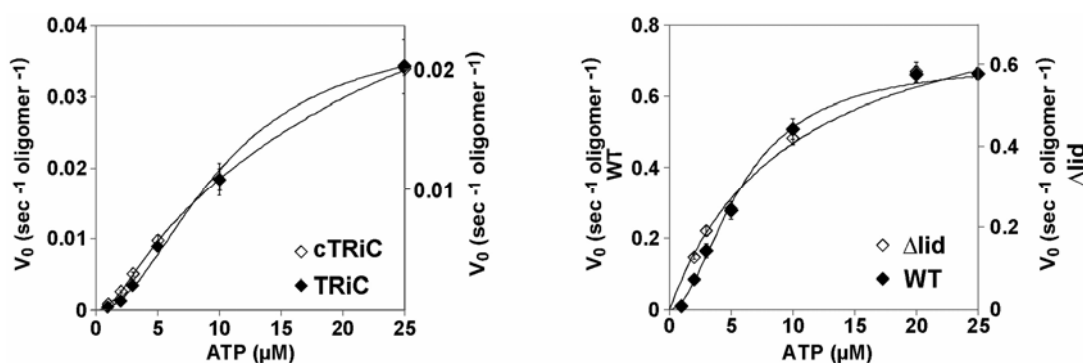


Figure 18. Direct comparison of the first allosteric transition in wild-type and lid-less chaperonin version. The data presented in Figure 17 are displayed from 0 to 25 μM ATP and the overlap of the kinetics wild-type and lid-less chaperonin versions is shown.

Negative allosteric coupling between rings affects ATP binding and hydrolysis

TRiC and Mm-Cpn display a second allosteric transition above 400 μM ATP, which results from *inter-ring* communication^{80,112} (**Fig. 19A,B**). These higher ATP concentrations overcome the negative cooperativity between the rings and as a result, the *trans*-ring also starts binding and hydrolyzing ATP^{80,112} (**Fig. 19C**).

To examine the nature of *inter-ring* communication in group II chaperonins, we extended our analysis to a broader range of ATP concentrations⁸⁰. The second allosteric transition observed for both TRiC and Mm-Cpn was reflected by a decreased hydrolysis rate at higher ATP concentrations (**Fig. 19A,B**), in contrast to

previous measurements for TRiC⁸⁰. Importantly, similar results were obtained for TRiC and Mm-Cpn^{WT}. Thus our results probably reflect a general property of group II chaperonins. Since both chaperonins used here were fully competent for substrate folding (**Fig. 10D** and **Fig. 16D**), the discrepancy with previous TRiC measurements could be explained by weakened *inter*-ring contacts in previous protein preparations, which may impair negative cooperativity.

The observation that the second allosteric transition produces a marked decrease in the rate of ATP hydrolysis suggests that in group II chaperonins, negative *inter*-ring communication prevents both ATP-bound rings from hydrolyzing ATP simultaneously at an optimal rate. Our findings suggest a model for how nested allosteric interactions in group II chaperonins allow them to function as two-stroke motors (**Fig. 19C**). In the absence of nucleotide, the two rings are virtually identical and in the symmetrically open T-state (**Fig. 19C**). At intermediate ATP concentrations (**Fig. 19C**, 0.2 mM ATP), the subunits in one ring (i.e. the *cis*-ring) undergo an allosteric transition to the R-state and bind ATP with positive cooperativity^{65,79}. As a result of the negative *inter*-ring cooperativity, ATP binding to the *cis*-ring induces a conformational change in the subunits of the *trans*-ring to a T'-state with lower affinity for ATP. This asymmetric state is characterized by an optimal ATPase activity ($v_{\max 1}$). At higher ATP concentrations (**Fig. 19C**; 1 mM ATP), the *trans*-ring also binds ATP but overall ATP hydrolysis becomes less efficient. We propose that this change corresponds to a different state of the enzyme, the R'/R'-state, where the negative cooperativity for ATP binding has been overcome and both rings are forced to adopt a conformation with a suboptimal ATPase rate ($v_{\max 2}$). Strikingly, similar results are observed for both TRiC and Mm-Cpn despite their widely different overall catalytic rates and subunit composition, suggesting that this type of allosteric regulation is conserved in all group II chaperonins.

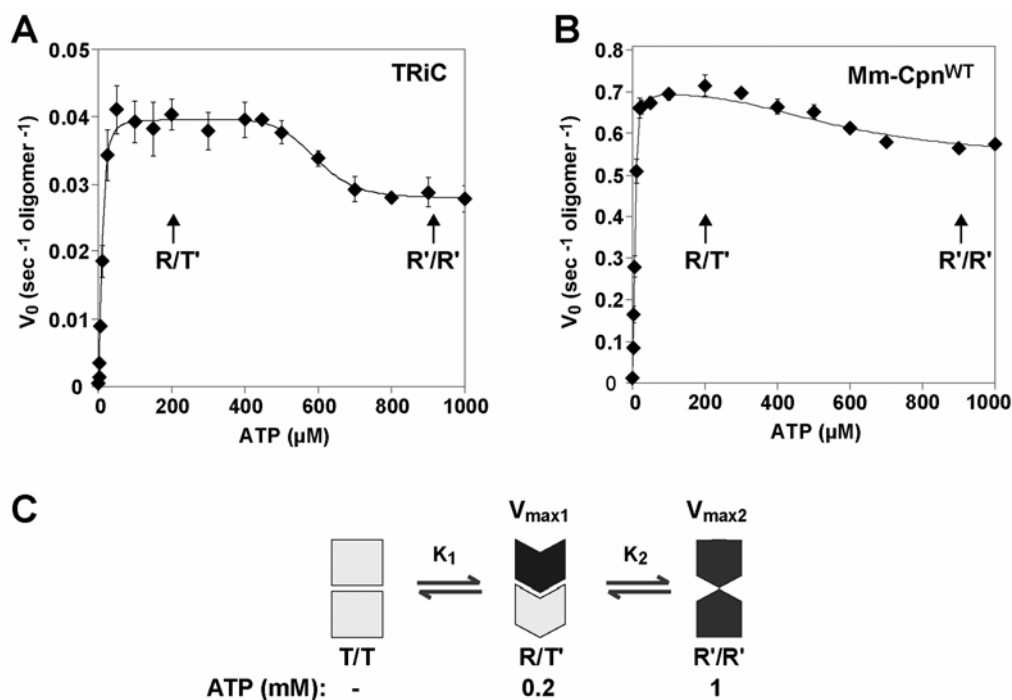


Figure 19. Negative allosteric coupling between rings affects ATP binding and hydrolysis. (A and B) Negative allosteric coupling between rings results in a second allosteric transition occurring at high ATP concentrations in wild-type chaperonins. Initial velocities of ATP hydrolysis by TRiC (A) and Mm-Cpn^{WT} (B) were plotted against the corresponding ATP concentrations (1 – 1000 μM ATP) and fitted to equation 2 (see methods). Each data point corresponds to the average of at least three independent experiments. The error bars represent the standard error of measurement (SEM). (C) Proposed conformational states for group II chaperonins at different ATP concentrations. T/T-state: in the absence of nucleotide, both rings reside in the “tense” (T) state, and the lid structure is not formed. This T/T complex is characterized by a low affinity for ATP. R/T'-state: at intermediate ATP concentrations (0.2 mM ATP) the *cis*-ring reaches saturation for ATP binding and hydrolysis and therefore assumes the R-state. At the same time the *trans*-ring is rendered in a conformational state T' with low affinity for ATP as a consequence of negative cooperativity between the rings. This asymmetric state is characterized by an optimal ATPase activity (v_{max1}). R'/R'-state: at high ATP concentrations (1 mM ATP) the negative cooperativity is overcome and both rings bind and hydrolyze ATP simultaneously. The two rings hinder each other, leading to the observed drop in the hydrolysis rate v_{max2} , which marks the transition to the R'/R'-state.

Negative allosteric coupling between rings drives a “two-stroke” motor cycle

The model suggested above predicts the formation of an asymmetric R/T'-state at intermediate ATP concentrations and a symmetric R'/R'-state at high ATP concentrations. This prediction was tested by exploiting the differential protease sensitivity of the lid in the open, T-state and the closed R-state. TRiC (Fig. 20A i) and

Mm-Cpn (**Fig. 20A ii**) were incubated in the absence of nucleotide or in the presence of either 0.2 or 1 mM ATP to generate the three states proposed by our model (**Fig. 19C**). The gamma-phosphate mimic AlF_x was included in the assays to stabilize the closed state^{72,78}. As expected, both rings were in the open conformation in the nucleotide-free T/T-state (**Fig. 20A**). In contrast, at high ATP concentrations (**Fig. 20A**, 1mM ATP), virtually all the apical lid segments were protected in both TRiC and Mm-Cpn^{WT}, yielding full length chaperonin, consistent with a R'/R'-state in which both rings are closed. Interestingly, incubation with an intermediate ATP concentration (**Fig. 20A**, 0.2 mM) reduced the level of protection of the lid segments of either mammalian or archaeal chaperonin to about half of the values obtained at high ATP concentrations, consistent with the idea that negative *inter*-ring cooperativity prevents the *trans*-ring from binding ATP. Importantly, this *lower* ATP concentration yields the *maximal* ATP hydrolysis rates, suggesting that the asymmetric conformation of the chaperonin induced by this ATP concentration is optimized for ATP cycling.

The observation of an asymmetric R/T' state at intermediate ATP concentrations raised the possibility that negative allosteric coupling between rings allows the inherently symmetrical group II chaperonins to function as “two-stroke” motors. To relate the regulation of ATPase activity to chaperonin function, we compared the protein folding activity of both TRiC and Mm-Cpn at either 0.2 or 1 mM ATP (**Fig. 20B, C**) TRiC-mediated actin folding was assessed using two independent folding assays, non-denaturing PAGE (**Fig. 20B i**) and protease susceptibility (**Fig. 20B ii**)⁷². Comparable folding yields and rates were observed at 0.2 or 1 mM ATP (**Fig. 20B, C i**). The protease susceptibility assay can distinguish between released folded actin, which yields a protease-resistant actin fragment of 34 kDa, and TRiC-encapsulated actin, as lid closure protects the full-length polypeptide (**Fig. 20B ii**)⁷². Of note, since similar levels of ³⁵S-actin protection were observed at 0.2 and 1 mM ATP, it appears that only one ring is functional for substrate folding and encapsulation, even at the higher ATP concentrations. Similar results were obtained for Mm-Cpn, as comparable yields and rates of rhodanese folding were observed at 0.2 and 1 mM ATP (**Fig. 20B ii**). Thus, the asymmetric R/T'-state supports optimal substrate folding rates.

Taken together these results support the idea that at intermediate ATP concentrations, negative *inter*-ring cooperativity establishes an asymmetric R/T'-state, with only one ring possessing a closed lid. Consistent with our model, structural evidence for an

asymmetric cycle of lid closure has been obtained for TRiC⁸³ and for archaeal thermosome^{81,82}. Importantly, our analysis provides a rationale as to how allosteric regulation of group II chaperonins allows these symmetrical complexes to function as a two-stroke machine without the assistance of an external GroES-like cofactor.

The second allosteric transition is absent in lid-less group II chaperonins

To examine the role of the apical lid segments in establishing the negative *inter*-ring cooperativity, we next extended our analysis to cTRiC and Mm-Cpn^{Δlid} (**Fig. 21**). Remarkably, there were significant differences in the kinetics of the lid-less and wild-type chaperonins. For both the archaeal and the eukaryotic chaperonins, absence of a functional lid completely abolished the second allosteric transition at higher ATP concentrations (**Fig. 21B, C; Table 6**; compare to **Fig.19A, B** for wild-type). We conclude that the lid segments not only synchronize subunits within one ring but also play an important role in the communication between the rings.

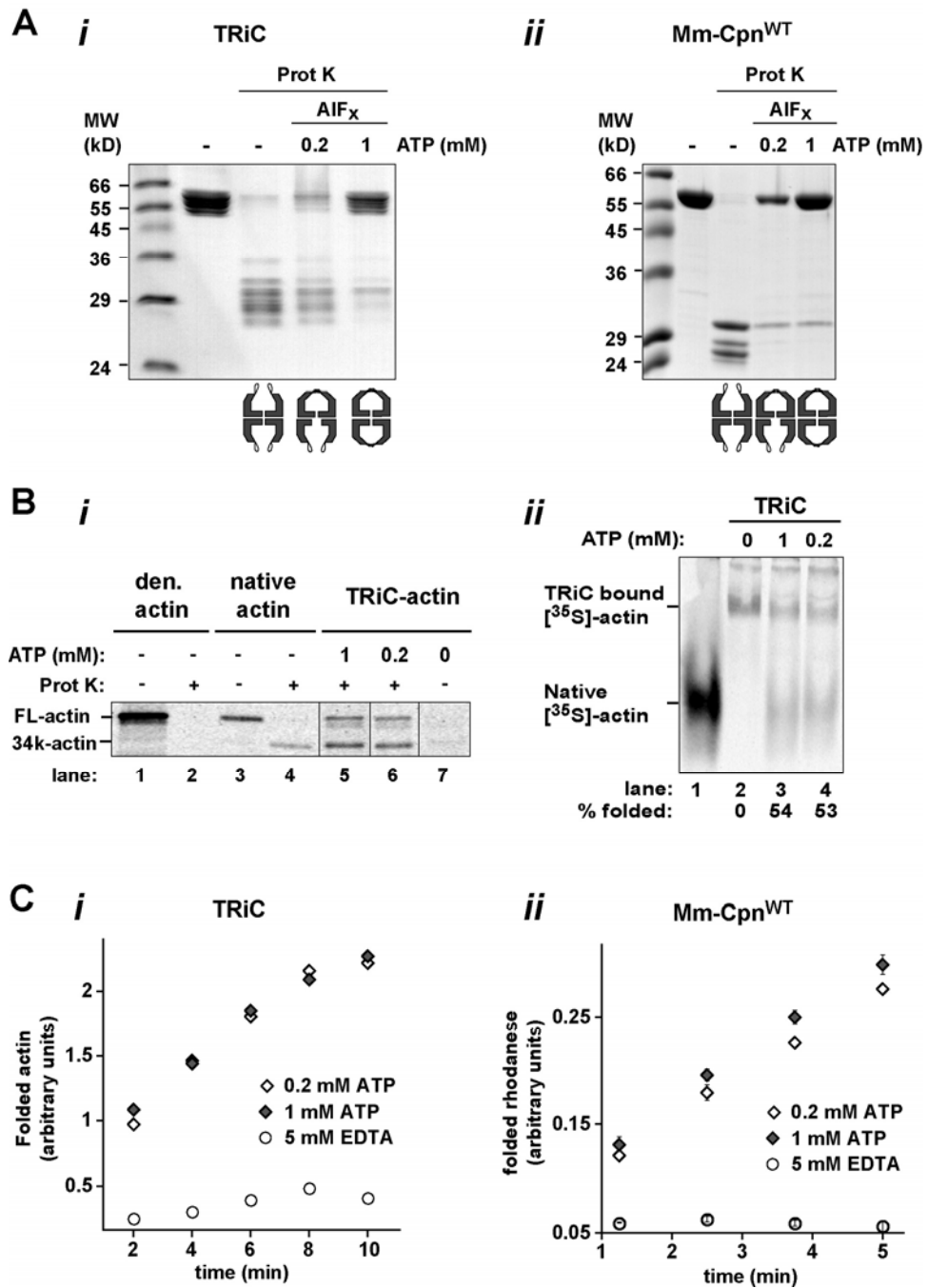


Figure 20. Group II chaperonins sample two different conformational states at intermediate and high ATP concentrations. (A) A biochemical assay to confirm the existence of the different conformational states proposed in (Fig. 19C). TRiC and Mm-Cpn^{WT} are fully protected from protease cleavage at 1mM ATP-AIF_x and therefore reside in a symmetrically closed complex, the R²/R²-state. The partial protection pattern at 0.2 mM ATP-AIF_x indicates the existence of an asymmetrically closed R/T²-state at intermediate ATP concentrations. (B, C) The asymmetric R/T²-state of group II chaperonins supports optimal substrate folding. (B) TRiC-mediated [³⁵S]-actin folding at 1 mM and 0.2 mM ATP, examined by (i) protease sensitivity and (ii) non-denaturing PAGE. (i) Nucleotide-dependent generation of native [³⁵S]-actin can be observed by the occurrence of the 34 kDa proteolytic fragment. The full-length actin band (FL-actin) in lane 5 and 6 corresponds to encapsulated substrate protein which is protease protected as shown previously⁷². (ii) About 50 % of bound [³⁵S]-actin was re-folded by TRiC in

the presence of 1 mM and 0.2 mM ATP (lane 3 and 4) and in the course of the experiment. Lane 1: native [35 S]-actin migration standard. (C) Substrate folding rates of TRiC and Mm-Cpn at 0.2 and 1 mM ATP (i) Time course of actin folding by TRiC in the absence of nucleotide (5 mM EDTA) and in the presence of 0.2 and 1 mM ATP. (ii) Time course of rhodanese folding by Mm-Cpn^{WT} in the absence of nucleotide (5 mM EDTA) and in the presence of 0.2 and 1 mM ATP.

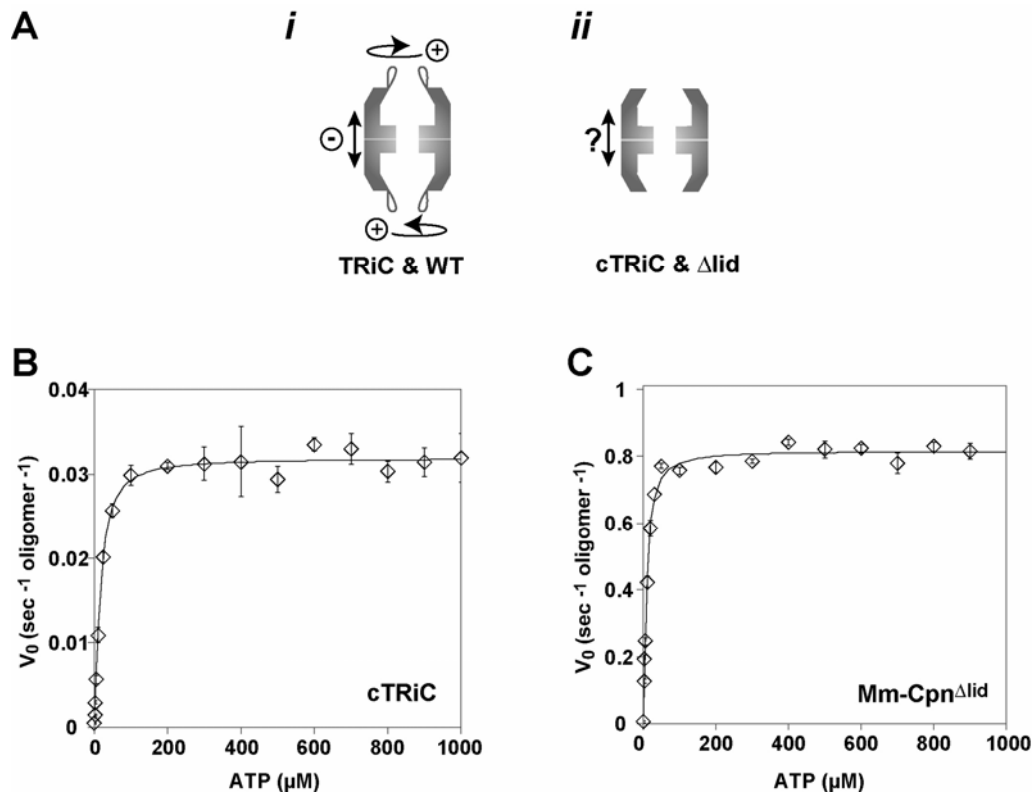


Figure 21. The built-in lid affects *inter*-ring communication of group II chaperonins. (A) (i) Nested allosteric coupling in group II chaperonins. Positive cooperativity within the subunits of one ring is nested into negative cooperativity between the two rings. (ii) The role of the lid in *inter*-ring communication was examined by kinetic analysis of lid-less chaperonins at high ATP concentrations. (B, C) The second allosteric transition, occurring at high ATP concentrations, is absent in the lid-less chaperonin versions. Initial velocities of ATP hydrolysis by cTRiC (B) and Mm-Cpn ^{Δ lid} (C), respectively, were plotted against the corresponding ATP concentrations (1 – 1000 μ M ATP) and fitted to equation 2 (see methods). Each data point corresponds to the average of at least three independent experiments. The error bars represent the standard error of measurement (SEM).

III.4. Positive cooperativity in the eukaryotic chaperonin TRiC is a sequential event driven by a gradient of affinities for ATP

To assemble a lid structure from building blocks provided by different subunits, ATP-induced conformational changes must occur in a synchronized fashion within the subunits of one ring. To this end, the subunits are coupled to an allosteric unit by *intra*-ring positive cooperativity in respect to ATP binding. The results presented in the previous chapter show that the apical protrusions themselves are required to establish positive cooperativity in group II chaperonins. During the positive allosteric transition from the T- to R-state in one ring of the bacterial chaperonin GroEL, all subunits act in an all or none reaction according to the MWC-model put forth by the scientists *Monod, Wyman, and Changeux* in 1965¹¹³. This concerted model of allostery postulates that subunits of multimeric enzymes are connected in such a way that a conformational change in one subunit is conferred simultaneously to all other subunits. Consequently, all subunits must exist in the same conformation at any time. However, due to integration of the built-in lid structure to the allosteric network in group II chaperonins, positive cooperative transition within the subunits of one ring in TRiC and Mm-Cpn might alternatively occur sequentially as described by the KNF-model proposed by the scientists *Koshland, Nemethy, and Filmer* in 1966¹¹⁴. This sequential model of allostery takes into account asymmetric conformations within the allosteric unit, as it would be the case during a domino-like transition around the ring of chaperonins. Consequently, the sequential model assumes that the conversion of one subunit from the T- to R-state induced by ligand binding does not induce the same conformational change to neighboring subunits. Interestingly, genetic analyses in *S. cerevisiae* indicated that the ATP-binding sites of the eight different TRiC subunits are not equivalent⁹¹. This led to the proposal that ATP binding indeed occurs in a sequential cooperative manner, unlike in the homo-oligomeric chaperonin GroEL, where ATP binding is a highly concerted allosteric event^{91,20}. Since substrate most likely binds to more than one subunit in TRiC^{86,109,115-117}, a sequentially occurring conformational change could impact the order with which different regions of the polypeptide are released from the binding sites and thereby determine the folding pathway of the substrate protein. This would be a mechanistic

feature unique to the eukaryotic chaperonin TRiC and could explain why GroEL as well as the archaeal group II chaperonin Mm-Cpn can bind to TRiC substrate proteins but fail to promote their folding^{71,84,85}.

A prediction of the sequential model of positive cooperativity in TRiC is that some subunits bind ATP with higher affinity than others. Accordingly, the “high affinity” subunits will bind ATP at lower ATP concentrations than the “low affinity” subunits. In order to determine which specific subunits of TRiC are occupied with ATP at different nucleotide concentrations we performed cross-link experiments with α -[³²P]-8-N₃-ATP and bovine TRiC. Subsequently, we determined which specific subunit bound ATP by separation of all subunits by RP-HPLC.

A gradient of affinities for ATP binding in TRiC

TRiC is a unique member of the chaperonin family since it is assembled from eight different subunits. The highest degree of sequence similarity between the subunits is found in regions of the equatorial and intermediate domains that constitute the ATP binding pocket¹¹⁸. In theory, all subunits within the TRiC complex would therefore be expected to have similar affinities for ATP, which is not compatible with the proposed sequential model of positive cooperativity^{91,20,119}.

In order to test whether all subunits display the same or different affinities for ATP, we cross-linked ATP to TRiC using α -[³²P]-8N₃-ATP at low, intermediate, and high ATP concentrations (**Fig. 22**). Note, that TRiC displays similar affinities for 8-N₃-ATP and ATP (**Fig. 23**). The photoactive azido (-N₃) group generates a highly reactive nitrene upon UV irradiation, which inserts either into the peptide backbone or into the amino acid side chain to which it is bound (ALT Inc., USA). After cross-linking, the eight different TRiC-subunits were separated by reversed-phase HPLC (RP-HPLC)⁵⁴ (**Fig. 22**, black profiles). Detection of co-eluting radioactivity allowed the assignment of the subunits covalently attached to nucleotide (**Fig. 22**, red profiles).

At low ATP concentrations (**Fig. 22C**, 10 μ M ATP), only CCT5 and to some extent also CCT4 could be cross-linked to ATP, at 0.2 mM ATP by contrast the cross-link intensity to CCT4 increased (**Fig. 22D**), and at 0.5 mM ATP, also CCT1 and to some extent CCT2 were cross-linked to ATP (**Fig. 22E**). Since all subunits can be cross-linked to ATP at saturating ATP concentrations (**Fig. 22F**, 2 mM ATP), it was

assumed that the UV-induced cross-link reaction between TRiC and 8-N₃-ATP was equally favored in all subunits.

We therefore conclude that there is a gradient of affinities for ATP established within the different subunits of TRiC (**Fig. 24**). At low ATP concentration, ATP predominantly binds to CCT5 and CCT4, which therefore possess the highest affinity, followed by CCT1 and CCT2. CCT3, 7, 8 and 6 are only occupied with nucleotide at high ATP concentrations and are therefore considered to have a low affinity for ATP.

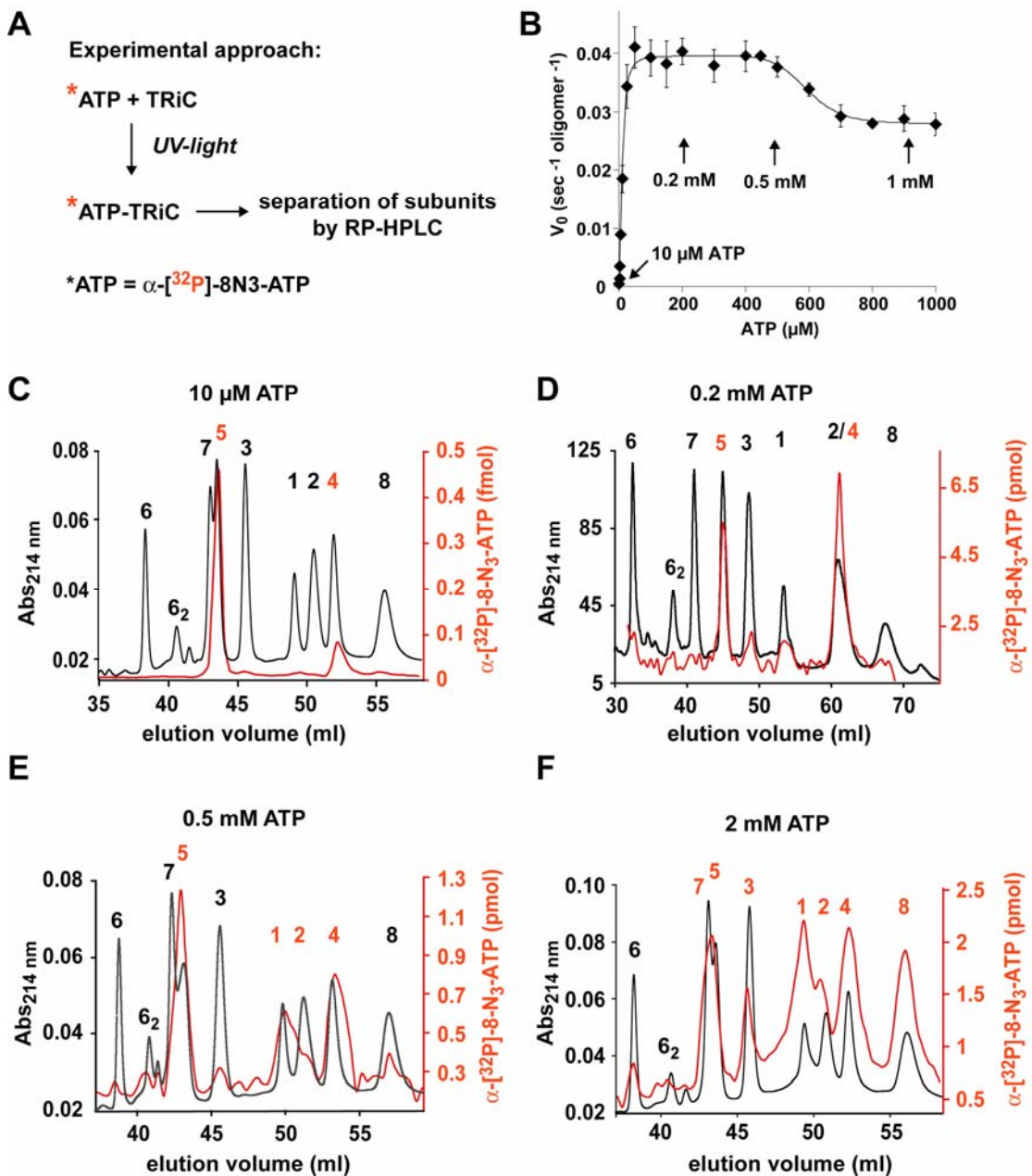
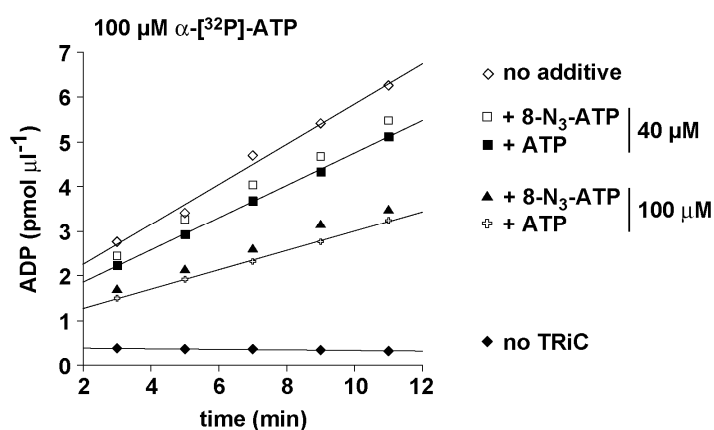
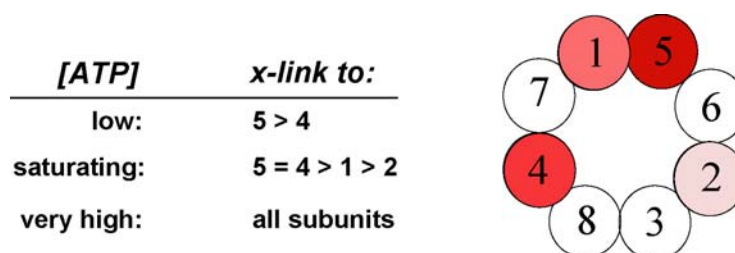


Figure 22. A gradient of affinities for ATP binding in TRiC.

(A) Experimental procedure. *ATP = α -[32 P]-8-N₃-ATP. (B) Initial velocities of the ATP hydrolysis rate of TRiC blotted against the corresponding ATP concentrations (compare **Fig. 19A**). The arrows point to the ATP concentrations for at which the cross-link experiments were performed. (C-F) The subunits in TRiC display different affinities for ATP. Separation of the subunits by RP-HPLC after cross-link of α -[32 P]-8-N₃-ATP at 10 μ M ATP (C), 0.2 mM ATP (D), 0.5 mM ATP (E) and 2 mM ATP (F). The UV-profile of the eluting subunits is shown in black whereas the specific radioactivity detected in each fraction is illustrated as the red profile. The numbers above every pike refer to the identity of the subunit (CCT1-8) as determined by mass-spectrometry⁸⁶. Red numbers imply that the corresponding subunit co-elutes with radioactively labeled nucleotide.

**Figure 23. TRiC has similar affinity for 8-N₃-ATP and ATP.** ATP hydrolysis of TRiC was measured at 100 μ M α -[32 P]-ATP in the presence of different additives as indicated.**Figure 24. A gradient of affinity for nucleotide binding within the different TRiC subunits.** Summary of the cross-link experiment shown in **Figure 22**. The model of the arrangement of the different TRiC subunits is taken from Liou and Willison, 1997¹³⁷. The subunits are colored in different shades of red according to their apparent affinities for nucleotide. Dark red = high affinity, light red = intermediate affinity, white = low affinity.

Not all subunits in TRiC cross-link to ATP at saturating conditions

Surprisingly, even at 1 mM ATP, a saturating ATP concentration as apparent from the equilibrium kinetics displayed in **Figure 22B**, ATP predominantly co-eluted with CCT5, 4, 1 and 2, whereas it cross-linked only weakly to CCT3 and not detectably to CCT6, CCT7 and CCT8 (**Fig. 25A**). To confirm that this results indeed corresponds to unequal occupation of the TRiC subunits with ATP and is not due to high off-rates of the ATP-hydrolysis products from CCT3, 6, 7 and 8, TRiC was incubated with 1 mM α -[³²P]-8N₃-ATP + AlF_x prior to UV irradiation (**Fig. 25B**). Addition of the gamma-phosphate mimic AlF_x allowed to irreversibly trap TRiC in a conformational state in which both rings adopt the nucleotide-induced closed conformation⁷². Intriguingly, even under those conditions only four out of the eight different TRiC subunits could be cross-linked to ATP (**Fig. 25B**). It was examined next whether the presence of bound substrate protein changes the occupancy of TRiC subunits with ATP but the cross-link results were identical in the presence and absence of denatured actin (**Fig. 25C, D**). Note that in agreement with this finding, the presence of substrate protein does not affect the rate of ATP hydrolysis in TRiC at saturating ATP concentrations (**Fig. 26**).

It therefore appears that not all subunits of TRiC are occupied with nucleotide at ATP concentrations that provide saturating conditions in respect to the kinetics of ATP hydrolysis^{79,80} (**Fig. 19**).

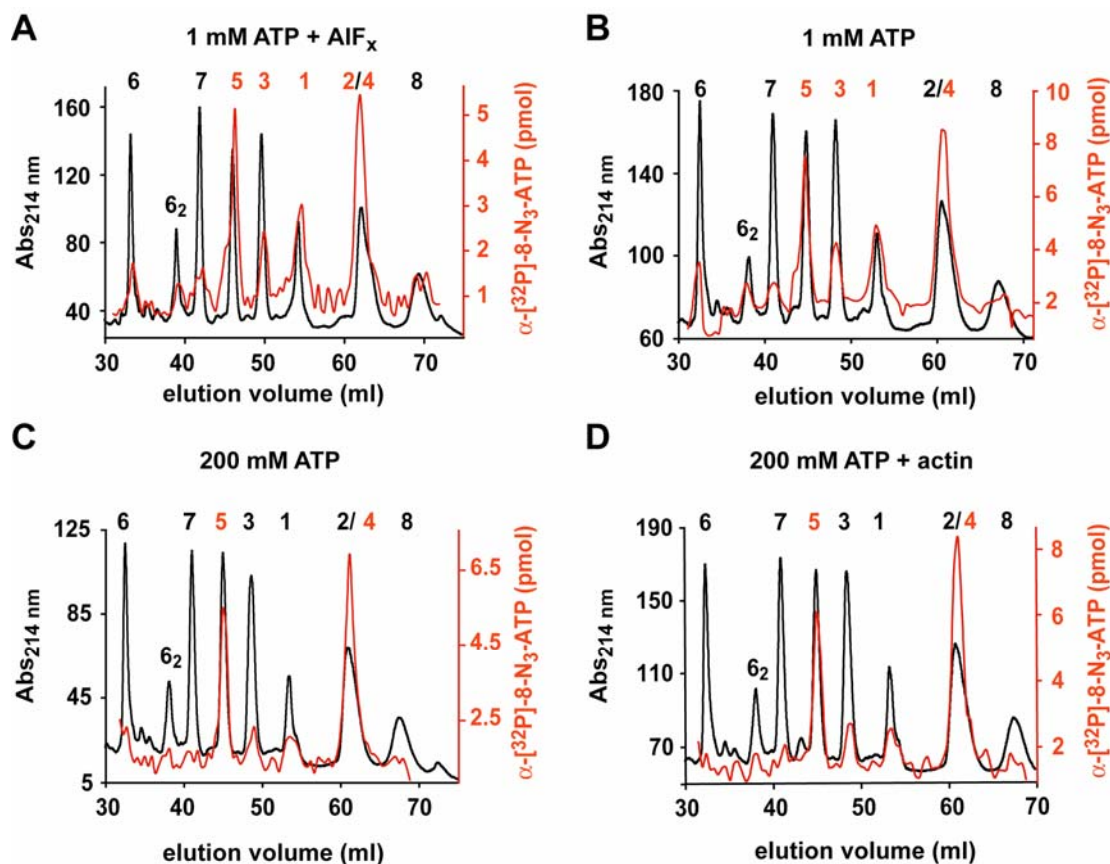


Figure 25. Not all subunits of TRiC are occupied with nucleotide even at saturating ATP concentrations and in the presence of substrate protein.

(A–D) Separation of the subunits by RP-HPLC after cross-link of α -[32 P]-8-N $_3$ -ATP at 1 mM ATP (A), 1 mM ATP in the presence of AIF $_x$ (B), 0.2 mM ATP (C) and 0.2 mM ATP in the presence of actin (D). The UV-profile of the eluting subunits is shown in black whereas the specific radioactivity detected in each fraction is illustrated as the red profile. The numbers above every peak refer to the identity of the subunit (CCT1-8) as determined by mass spectrometry⁸⁶. Red numbers imply that the corresponding subunit co-elutes with radioactively labeled nucleotide.

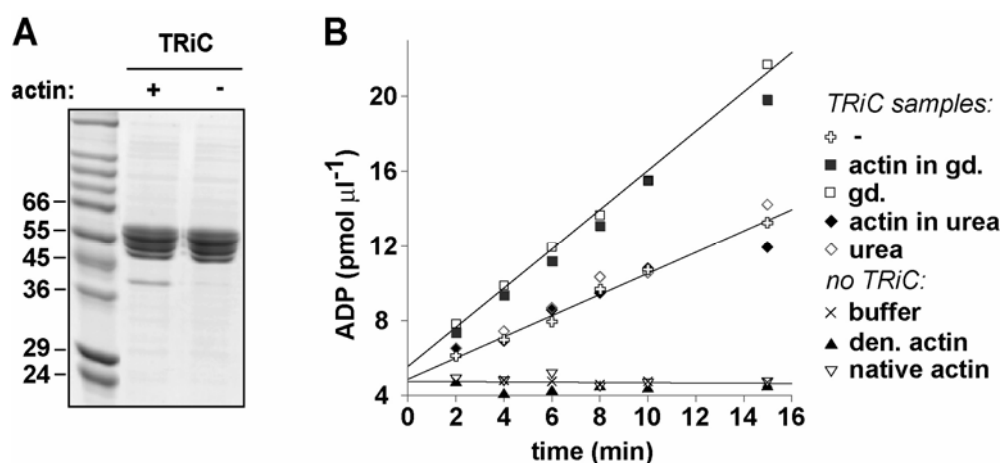


Figure 26. Presence of substrate protein does not influence the rate of ATP hydrolysis in TRiC. (A) Reactions containing TRiC in the presence and absence of actin were analyzed by SDS-PAGE and subsequent Coomassie staining. (B) The presence of 60 mM guanidine/HCl (gd.) but not the presence of 80 mM urea stimulates the rate of ATP hydrolysis by TRiC. Bound substrate protein has no additional effect. ATPase activity of TRiC in the presence of different supplements was measured at 1 mM α -[^{32}P]-ATP.

Stoichiometry of TRiC-nucleotide complexes under equilibrium conditions

The cross-link approach described above describes the selective binding of nucleotide to the different TRiC subunits in a qualitative fashion but does not allow to draw quantitative conclusions. We therefore applied filter-binding experiments or, alternatively, gel filtration analyses to determine the stoichiometry of TRiC-nucleotide complexes at saturating ATP concentration (1 mM ATP, **Table 7**).

The filter-binding assay is a very time efficient procedure and thus more likely to yield reliable stoichiometries for ligands with high off-rates. However, due to background problems in the presence of AlF_x , we used the gel filtration assay under certain conditions.

The stoichiometry of TRiC and ATP at 1 mM ATP is found to be nine or ten nucleotides per oligomeric complex, as determined by the filter binding assay, and seven nucleotides according to gel filtration analysis (**Table 7**). This apparent difference most likely reflects the fact that some nucleotide may be dissociating from the chaperonins during the slower gel filtration process. However, this effect is absent in subsequent experiments where stably associated TRiC nucleotide complexes were analyzed, in which nucleotide was either cross-linked to TRiC or trapped by the addition of AlF_x . Interestingly, we obtained the same stoichiometry for TRiC cross-

linked to α -[^{32}P]-8N₃-ATP in the presence of AlF_x and for TRiC incubated with α -[^{32}P]-ATP and AlF_x, namely nine nucleotides per complex (**Table 7**). This is consistent with the values obtained for α -[^{32}P]-ATP in the absence of AlF_x and indicates that only half of the subunits are bound to nucleotide under saturating conditions.

Table 7. Stoichiometry of chaperonins nucleotide complexes

condition	nucleotides/ oligomer	
	filter-binding	gel filtration
<u>TRiC:</u>		
[α ³² P]-ATP	9.6 (± 0.5)	7.1 (± 1.3)
[α ³² P]-8-N ₃ -ATP, x-linked	-	6.4 (± 2.3)
[α ³² P]-ATP + AlF _x	-	9.1 (± 0.8)
[α ³² P]- 8-N ₃ -ATP + AlF _x , x-linked	-	8.6 (± 1.0)
<u>GroEL/ES:</u>		
[α ³² P]-ATP	8.4 (± 0.6)	2.5 (± 0.3)
[α ³² P]-8-N ₃ -ATP, x-linked	-	7.8 (± 1.0)
[α ³² P]-ATP + AlF _x	-	7.2 (± 0.4)
[α ³² P]- 8-N ₃ -ATP + AlF _x , x-linked	-	14.4 (± 3.1)

As a control, the same stoichiometry experiments were performed for GroEL, whose nucleotide cycle has been established by previous analyses^{29,120,121}. GroEL incubated with its lid-cofactor GroES and α -[^{32}P]-ATP was found to bind two or three nucleotides, as determined by gel filtration, and eight nucleotides according to the filter-binding assay (**Table 7**). The latter experiment seems more suitable under those conditions (as discussed above) and corresponds well with data from previous studies¹²⁰. Although GroEL/ES bound to seven nucleotides when incubated with α -[^{32}P]-ATP and AlF_x (**Table 7**), cross-linking of α -[^{32}P]-8N₃-ATP to GroEL/ES in the presence of AlF_x resulted in fourteen bound nucleotides per oligomeric complex (**Table 7**). In agreement with previous studies¹²¹, all subunits of GroEL are therefore occupied with nucleotide under those conditions. This result suggests that 8-N₃-ATP cross-links to chaperonins in a quantitative manner. It furthermore proves, that the gel filtration analysis is an appropriate method to determine the stoichiometry of

nucleotide binding in chaperonins, given that the complex has been stabilized by cross-linking or addition of AlF_x .

In summary it can be concluded that only half of the TRiC subunits bind ATP under saturating conditions and even in the presence of ATP and AlF_x , were TRiC adopts a conformation with both rings closed⁷² only half of its subunits are bound to nucleotide. In combination with the cross-link data this strongly suggests that only a subset of all TRiC subunits bind nucleotide under saturating conditions. Our data are consistent with a model where nucleotides are only bound to CCT4, 5, 1 and 2 in both rings.

ATP binding to CCT6 is dispensable for TRiC's catalytic cycle *in vivo*

Motivated by our *in vitro* data, we proceeded to test the possibility that ATP binding to a subset of the TRiC subunits might not be required for TRiC activity *in vivo*.

In the eukaryotic cytosol, TRiC cooperates with chaperones from the Hsp70 family and the jellyfish-like chaperone GiM/prefoldin in the co-translational folding pathway of a variety of essential cytosolic proteins, such as the cytoskeletal proteins actin and tubulin⁴⁵⁻⁴⁷. Chromosomal deletion of either TRiC subunit by itself is lethal in haploid cells of the yeast *S. cerevisiae*, but it can be complemented by providing the respective *cctx*-gene on a plasmid. Lin *et al.*, (1997)⁹¹ have previously reported that the *cct6-24* mutant of *S. cerevisiae*, in which the GDGTT putative ATP binding motif has been exchanged for AAAAA, was viable and grew normally on a variety of media at various temperatures⁹¹. The GDGTT-motif is conserved in all chaperonin sequences¹²² and mutation of the conserved Asp-87 in this motif is sufficient to abolish ATP binding in GroEL¹²³. In order to investigate whether this finding for CCT6 could be extended to all other TRiC subunits, we constructed and tested mutants in *cct1* – *cct8* bearing alanine replacements in the putative ATP binding motifs in *S. cerevisiae* (Stephen Tam, unpublished data). It turned out that, in contrast to CCT6, ATP binding to all other TRiC subunits is required for viability in yeast since introduction of the respective plasmids carrying the GDGTT/AAAAA replacement could not restore viability. It is intriguing, however, that ATP binding to CCT6 seems not to be essential for function, especially since it corresponds well with the *in vitro* finding that ATP cannot be cross-linked to CCT6 efficiently even at high ATP concentrations (**Fig. 22E**). In order to prove that ATP binding and hydrolysis in CCT6 is not only dispensable for viability but also not required for an efficient

catalytic cycle of TRiC, we compared the rate of co-translational actin folding in a wild-type and mutant yeast background (**Fig. 27**). To this end we performed a pulse-chase experiment in a haploid yeast-strain that carried a deletion in the chromosomal copy of *cct6* and contained either the wild-type or the mutant allele *cct6-24* on a plasmid (**Fig. 27A**). The folding rate of newly translated pulse-labeled actin was examined by pull-down of native actin using DNaseI covalently attached to beads⁹⁹ at different time-points during the pulse and after the chase (**Fig. 27B**). In a parallel approach, we immunoprecipitated TRiC to observe the kinetics of transient association and dissociation of pulse-labeled, co-immunoprecipitated actin with TRiC (**Fig. 27C**). As apparent from **Figure 27B** and **C**, both the rate of co-translational actin folding as well as the kinetics of actin cycling through TRiC are essentially the same in the wild-type and mutant backgrounds. This result suggests that ATP binding to CCT6 is dispensable for TRiC's catalytic cycle *in vivo*.

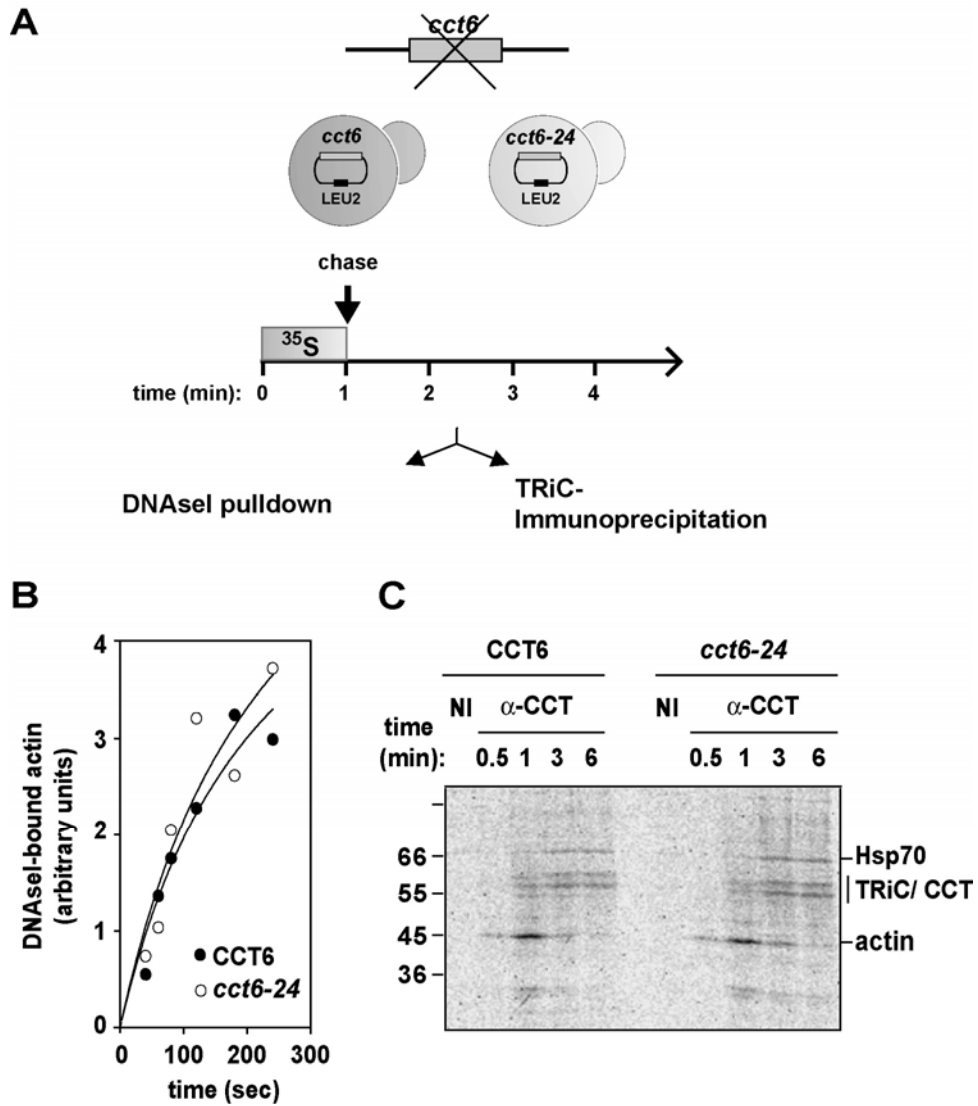


Figure 27. ATP binding to CCT6 is dispensable for TRiC's catalytic cycle *in vivo*. (A) Experimental strategy. (B) ATP binding to CCT6 is not required for efficient actin folding in the cytosol. Rate of co-translational folding of pulse-labeled actin in yeast cells expressing either the wild type CCT6-subunit or the mutant version CCT6_{GDGTT/AAAAA}. The error bars represent the standard error of measurement (SEM). (C) ATP binding to CCT6 is not required for TRiC's catalytic cycle. The association and dissociation kinetic of pulse-labeled actin and TRiC was determined by TRiC immunoprecipitation. An autoradiogram is shown and radiolabeled bands corresponding to immunoprecipitated TRiC as well as co-immunoprecipitated actin and Hsp70 are marked.

IV. Discussion

IV.1. Allosteric regulation in group II chaperonins

Opening and closure of the built-in lid in group II chaperonins requires the coordinated action of all subunits within a ring, controlled by ATP binding and hydrolysis in the distant equatorial domains. The lid segments are required to integrate the subunits within a ring into an allosteric unit and therefore synchronize *intra*-ring conformational changes. Although the lid is located far away from the *inter*-ring contacts, the lid structure also plays a role in modulating *inter*-ring communication.

Similar allosteric coupling within the subunits of a ring is achieved by different strategies in Group I and group II chaperonins

The phenomenon of nested cooperativity has been observed in all chaperonins. Strikingly, we find that group I and group II chaperonins employ different strategies to establish the same type of allostery. Allosteric coupling of subunits within one ring is intrinsic to GroEL and only modulated by the GroES cofactor^{58-60,64,111}. Instead, we find that group II chaperonins depend on their built-in lids to coordinate *intra*-ring communication. The requirement for the built-in lid to achieve positive cooperativity in group II chaperonins is surprising, given their overall similarity with their bacterial counterparts. However, in GroEL the lid is already preformed, and lid closure merely requires an increased affinity of GroEL for its cofactor. Instead, in group II chaperonins, the lid must be created in a coordinated manner during ATP hydrolysis within the ring. It is tempting to speculate that the structural challenges associated with having an integrated lid may be incompatible with the allosteric regulation of bacterial chaperonins, thus forcing the emergence of novel allosteric networks in group II chaperonins.

Allosteric network in group I chaperonins

In the bacterial chaperonin GroEL, positive cooperativity depends on a salt-bridge network connecting R197 in the apical domain of one subunit with E386 in the intermediate domain of the neighboring subunit^{59,124-126}. This salt-bridge network,

established in the nucleotide-free T-state, creates physical tension within the subunits of one ring. Conformational changes upon ATP binding to one subunit break this tight salt bridge as the respective intermediate domain moves downwards in order to contribute residues for the coordination of ATP. This ATP induced conformational change in the intermediate domain is stabilized by the formation of a new salt bridge between E386 and the residue K80 in the equatorial domain of the neighboring subunit. The apical domains which are no longer fixed to neighboring intermediate domains are much more flexible and relax simultaneously to a conformation described as the R state with high affinity for ATP and the lid cofactor GroES¹²⁵.

Allosteric network of group II chaperonins

Although the structural basis of allosteric coupling in group II chaperonins must await a better characterization of the ATP-bound, open state, it is clear that amino acids contributing to the salt bridge network between apical and intermediate domains in GroEL are not conserved in TRiC and the thermosome. Supported by our finding that lid-less chaperonins are no longer coupled by positive cooperativity, a picture emerges in which the corresponding network has been relocated upwards into the apical protrusions. Notably, in contrast to group I chaperonins in this system the nucleotide-free T-state is relaxed, while the closed R-state induced by ATP-hydrolysis appears to be under physical tension, since the apical domains have to come in close proximity to form the lid structure. These distinct allosteric strategies of group II chaperonins may originate from the unique mechanistic requirements of having a built-in lid. Since ATP hydrolysis hides the substrate binding sites from the cavity (**Fig. 11, Fig. 13 and Fig. 15**), it is possible that incorporating the lid into the allosteric network may help ensure that the lid is formed prior to substrate release.

Influence of the built-in lid on *inter-ring* communication

Our analysis indicated that the built-in lid also affects *inter-ring* communication (**Fig. 21**). We envision two possible models that could account for these observations. First, removing the lid could abolish both positive and negative allosteric coupling so that all 16 subunits bind and hydrolyze ATP independently. However, since all subunits in both rings would be hydrolyzing ATP simultaneously under saturating conditions, this scenario would predict that the lid-less variants reach a higher maximal hydrolysis rate, v_{\max} , than intact chaperonins. Indeed, such behavior has been

observed for GroEL mutants with distorted *inter*-ring communication^{127,128}. However, the results presented in chapter III.3. of the present work are not consistent with this possibility (compare **Fig. 19A, B** and **Fig. 21B, C**). Accordingly, an alternative model is favored whereby the formation of a functional lid structure is not required for negative cooperativity, but serves to slow down the ATPase cycle by stabilizing the closed state. This model is consistent with different lines of evidence obtained for TRiC and the archaeal thermosome which indicate that lid opening is the rate-limiting step in the ATPase cycle^{72,129}. First, steady state measurements at high ATP concentrations indicate that for TRiC the closed post-hydrolysis state dominates the kinetic ATPase cycle⁷². In agreement with this idea, kinetic analysis of the thermosome revealed that ADP + Pi release are rate-limiting, leading to a long-lived post-hydrolysis state¹²⁹; furthermore, the *trans*-ring is prevented from hydrolyzing ATP until Pi and ADP are released from the *cis*-ring. Taken together with our results, these findings suggest that formation of the closed lid structure delays the release of the hydrolysis products ADP and Pi, thus extending the duration of the ATPase cycle in the *cis*-ring. At saturating ATP concentrations this would effectively slow down the steady state ATPase rate, as observed experimentally for both TRiC (**Fig. 19A**) and Mm-Cpn (**Fig. 19B**). Since the lid-less chaperonins do not have a closed lid to slow down release of ADP and Pi in the *cis*-ring, the inhibition of hydrolysis in the *trans*-ring would not be observed. This is consistent with the faster turnover rate observed at high ATP concentrations for the lid-less chaperonins (**Fig. 21B, C**). In addition to explaining all available data, this model reveals that the lid acts as a timing device that regulates the duration of the folding-active state.

Our study provides a striking example of how incorporation of a slight structural variation, namely the built-in lid, into the conserved chaperonin architecture forced the archaeal and eukaryotic complexes to evolve a different strategy in order to maintain their regulation through nested cooperativity. Defining the structural basis of *inter*-subunit communication in eukaryotic and archaeal chaperonins may thus provide insights into the plasticity of allosteric networks.

IV.2. Positive cooperativity in group II chaperonins propagates sequentially

Lid formation in group II chaperonins could occur in two different ways. On the one hand it could involve a concerted interaction between all apical protrusions according to the MWC-model¹¹³. On the other hand, based on the KNF-model¹¹⁴ the conformational change could propagate sequentially via domino-like interactions between apical protrusions. Our finding that subunits in the hetero-oligomeric chaperonin TRiC display different affinities for ATP strongly suggests a sequential type of allosteric transition.

What is the structural feature common to all high affinity subunits?

The data presented in the present study suggest the existence of a gradient of affinities within the subunits of TRiC, whereby CCT5 has the highest affinity followed by CCT 4, CCT1 and CCT2, whereas CCT 3, CCT6, CCT7 and CCT8 are classified as low-affinity subunits (**Fig. 24**). The structural feature that discriminates low- and high-affinity subunits remains to be identified. Sequence alignment of the eight different CCT genes of *S. cerevisiae* shows an overall low level of sequence identity (25-35%), with the highest conservation being found in the regions harboring residues responsible for ATP binding and hydrolysis¹¹⁸. **Figure 28** shows a sequence alignment of all eight yeast CCT proteins, focusing on the regions that, according to the crystal structure of the thermosome beta subunit (*T.a. beta*)³⁴, form the ATP binding pocket. It is apparent from this alignment that most of the residues involved in coordinating the nucleotide are highly conserved. CCT6 and CCT8 show a few discrepancies, but it still remains to be biochemically proven that these amino acid changes result in lower affinity for ATP. High resolution structural information on the hetero-oligomeric TRiC complex will be necessary to elucidate the nature of the differences that must exist between the conserved ATP binding pockets of the different subunits.

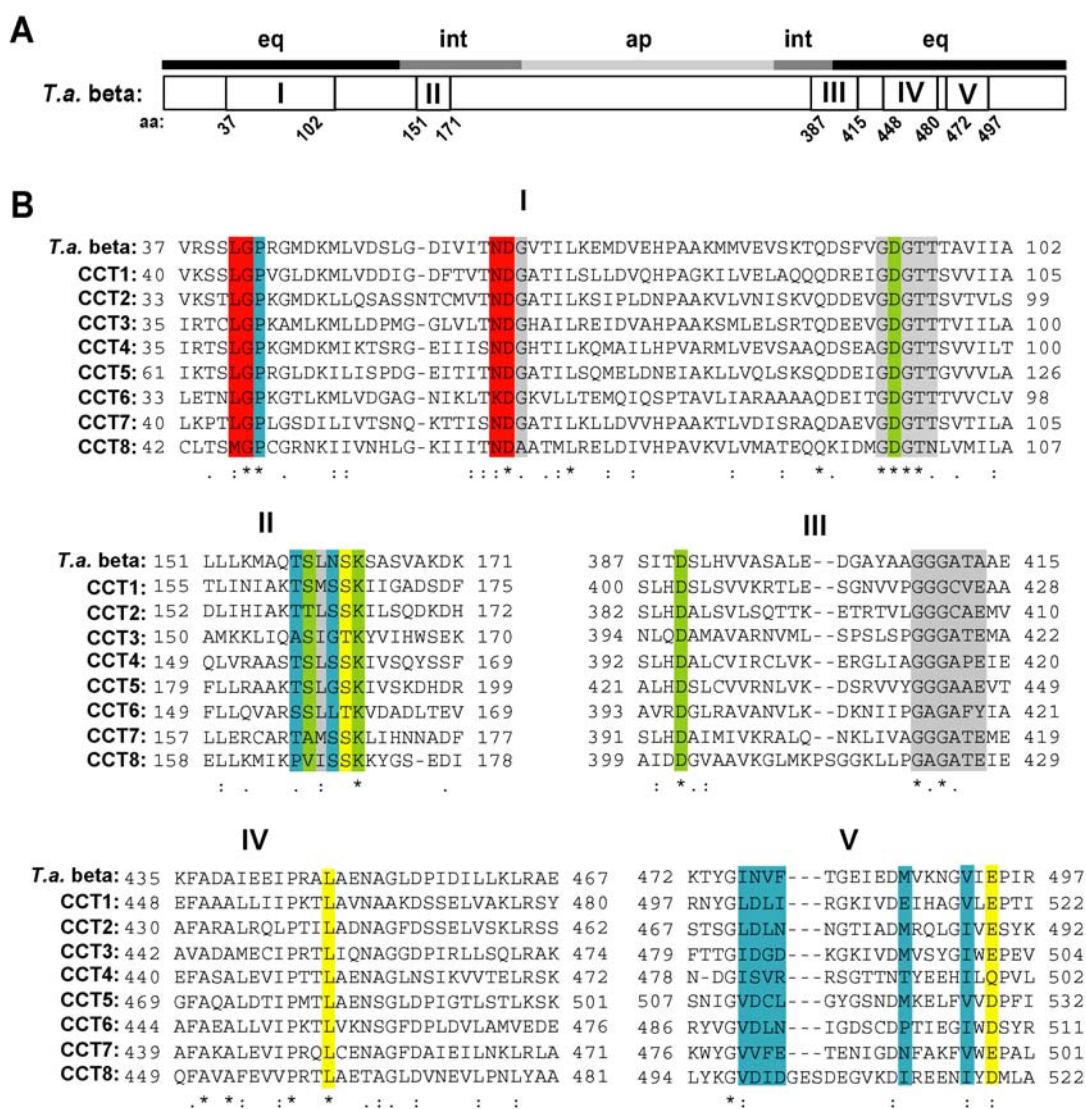


Figure 28. Alignment of the amino acid sequence from the nucleotide binding pocket of CCT1-8 from *S. cerevisiae*. (A) Schematic presentation of the domain arrangement in the linear amino acid sequence of the beta subunit of the thermosome from *T. acidophilum*. The regions (I–V) that harbor residues contributing to the ATP binding pocket are highlighted. *T.a. beta*: *T. acidophilum* thermosome beta-subunit; eq: equatorial domain, int: intermediate domain, ap: apical domain; aa: amino acid. (B) Sequence alignment of the regions I-V highlighted in (A) between the beta subunit of the thermosome and all eight subunits of the TRiC complex (CCT1- CCT8) from *S. cerevisiae*. Residues that, according to the crystal structure of the thermosome beta-subunit, directly interact with nucleotide are highlighted in color. Red: coordinate phosphates; blue: interact with purin-base; yellow: interacts with ribose; green: coordinates magnesium; grey: no direct contact but establish the pocket like structure. The sequence alignment was generated using the ClustalW software¹³⁸. * = identical residues in all aligned sequences, : = functionally conserved residues in all aligned sequences.

The order of sequential ATP-induced allosteric transitions in one ring of TRiC

Interpretation of our data in the light of the proposed subunits arrangement within a ring in TRiC⁹¹ (**Fig. 24** and **29A**) indicates that the high affinity subunits might not be located next to each other. A typical KNF-type transition¹¹⁴ in which the highest affinity subunit would bind to ATP first and induce a transition in its immediate neighbor resulting in sequential propagation of nucleotide binding seems therefore unlikely.

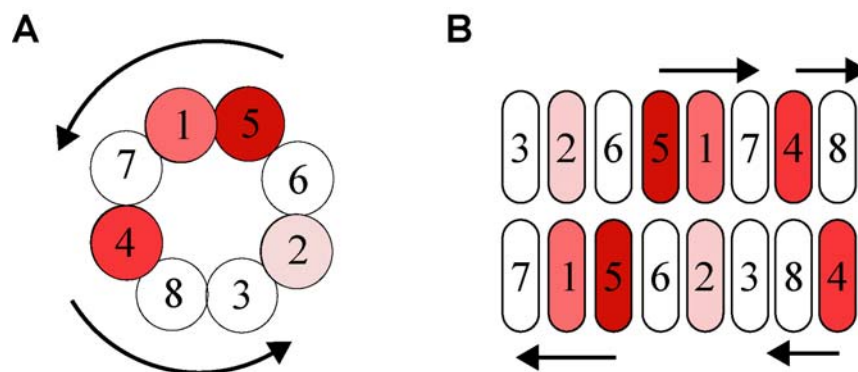


Figure 29. Model of the subunit arrangement in the TRiC complex. (A) Proposed subunit arrangement within one ring of TRiC according to Liou and Willison, 1997¹³⁷. The relative affinity of the different subunits for nucleotide is expressed by different shades of red. Dark red = high affinity, light red = intermediate affinity, white = low affinity. The arrows indicate the proposed direction of the sequential cooperative conformational change within one ring of TRiC. (B) Proposed *inter-ring* contacts according to Martin-Benito *et al.*, 2007¹³⁰. The coloring of the subunits corresponds to (A).

However, it needs to be emphasized that in the present study the occupation of the subunits with ATP rather than conformational changes were investigated. Cryo-EM analysis of one ring in TRiC revealed the presence of asymmetry at low ATP concentrations¹¹⁹. Conformational changes started in the region of CCT1/7/4/8 and ended at CCT2 (**Fig. 29A**). The data presented here confirm the suggested sequential allosteric transition and allow completing the model by providing two pieces of information: First, CCT5 can be assigned as the subunit that binds to ATP first, and second the transition propagates counter-clockwise via the subunits CCT4, 1 and 2 ending at CCT6. Intriguingly, the cryo-EM study¹¹⁹ reports retained symmetry at intermediate ATP concentrations, when only the high affinity subunits are bound to ATP according to the cross-link experiments. This suggests that conformational

changes can propagate sequentially throughout the ring and result in a symmetrically closed active state although only every second or third subunit actually binds to nucleotide. According to this model, positive cooperativity between neighboring subunits is strong enough to induce conformational changes even in subunits without bound nucleotide.

A recent report provides insight in the *inter-ring* arrangement of TRiC subunits¹³⁰. It appears that the up/down *inter-ring* communication always involves two different CCT subunits in all eight positions¹³⁰ (**Fig. 29B**). Intriguingly, the two rings are rotated against each other such that the subunit with highest affinity for ATP, namely CCT5 sits directly on top of CCT6, the subunit with lowest affinity for ATP and dispensable for TRiC's catalytic cycle in yeast. How this distinct *inter-ring* arrangement affects the function of TRiC as a two-stroke molecular machine will be subject of future investigations.

Given that substrate proteins might be bound to more than one subunit within a ring^{86, 117} a conformational change that occurs sequentially throughout the subunits of a ring can impact the mechanism of substrate release from the binding sites and may therefore influence the folding mechanism. It might also enable the TRiC complex to sequester parts of complex substrates until all players are assembled to a final structure.

Do the low affinity subunits fulfill a regulatory function?

Why only four of the eight subunits bind to ATP under saturating conditions remains to be investigated. Obviously, it would save energy if ATP hydrolysis in four out of the eight subunits in TRiC were sufficient to promote substrate folding. However, the energy supply of the cytoplasm is likely not to be limiting under conditions in which protein synthesis occurs. Additionally, one would expect less conservation in the ATP binding pockets if they completely lost their essential function during evolution.

One alternative explanation could be that the affinity of the subunits for nucleotide changes upon interaction of TRiC with a co-factor. If occupation of all eight subunits in TRiC significantly influences the turnover rate of this molecular machine, changing the nucleotide occupation could provide a regulatory switch. GimC has been discussed as a possible co-chaperone for TRiC as the release of actin from TRiC is five- to eightfold slower in GimC-deficient cells⁴⁵, suggesting that GimC activates TRiC's catalytic cycle. Additionally, the Phlp1 protein was shown to bind to TRiC in

its native conformation^{131,132} and to inhibit its ATPase activity when present in a trimetric complex with TRiC and substrate proteins, such as actin or tubulin¹³¹. It would be interesting to test biochemically whether those two potential co-factors change the occupation pattern of TRiC under saturating ATP concentrations.

IV.3. The apical protrusions and the conformational cycle of group II chaperonins

This study uncovers a remarkable degree of mechanistic and functional conservation between group II chaperonins from eukaryotic and archaeal origin. In both cases, the built-in lid is in the open state upon ATP binding and closes during ATP hydrolysis. In the following section the data are discussed in context of the ATPase cycle of group II chaperonins, focusing on two steps in more detail, namely ATP binding and ATP hydrolysis.

Conformational changes in group II chaperonins upon binding of ATP

As illustrated in **Figure 30**, group II chaperonins are predominantly in the open conformation in the absence of nucleotide. Structural analysis of the isolated apical domain of mouse CCT γ ¹³³ as well as the apical domains in the thermosome^{134,135} revealed that the tips of the apical protrusions have little propensity to adopt a defined structure in solution. This observation suggests that the apical protrusions may provide *inter*-subunit interactions in different stages of TRiC's functional cycle and corresponds well with their function in establishing positive cooperativity within the subunits of a ring. Since positive and negative allosteric coupling between subunits is achieved at the level of ATP binding⁷⁹ we propose the existence of a distinct conformation of the helical protrusions in the ATP-bound pre-hydrolysis state. At this stage of the conformational cycle of group II chaperonins the apical protrusions reside in the "open" conformation and are likely to form tight contacts between neighboring subunits which are responsible for the allosteric coupling. In accordance with the results presented in this work (**Fig. 13** and **Fig. 15**), the substrate binding sites are available in the ATP-bound state, however, changes in the affinity for substrate might occur. Additionally, ATP binding induces a conformational change within the N- and C-terminus of the subunits that renders those regions, located in the equatorial domains, protected from protease digestion (**Fig. 10C**). A correlation between those

structural rearrangements within the *inter*-ring contacts and negative allosteric communication between the rings seems likely but needs to be proven.

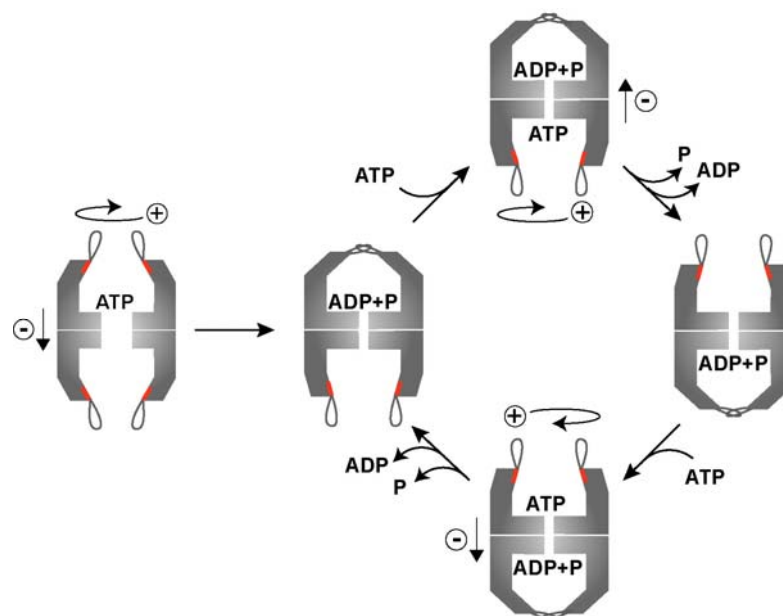


Figure 30. The built-in lid controls the ATPase cycle of group II chaperonins. ATP binding to subunits in one ring is a cooperative event communicated by the apical protrusions. Subsequent formation of the iris-like lid during ATP hydrolysis stabilizes an asymmetric conformation with strong negative cooperativity between the rings, which enables group II chaperonins to function as a “two-stroke” engine.

ATP hydrolysis is the central step in the folding cycle of group II chaperonins

Steady state and kinetic measurements for TRiC^{79,80} and the thermosome¹²⁹ indicate that the ATP-bound, open state is rather transient. Subsequent ATP hydrolysis initiates significant conformational rearrangements (**Fig. 30**) in both the substrate binding sites and the apical protrusions which lead to the ejection of bound substrate protein into the central chamber (**Fig. 11**, **Fig. 13** and **Fig. 15**) and to the formation of the iris-like lid structure²⁰ (**Fig. 7** and **Fig. 9**). Future research is aimed towards elucidating the precise sequence of the distinct conformational changes during ATP hydrolysis. To this end, single tryptophan residues were introduced in the potential substrate binding site⁸⁶ and the apical protrusions of Mm-Cpn, utilizing the advantage that Mm-Cpn does not contain any tryptophan residue in its primary sequence. Measuring changes in tryptophan fluorescence in these mutant forms upon addition of nucleotide using a stopped flow apparatus will provide insight into the order of events

corresponding to lid closure and substrate release respectively. Notably, the finding that substrate is ejected in the central cavity of Mm-Cpn and does not remain bound to the initial substrate binding sites as previously suggested¹¹⁷ points to an Anfinsen-cage like function of the central cavity¹¹⁰.

What is the signal for re-opening of the lid?

The lid probably remains closed in the post-hydrolysis ADP+Pi state since re-opening of the stable iris-like lid structure seems to be the rate-limiting step in the conformational cycle¹²⁹(**Fig. 30**). Due to negative *inter*-ring cooperativity^{79,129,136}, ATP hydrolysis in the *trans*-ring can only occur once the products of ATP hydrolysis have dissociated from the *cis*-ring, although the precise mechanism that unravels the stable lid structure as well as the signal that induces lid opening remains undefined.

Because the closed conformation is the folding-active state lid opening upon ADP and Pi release serves as a timer mechanism that regulates the length of substrate encapsulation in the folding chamber. Interestingly, despite having similar mechanisms, TRiC and Mm-Cpn have strikingly different ATP turnover rates (compare **Fig. 19A** and **B**), suggesting that the substrate residence time within the chamber may be fine-tuned to suit the folding requirements of different cellular environments.

V. Summary

Chaperonins are highly allosteric double-ring ATPases that mediate cellular protein folding. ATP binding and hydrolysis control opening and closing of the central chaperonin chamber which transiently provides a protected environment for protein folding. During evolution, two distinct strategies to close the chaperonin chamber have emerged. Archaeal and eukaryotic chaperonins contain a built-in lid, whereas bacterial chaperonins use a ring-shaped cofactor as a detachable lid.

The present work contributes to the current mechanistical understanding of group II chaperonins by unraveling key functions of the built-in lid. In addition to physically encapsulating the substrate, the lid-forming apical protrusions also play a key role in regulating chaperonin function and ensuring its activity as a “two-stroke” molecular machine. By comparative investigation of two distinct chaperonin systems, namely TRiC and Mm-Cpn, this study uncovers a remarkable degree of mechanistic and functional conservation between group II chaperonins from eukaryotic and archaeal origin, despite their evolutionary distance.

In particular the following conclusions can be drawn from the present work:

- 1) The helical protrusions of group II chaperonins assemble into an iris-like structure that indeed functions as a lid on top of the cavity and is necessary to physically encapsulate substrate proteins. Substrate is released from the binding sites during a conformational change that is induced by ATP hydrolysis and occurs independently of but with similar timing as lid formation. This observation argues against a folding mechanism whereby the substrate remains associated with the binding sites during the folding cycle.
- 2) In both eukaryotic and archaeal chaperonins the lid-forming segments are required to integrate the subunits within a ring into an allosteric unit and, therefore, to synchronize *intra*-ring conformational changes. The concerted action of subunits within a ring appears essential for optimal chaperonin function since lid-less

chaperonins cannot promote efficient substrate folding, even though they are still able to hydrolyze ATP.

- 3) In both eukaryotic and archaeal chaperonins negative *inter*-ring coupling leads to the alternation of allosteric states that causes group II chaperonins to function as “two-stroke” motors. Although the lid is located far away from the *inter*-ring contacts, the lid structure also plays a role in modulating *inter*-ring communication.
- 4) The discovery of a gradient of affinities for ATP within the eight different TRiC subunits provides biochemical evidence for a sequential model of the positive cooperative transition within a ring of the eukaryotic chaperonin TRiC. Moreover it is suggested that ATP binding to all eight subunits might not be required for an optimal folding cycle.

VI. References

1. Thomas, P.J., Qu, B.H. and Pedersen, P.L. Defective protein folding as a basis of human disease. *Trends Biochem Sci* **20**, 456-9 (1995).
2. Dobson, C.M. Protein misfolding, evolution and disease. *Trends Biochem Sci* **24**, 329-32 (1999).
3. Anfinsen, C.B. Principles that govern the folding of protein chains. *Science* **181**, 223-30 (1973).
4. Dobson, C.M. & Hore, P.J. Kinetic studies of protein folding using NMR spectroscopy. *Nat Struct Biol* **5**, 504-7 (1998).
5. Dobson, C.M. Protein folding. Solid evidence for molten globules. *Curr Biol* **4**, 636-40 (1994).
6. Elowitz, M.B., Surette, M.G., Wolf, P.E., Stock, J.B. and Leibler, S. Protein mobility in the cytoplasm of Escherichia coli. *J Bacteriol* **181**, 197-203 (1999).
7. Zimmerman, S.B. and Trach, S.O. Estimation of macromolecule concentrations and excluded volume effects for the cytoplasm of Escherichia coli. *J Mol Biol* **222**, 599-620 (1991).
8. Minton, A.P. Protein folding: Thickening the broth. *Curr Biol* **10**, R97-9 (2000).
9. Zimmerman, S.B. and Minton, A.P. Macromolecular crowding: biochemical, biophysical, and physiological consequences. *Annu Rev Biophys Biomol Struct* **22**, 27-65 (1993).
10. Ellis, R.J. and Minton, A.P. Protein aggregation in crowded environments. *Biol Chem* **387**, 485-97 (2006).
11. Hartl, F.U. and Hayer-Hartl, M. Molecular chaperones in the cytosol: from nascent chain to folded protein. *Science* **295**, 1852-8 (2002).
12. Frydman, J. Folding of newly translated proteins in vivo: the role of molecular chaperones. *Annu Rev Biochem* **70**, 603-47 (2001).
13. Agashe, V.R. and Hartl, F.U. Roles of molecular chaperones in cytoplasmic protein folding. *Semin Cell Dev Biol* **11**, 15-25 (2000).
14. Young, J.C., Agashe, V.R., Siegers, K. and Hartl, F.U. Pathways of chaperone-mediated protein folding in the cytosol. *Nat Rev Mol Cell Biol* **5**, 781-91 (2004).
15. Hartl, F.U. Molecular chaperones in cellular protein folding. *Nature* **381**, 571-9 (1996).

16. Bukau, B. & Horwich, A.L. The Hsp70 and Hsp60 chaperone machines. *Cell* **92**, 351-66 (1998).
17. Neupert, W. and Herrmann, J.M. Translocation of proteins into mitochondria. *Annu Rev Biochem* (2007).
18. Bukau, B., Weissman, J. and Horwich, A. Molecular chaperones and protein quality control. *Cell* **125**, 443-51 (2006).
19. Hohfeld, J., Cyr, D.M. and Patterson, C. From the cradle to the grave: molecular chaperones that may choose between folding and degradation. *EMBO Rep* **2**, 885-90 (2001).
20. Mayer, M.P. and Bukau, B. Hsp70 chaperones: cellular functions and molecular mechanism. *Cell Mol Life Sci* **62**, 670-84 (2005).
21. Macario, A.J., Lange, M., Ahring, B.K. and De Macario, E.C. Stress genes and proteins in the archaea. *Microbiol Mol Biol Rev* **63**, 923-67, table of contents (1999).
22. Szabo, A., Langer, T., Schroder, H., Flanagan, J., Bukau, B. and Hartl, F.U. The ATP hydrolysis-dependent reaction cycle of the *Escherichia coli* Hsp70 system DnaK, DnaJ, and GrpE. *Proc Natl Acad Sci U S A* **91**, 10345-9 (1994).
23. McCarty, J.S., Buchberger, A., Reinstein, J. and Bukau, B. The role of ATP in the functional cycle of the DnaK chaperone system. *J Mol Biol* **249**, 126-37 (1995).
24. Glover, J.R. and Lindquist, S. Hsp104, Hsp70, and Hsp40: a novel chaperone system that rescues previously aggregated proteins. *Cell* **94**, 73-82 (1998).
25. Pfund, C., Lopez-Hoyo, N., Ziegelhoffer, T., Schilke, B.A., Lopez-Buesa, P., Walter, W.A., Wiedmann, M. and Craig, E.A. The molecular chaperone Ssb from *Saccharomyces cerevisiae* is a component of the ribosome-nascent chain complex. *EMBO J* **17**, 3981-9 (1998).
26. Yan, W., Schilke, B., Pfund, C., Walter, W., Kim, S. and Craig, E.A. Zuotin, a ribosome-associated DnaJ molecular chaperone. *EMBO J* **17**, 4809-17 (1998).
27. Gautschi, M., Lilie, H., Funfschilling, U., Mun, A., Ross, S., Lithgow, T., Rucknagel, P. and Rospert, S. RAC, a stable ribosome-associated complex in yeast formed by the DnaK-DnaJ homologs Ssz1p and zuotin. *Proc Natl Acad Sci U S A* **98**, 3762-7 (2001).
28. Huang, P., Gautschi, M., Walter, W., Rospert, S. and Craig, E.A. The Hsp70 Ssz1 modulates the function of the ribosome-associated J-protein Zuo1. *Nat Struct Mol Biol* **12**, 497-504 (2005).

29. Horwich, A.L., Farr, G.W. and Fenton, W.A. GroEL-GroES-mediated protein folding. *Chem Rev* **106**, 1917-30 (2006).
30. Xu, Z., Horwich, A.L. and Sigler, P.B. The crystal structure of the asymmetric GroEL-GroES-(ADP)₇ chaperonin complex. *Nature* **388**, 741-50 (1997).
31. Ellis, R.J. Protein folding: importance of the Anfinsen cage. *Curr Biol* **13**, R881-3 (2003).
32. Tang, Y.C., Chang, H.C., Roeben, A., Wischnewski, D., Wischnewski, N., Kerner, M.J., Hartl, F.U. and Hayer-Hartl, M. Structural features of the GroEL-GroES nano-cage required for rapid folding of encapsulated protein. *Cell* **125**, 903-14 (2006).
33. Shtilerman, M., Lorimer, G.H. and Englander, S.W. Chaperonin function: folding by forced unfolding. *Science* **284**, 822-5 (1999).
34. Ditzel, L., Lowe, J., Stock, D., Stetter, K.O., Huber, H., Huber, R. and Steinbacher, S. Crystal structure of the thermosome, the archaeal chaperonin and homolog of CCT. *Cell* **93**, 125-38 (1998).
35. Shomura, Y., Yoshida, T., Iizuka, R., Maruyama, T., Yohda, M. and Miki, K. Crystal structures of the group II chaperonin from *Thermococcus* strain KS-1: steric hindrance by the substituted amino acid, and inter-subunit rearrangement between two crystal forms. *J Mol Biol* **335**, 1265-78 (2004).
36. Albanese, V., Yam, A.Y., Baughman, J., Parnot, C. and Frydman, J. Systems analyses reveal two chaperone networks with distinct functions in eukaryotic cells. *Cell* **124**, 75-88 (2006).
37. Frydman, J., Erdjument-Bromage, H., Tempst, P. and Hartl, F.U. Co-translational domain folding as the structural basis for the rapid de novo folding of firefly luciferase. *Nat Struct Biol* **6**, 697-705 (1999).
38. Parsell, D.A. and Lindquist, S. The function of heat-shock proteins in stress tolerance: degradation and reactivation of damaged proteins. *Annu Rev Genet* **27**, 437-96 (1993).
39. Agashe, V.R., Guha, S., Chang, H.C., Genevaux, P., Hayer-Hartl, M., Stemp, M., Georgopoulos, C., Hartl, F.U. and Barral, J.M. Function of trigger factor and DnaK in multidomain protein folding: increase in yield at the expense of folding speed. *Cell* **117**, 199-209 (2004).
40. Netzer, W.J. and Hartl, F.U. Recombination of protein domains facilitated by co-translational folding in eukaryotes. *Nature* **388**, 343-9 (1997).

41. Kramer, G., Rauch, T., Rist, W., Vorderwulbecke, S., Patzelt, H., Schulze-Specking, A., Ban, N., Deuerling, E. and Bukau, B. L23 protein functions as a chaperone docking site on the ribosome. *Nature* **419**, 171-4 (2002).
42. Maier, T., Ferbitz, L., Deuerling, E. and Ban, N. A cradle for new proteins: trigger factor at the ribosome. *Curr Opin Struct Biol* **15**, 204-12 (2005).
43. Deuerling, E., Schulze-Specking, A., Tomoyasu, T., Mogk, A. and Bukau, B. Trigger factor and DnaK cooperate in folding of newly synthesized proteins. *Nature* **400**, 693-6 (1999).
44. Ewalt, K.L., Hendrick, J.P., Houry, W.A. and Hartl, F.U. In vivo observation of polypeptide flux through the bacterial chaperonin system. *Cell* **90**, 491-500 (1997).
45. Siegers, K., Waldmann, T., Leroux, M.R., Grein, K., Shevchenko, A., Schiebel, E. and Hartl, F.U. Compartmentation of protein folding in vivo: sequestration of non-native polypeptide by the chaperonin-GimC system. *EMBO J* **18**, 75-84 (1999).
46. Siegers, K., Bolter, B., Schwarz, J.P., Bottcher, U.M., Guha, S. and Hartl, F.U. TRiC/CCT cooperates with different upstream chaperones in the folding of distinct protein classes. *EMBO J* **22**, 5230-40 (2003).
47. Thulasiraman, V., Yang, C.F. and Frydman, J. In vivo newly translated polypeptides are sequestered in a protected folding environment. *EMBO J* **18**, 85-95 (1999).
48. Frydman, J. and Hartl, F.U. Principles of chaperone-assisted protein folding: differences between in vitro and in vivo mechanisms. *Science* **272**, 1497-502 (1996).
49. Yam, A.Y., Albanese, V., Lin, H.T. and Frydman, J. Hsp110 cooperates with different cytosolic HSP70 systems in a pathway for de novo folding. *J Biol Chem* **280**, 41252-61 (2005).
50. Vainberg, I.E., Lewis, S.A., Rommelaere, H., Ampe, C., Vandekerckhove, J., Klein, H.L. and Cowan, N.J. Prefoldin, a chaperone that delivers unfolded proteins to cytosolic chaperonin. *Cell* **93**, 863-73 (1998).
51. Feldman, D.E., Thulasiraman, V., Ferreyra, R.G. and Frydman, J. Formation of the VHL-elongin BC tumor suppressor complex is mediated by the chaperonin TRiC. *Mol Cell* **4**, 1051-61 (1999).

52. Melville, M.W., McClellan, A.J., Meyer, A.S., Darveau, A. and Frydman, J. The Hsp70 and TRiC/CCT chaperone systems cooperate in vivo to assemble the von Hippel-Lindau tumor suppressor complex. *Mol Cell Biol* **23**, 3141-51 (2003).
53. Rospert, S. and Chacinska, A. Distinct yet linked: chaperone networks in the eukaryotic cytosol. *Genome Biol* **7**, 208 (2006).
54. Spiess, C., Meyer, A.S., Reissmann, S. and Frydman, J. Mechanism of the eukaryotic chaperonin: protein folding in the chamber of secrets. *Trends Cell Biol* **14**, 598-604 (2004).
55. Sigler, P.B., Xu, Z., Rye, H.S., Burston, S.G., Fenton, W.A. and Horwich, A.L. Structure and function in GroEL-mediated protein folding. *Annu Rev Biochem* **67**, 581-608 (1998).
56. Gutsche, I., Essen, L.O. and Baumeister, W. Group II chaperonins: new TRiC(k)s and turns of a protein folding machine. *J Mol Biol* **293**, 295-312 (1999).
57. Kubota, H., Hynes, G. and Willison, K. The chaperonin containing t-complex polypeptide 1 (TCP-1). Multisubunit machinery assisting in protein folding and assembly in the eukaryotic cytosol. *Eur J Biochem* **230**, 3-16 (1995).
58. Roseman, A.M., Chen, S., White, H., Braig, K. and Saibil, H.R. The chaperonin ATPase cycle: mechanism of allosteric switching and movements of substrate-binding domains in GroEL. *Cell* **87**, 241-51 (1996).
59. Ranson, N.A., Clare, D.K., Farr, G.W., Houldershaw, D., Horwich, A.L. and Saibil, H.R. Allosteric signaling of ATP hydrolysis in GroEL-GroES complexes. *Nat Struct Mol Biol* **13**, 147-52 (2006).
60. Ranson, N.A., Farr, G.W., Roseman, A.M., Gowen, B., Fenton, W.A., Horwich, A.L. and Saibil, H.R. ATP-bound states of GroEL captured by cryo-electron microscopy. *Cell* **107**, 869-79 (2001).
61. Horovitz, A., Fridmann, Y., Kafri, G. and Yifrach, O. Review: allostery in chaperonins. *J Struct Biol* **135**, 104-14 (2001).
62. Saibil, H.R., Horwich, A.L. and Fenton, W.A. Allostery and protein substrate conformational change during GroEL/GroES-mediated protein folding. *Adv Protein Chem* **59**, 45-72 (2001).
63. Swain, J.F. and Gierasch, L.M. The changing landscape of protein allostery. *Curr Opin Struct Biol* **16**, 102-8 (2006).
64. Yifrach, O. and Horovitz, A. Nested cooperativity in the ATPase activity of the oligomeric chaperonin GroEL. *Biochemistry* **34**, 5303-8 (1995).

65. Yifrach, O. and Horovitz, A. Transient kinetic analysis of adenosine 5'-triphosphate binding-induced conformational changes in the allosteric chaperonin GroEL. *Biochemistry* **37**, 7083-8 (1998).
66. Braig, K., Otwinowski, Z., Hegde, R., Boisvert, D.C., Joachimiak, A., Horwich, A.L. and Sigler, P.B. The crystal structure of the bacterial chaperonin GroEL at 2.8 Å. *Nature* **371**, 578-86 (1994).
67. Chandrasekhar, G.N., Tilly, K., Woolford, C., Hendrix, R. and Georgopoulos, C. Purification and properties of the groES morphogenetic protein of *Escherichia coli*. *J Biol Chem* **261**, 12414-9 (1986).
68. Weissman, J.S., Rye, H.S., Fenton, W.A., Beechem, J.M. and Horwich, A.L. Characterization of the active intermediate of a GroEL-GroES-mediated protein folding reaction. *Cell* **84**, 481-90 (1996).
69. Rye, H.S., Burston, S.G., Fenton, W.A., Beechem, J.M., Xu, Z., Sigler, P.B. and Horwich, A.L. Distinct actions of cis and trans ATP within the double ring of the chaperonin GroEL. *Nature* **388**, 792-8 (1997).
70. Rye, H.S., Roseman, A.M., Chen, S., Furtak, K., Fenton, W.A., Saibil, H.R. and Horwich, A.L. GroEL-GroES cycling: ATP and nonnative polypeptide direct alternation of folding-active rings. *Cell* **97**, 325-38 (1999).
71. Melki, R. and Cowan, N.J. Facilitated folding of actins and tubulins occurs via a nucleotide-dependent interaction between cytoplasmic chaperonin and distinctive folding intermediates. *Mol Cell Biol* **14**, 2895-904 (1994).
72. Meyer, A.S., Gillespie, J.R., Walther, D., Millet, I.S., Doniach, S. and Frydman, J. Closing the folding chamber of the eukaryotic chaperonin requires the transition state of ATP hydrolysis. *Cell* **113**, 369-81 (2003).
73. Gutsche, I., Holzinger, J., Rossle, M., Heumann, H., Baumeister, W. and May, R.P. Conformational rearrangements of an archaeal chaperonin upon ATPase cycling. *Curr Biol* **10**, 405-8 (2000).
74. Gutsche, I., Mihalache, O., Hegerl, R., Typke, D. and Baumeister, W. ATPase cycle controls the conformation of an archaeal chaperonin as visualized by cryo-electron microscopy. *FEBS Lett* **477**, 278-82 (2000).
75. Gutsche, I., Holzinger, J., Rauh, N., Baumeister, W. and May, R.P. ATP-induced structural change of the thermosome is temperature-dependent. *J Struct Biol* **135**, 139-46 (2001).

76. Iizuka, R., Yoshida, T., Shomura, Y., Miki, K., Maruyama, T., Odaka, M. and Yohda, M. ATP binding is critical for the conformational change from an open to closed state in archaeal group II chaperonin. *J Biol Chem* **278**, 44959-65 (2003).
77. Melki, R., Batelier, G., Soulie, S. and Williams, R.C., Jr. Cytoplasmic chaperonin containing TCP-1: structural and functional characterization. *Biochemistry* **36**, 5817-26 (1997).
78. Iizuka, R., Yoshida, T., Ishii, N., Zako, T., Takahashi, K., Maki, K., Inobe, T., Kuwajima, K. and Yohda, M. Characterization of archaeal group II chaperonin-ADP-metal fluoride complexes: implications that group II chaperonins operate as a "two-stroke engine". *J Biol Chem* **280**, 40375-83 (2005).
79. Kafri, G. and Horovitz, A. Transient kinetic analysis of ATP-induced allosteric transitions in the eukaryotic chaperonin containing TCP-1. *J Mol Biol* **326**, 981-7 (2003).
80. Kafri, G., Willison, K.R. and Horovitz, A. Nested allosteric interactions in the cytoplasmic chaperonin containing TCP-1. *Protein Sci* **10**, 445-9 (2001).
81. Schoehn, G., Hayes, M., Cliff, M., Clarke, A.R. and Saibil, H.R. Domain rotations between open, closed and bullet-shaped forms of the thermosome, an archaeal chaperonin. *J Mol Biol* **301**, 323-32 (2000).
82. Schoehn, G., Quaiter-Randall, E., Jimenez, J.L., Joachimiak, A. and Saibil, H.R. Three conformations of an archaeal chaperonin, TF55 from *Sulfolobus shibatae*. *J Mol Biol* **296**, 813-9 (2000).
83. Llorca, O., Smyth, M.G., Carrascosa, J.L., Willison, K.R., Radermacher, M., Steinbacher, S. and Valpuesta, J.M. 3D reconstruction of the ATP-bound form of CCT reveals the asymmetric folding conformation of a type II chaperonin. *Nat Struct Biol* **6**, 639-42 (1999).
84. Frydman, J., Nimmegern, E., Erdjument-Bromage, H., Wall, J.S., Tempst, P. and Hartl, F.U. Function in protein folding of TRiC, a cytosolic ring complex containing TCP-1 and structurally related subunits. *EMBO J* **11**, 4767-78 (1992).
85. Tian, G., Vainberg, I.E., Tap, W.D., Lewis, S.A. and Cowan, N.J. Specificity in chaperonin-mediated protein folding. *Nature* **375**, 250-3 (1995).
86. Spiess, C., Miller, E.J., McClellan, A.J. and Frydman, J. Identification of the TRiC/CCT substrate binding sites uncovers the function of subunit diversity in eukaryotic chaperonins. *Mol Cell* **24**, 25-37 (2006).

87. Feldman, D.E., Spiess, C., Howard, D.E. and Frydman, J. Tumorigenic mutations in VHL disrupt folding in vivo by interfering with chaperonin binding. *Mol Cell* **12**, 1213-24 (2003).
88. Tam, S., Geller, R., Spiess, C. and Frydman, J. The chaperonin TRiC controls polyglutamine aggregation and toxicity through subunit-specific interactions. *Nat Cell Biol* **8**, 1155-62 (2006).
89. Behrends, C., Langer, C.A., Boteva, R., Bottcher, U.M., Stemp, M.J., Schaffar, G., Rao, B.V., Giese, A., Kretzschmar, H., Siegers, K. and Hartl, F.U. Chaperonin TRiC promotes the assembly of polyQ expansion proteins into nontoxic oligomers. *Mol Cell* **23**, 887-97 (2006).
90. Kitamura, A., Kubota, H., Pack, C.G., Matsumoto, G., Hirayama, S., Takahashi, Y., Kimura, H., Kinjo, M., Morimoto, R.I. and Nagata, K. Cytosolic chaperonin prevents polyglutamine toxicity with altering the aggregation state. *Nat Cell Biol* **8**, 1163-70 (2006).
91. Lin, P. and Sherman, F. The unique hetero-oligomeric nature of the subunits in the catalytic cooperativity of the yeast Cct chaperonin complex. *Proc Natl Acad Sci U S A* **94**, 10780-5 (1997).
92. Miller, D.M., Delgado, R., Chirgwin, J.M., Hardies, S.C. and Horowitz, P.M. Expression of cloned bovine adrenal rhodanese. *J Biol Chem* **266**, 4686-91 (1991).
93. Lin, P., Cardillo, T.S., Richard, L.M., Segel, G.B. and Sherman, F. Analysis of mutationally altered forms of the Cct6 subunit of the chaperonin from *Saccharomyces cerevisiae*. *Genetics* **147**, 1609-33 (1997).
94. Weissman, J.S., Kashi, Y., Fenton, W.A. and Horwich, A.L. GroEL-mediated protein folding proceeds by multiple rounds of binding and release of nonnative forms. *Cell* **78**, 693-702 (1994).
95. Sambrook, J., Fritsch, E.F. and Maniatis, T. *Molecular Cloning - A Laboratory Manual, 2nd Edition.*, (Cold Spring Harbour Laboratory Press, 1989).
96. Laemmli, U.K. Cleavage of structural proteins during the assembly of the head of bacteriophage T4. *Nature* **227**, 680-5 (1970).
97. Weber, F. and Hayer-Hartl, M. Refolding of bovine mitochondrial rhodanese by chaperonins GroEL and GroES. *Methods Mol Biol* **140**, 117-26 (2000).
98. Martin, J. and Hartl, F.U. The effect of macromolecular crowding on chaperonin-mediated protein folding. *Proc Natl Acad Sci U S A* **94**, 1107-12 (1997).

99. Thulasiraman, V., Ferreyra, R.G. and Frydman, J. Folding assays. Assessing the native conformation of proteins. *Methods Mol Biol* **140**, 169-77 (2000).
100. Schwede, T., Kopp, J., Guex, N. and Peitsch, M.C. SWISS-MODEL: An automated protein homology-modeling server. *Nucleic Acids Res* **31**, 3381-5 (2003).
101. Kusmierczyk, A.R. and Martin, J. Nucleotide-dependent protein folding in the type II chaperonin from the mesophilic archaeon *Methanococcus maripaludis*. *Biochem J* **371**, 669-73 (2003).
102. Burston, S.G., Weissman, J.S., Farr, G.W., Fenton, W.A. and Horwich, A.L. Release of both native and non-native proteins from a cis-only GroEL ternary complex. *Nature* **383**, 96-9 (1996).
103. Tatusov, R.L., Galperin, M.Y., Natale, D.A. and Koonin, E.V. The COG database: a tool for genome-scale analysis of protein functions and evolution. *Nucleic Acids Res* **28**, 33-6 (2000).
104. Szpikowska, B.K., Swiderek, K.M., Sherman, M.A. and Mas, M.T. MgATP binding to the nucleotide-binding domains of the eukaryotic cytoplasmic chaperonin induces conformational changes in the putative substrate-binding domains. *Protein Sci* **7**, 1524-30 (1998).
105. Fisher, A.J., Smith, C.A., Thoden, J.B., Smith, R., Sutoh, K., Holden, H.M. and Rayment, I. X-ray structures of the myosin motor domain of *Dictyostelium discoideum* complexed with MgADP.BeFx and MgADP.AlF₄. *Biochemistry* **34**, 8960-72 (1995).
106. Rayment, I., Smith, C. and Yount, R.G. The active site of myosin. *Annu Rev Physiol* **58**, 671-702 (1996).
107. Ueno, T., Taguchi, H., Tadakuma, H., Yoshida, M. and Funatsu, T. GroEL mediates protein folding with a two successive timer mechanism. *Mol Cell* **14**, 423-34 (2004).
108. Cliff, M.J., Limpkin, C., Cameron, A., Burston, S.G. and Clarke, A.R. Elucidation of steps in the capture of a protein substrate for efficient encapsulation by GroE. *J Biol Chem* **281**, 21266-75 (2006).
109. Llorca, O., Martin-Benito, J., Ritco-Vonsovici, M., Grantham, J., Hynes, G.M., Willison, K.R., Carrascosa, J.L. and Valpuesta, J.M. Eukaryotic chaperonin CCT stabilizes actin and tubulin folding intermediates in open quasi-native conformations. *EMBO J* **19**, 5971-9 (2000).

110. Brinker, A., Pfeifer, G., Kerner, M.J., Naylor, D.J., Hartl, F.U. and Hayer-Hartl, M. Dual function of protein confinement in chaperonin-assisted protein folding. *Cell* **107**, 223-33 (2001).
111. Inbar, E. and Horovitz, A. GroES promotes the T to R transition of the GroEL ring distal to GroES in the GroEL-GroES complex. *Biochemistry* **36**, 12276-81 (1997).
112. Kusmierczyk, A.R. and Martin, J. Nested cooperativity and salt dependence of the ATPase activity of the archaeal chaperonin Mm-cpn. *FEBS Lett* **547**, 201-4 (2003).
113. Monod, J., Wyman, J. and Changeux, J.P. On the nature of allosteric transitions: A plausible model. *J Mol Biol* **12**, 88-118 (1965).
114. Koshland, D.E., Jr., Nemethy, G. and Filmer, D. Comparison of experimental binding data and theoretical models in proteins containing subunits. *Biochemistry* **5**, 365-85 (1966).
115. Etchells, S.A., Meyer, A.S., Yam, A.Y., Roobol, A., Miao, Y., Shao, Y., Carden, M.J., Skach, W.R., Frydman, J. and Johnson, A.E. The cotranslational contacts between ribosome-bound nascent polypeptides and the subunits of the hetero-oligomeric chaperonin TRiC probed by photocross-linking. *J Biol Chem* **280**, 28118-26 (2005).
116. Llorca, O., Martin-Benito, J., Gomez-Puertas, P., Ritco-Vonsovici, M., Willison, K.R., Carrascosa, J.L. and Valpuesta, J.M. Analysis of the interaction between the eukaryotic chaperonin CCT and its substrates actin and tubulin. *J Struct Biol* **135**, 205-18 (2001).
117. Llorca, O., Martin-Benito, J., Grantham, J., Ritco-Vonsovici, M., Willison, K.R., Carrascosa, J.L. and Valpuesta, J.M. The 'sequential allosteric ring' mechanism in the eukaryotic chaperonin-assisted folding of actin and tubulin. *EMBO J* **20**, 4065-75 (2001).
118. Kim, S., Willison, K.R. and Horwich, A.L. Cytosolic chaperonin subunits have a conserved ATPase domain but diverged polypeptide-binding domains. *Trends Biochem Sci* **19**, 543-8 (1994).
119. Rivenzon-Segal, D., Wolf, S.G., Shimon, L., Willison, K.R. and Horovitz, A. Sequential ATP-induced allosteric transitions of the cytoplasmic chaperonin containing TCP-1 revealed by EM analysis. *Nat Struct Mol Biol* **12**, 233-7 (2005).

120. Bochkareva, E.S., Lissin, N.M., Flynn, G.C., Rothman, J.E. and Girshovich, A.S. Positive cooperativity in the functioning of molecular chaperone GroEL. *J Biol Chem* **267**, 6796-800 (1992).
121. Taguchi, H., Tsukuda, K., Motojima, F., Koike-Takeshita, A. and Yoshida, M. BeF(x) stops the chaperonin cycle of GroEL-GroES and generates a complex with double folding chambers. *J Biol Chem* **279**, 45737-43 (2004).
122. Kubota, H., Hynes, G., Carne, A., Ashworth, A. and Willison, K. Identification of six Tcp-1-related genes encoding divergent subunits of the TCP-1-containing chaperonin. *Curr Biol* **4**, 89-99 (1994).
123. Fenton, W.A., Kashi, Y., Furtak, K. and Horwich, A.L. Residues in chaperonin GroEL required for polypeptide binding and release. *Nature* **371**, 614-9 (1994).
124. Yifrach, O. and Horovitz, A. Two lines of allosteric communication in the oligomeric chaperonin GroEL are revealed by the single mutation Arg196-->Ala. *J Mol Biol* **243**, 397-401 (1994).
125. White, H.E., Chen, S., Roseman, A.M., Yifrach, O., Horovitz, A. and Saibil, H.R. Structural basis of allosteric changes in the GroEL mutant Arg197-->Ala. *Nat Struct Biol* **4**, 690-4 (1997).
126. Danziger, O., Rivenzon-Segal, D., Wolf, S.G. and Horovitz, A. Conversion of the allosteric transition of GroEL from concerted to sequential by the single mutation Asp-155 -> Ala. *Proc Natl Acad Sci U S A* **100**, 13797-802 (2003).
127. Aharoni, A. and Horovitz, A. Inter-ring communication is disrupted in the GroEL mutant Arg13 --> Gly; Ala126 --> Val with known crystal structure. *J Mol Biol* **258**, 732-5 (1996).
128. Sewell, B.T., Best, R.B., Chen, S., Roseman, A.M., Farr, G.W., Horwich, A.L. and Saibil, H.R. A mutant chaperonin with rearranged inter-ring electrostatic contacts and temperature-sensitive dissociation. *Nat Struct Mol Biol* **11**, 1128-33 (2004).
129. Bigotti, M.G., Bellamy, S.R. and Clarke, A.R. The asymmetric ATPase cycle of the thermosome: elucidation of the binding, hydrolysis and product-release steps. *J Mol Biol* **362**, 835-43 (2006).
130. Martin-Benito, J., Grantham, J., Boskovic, J., Brackley, K.I., Carrascosa, J.L., Willison, K.R. and Valpuesta, J.M. The inter-ring arrangement of the cytosolic chaperonin CCT. *EMBO Rep* (2007).

131. Stirling, P.C., Cuellar, J., Alfaro, G.A., El Khadali, F., Beh, C.T., Valpuesta, J.M., Melki, R. and Leroux, M.R. PhLP3 modulates CCT-mediated actin and tubulin folding via ternary complexes with substrates. *J Biol Chem* **281**, 7012-21 (2006).
132. McLaughlin, J.N., Thulin, C.D., Hart, S.J., Resing, K.A., Ahn, N.G. and Willardson, B.M. Regulatory interaction of phosphoducin-like protein with the cytosolic chaperonin complex. *Proc Natl Acad Sci U S A* **99**, 7962-7 (2002).
133. Pappenberger, G., Wilsher, J.A., Roe, S.M., Counsell, D.J., Willison, K.R. and Pearl, L.H. Crystal structure of the CCTgamma apical domain: implications for substrate binding to the eukaryotic cytosolic chaperonin. *J Mol Biol* **318**, 1367-79 (2002).
134. Heller, M., John, M., Coles, M., Bosch, G., Baumeister, W. and Kessler, H. NMR studies on the substrate-binding domains of the thermosome: structural plasticity in the protrusion region. *J Mol Biol* **336**, 717-29 (2004).
135. Bosch, G., Baumeister, W. and Essen, L.O. Crystal structure of the beta-apical domain of the thermosome reveals structural plasticity in the protrusion region. *J Mol Biol* **301**, 19-25 (2000).
136. Bigotti, M.G. and Clarke, A.R. Cooperativity in the thermosome. *J Mol Biol* **348**, 13-26 (2005).
137. Liou, A.K. and Willison, K.R. Elucidation of the subunit orientation in CCT (chaperonin containing TCP1) from the subunit composition of CCT micro-complexes. *EMBO J* **16**, 4311-6 (1997).
138. Chenna, R., Sugawara, H., Koike, T., Lopez, R., Gibson, T.J., Higgins, D.G. and Thompson, J.D. Multiple sequence alignment with the Clustal series of programs. *Nucleic Acids Res* **31**, 3497-500 (2003).

ACKNOWLEDGEMENTS:

I want to thank Dr. Judith Frydman for inviting me to be a part of her lab – a fantastic place where I not only experienced excellent science, but met a number of amazing people. Aside from her seemingly endless source of knowledge, ideas, and solutions, Judith was (and is) a truly valuable mentor and I am eternally grateful for her unwavering trust and believe in me.

I am very grateful to Prof. Dr. August Böck for his substantial involvement throughout my thesis, especially during the revision and submission process. His advice and support were invaluable.

I owe thanks to the “Studienstiftung des Deutschen Volkes” for supporting this work with a fellowship.

I want to thank our collaborator Prof. Dr. Wah Chiu of the National Center for Molecular Imaging as well as the member of his lab, especially Junjie Zhang (George) and Christopher Booth. Wah’s energy and enthusiasm combined with his organizational skills were really inspiring and made this collaboration very productive.

Thanks also to Dr. Charles Parnot for his help fitting the kinetic data and for his incredible patience and optimism while teaching me basic math.

I want to thank all members of the Frydman- Kopito- and Nelson- lab for providing such an amazing work atmosphere. I owe particular thanks to the permanent residents

of “little Germany” as well as all the frequent visitors who came to discuss science, chat, moon-walk, drink beers or simply have a glance at Christophs David Hasselhoff calender. I really enjoyed your company and I will never forget the good times!

I got very lucky to be able to work together with Nick for the last couple of months. His great enthusiasm and sincerity made it easy and very inspiring to hand over all projects. I want to thank him for his patience with my impatience and for his friendship.

I owe very special thanks to Vero Albanese, Charles Parnot and their three amazing children: Madeleine, Oscar, and Victoria. Their friendship and love is invaluable and they will always be part of our family.

Thanks also to Steffi, Melanie and Christiane for their friendship.

I thank my parents for their love and trust. They encouraged me early on to make my own decisions and provided reliable mental and financial support during all those years.

Last but not least I thank Martin for being the husband and friend I had always dreamed of.

Hiermit erkläre ich ehrenwörtlich, dass ich die Dissertation mit dem Titel

Mechanism of Action of Group II Chaperonins:

Impact of the Built-in Lid on the Conformational Cycle

selbständig und ohne unerlaubte Hilfe angefertigt habe.

Marburg, den 21.Mai 2007

Stefanie Reissmann

Hiermit erkläre ich, dass ich nie anderweitig ohne Erfolg versucht habe eine Dissertation einzureichen oder mich der Doktorprüfung zu unterziehen.

Marburg, den 21.Mai 2007

Stefanie Reissmann

Hiermit erkläre ich, dass ich die hier vorliegende Dissertation mit dem Titel

Mechanism of Action of Group II Chaperonins:

Impact of the Built-in Lid on the Conformational Cycle

nicht ganz oder in wesentlichen Teilen einer anderen Prüfungskommission vorgelegt habe.

Marburg, den 21.Mai 2007

Stefanie Reissmann

Curriculum vitae

Stefanie Reissmann

Education:

- 01/07 – current **MPI für terrestrische Mikrobiologie**, Marburg, Germany
Research assistant in the laboratory of Prof. Gero Steinberg
- 01/03 – 08/2007 **LMU München**, Munich, Germany
Dissertation in biology, supervisor: Prof. A. Böck
Dissertation carried out at
- 01/03 – 12/06 **Stanford University**, Stanford, USA
in the laboratory of Prof. J. Frydman, Department of Biological Sciences
- 03/02 – 10/02: **LMU München**, Munich, Germany
Research associate in the laboratory of Prof. A. Böck
- 10/95 - 01/02: **LMU München**, Munich, Germany
study of Biology and Chemistry in order to become a teacher at the
“Gymnasium”
Degree: „Staatsexamen“
- 10/95 - 03/02: **LMU München**, Munich, Germany
study of biology, main subject: microbiology
Thesis topic: "Isolation and characterization of the SelB homolog from
Drosophila melanogaster".
Degree: “Diplom”

Fellowships:

- 12/02 – 05/05 „Promotionsstipendium“ of the “Studienstiftung des Deutschen Volkes“
- 05/05 EMBO-FEBS Travel award to attend the workshop „Biology of
Molecular Chaperones” in Zakopane, Poland, 28 May – 2 June, 2005

Publications:

- Reissmann S., Hochleitner E., Wang H., Paschos A., Lottspeich F., Glass R.S. and Böck A. (2003) Taming of a poison: Biosynthesis of the NiFe-Hydrogenase Cyanide Ligands. *Science* **299**, 1067-70
- Blokesch M., Paschos A., Bauer A., Reissmann S., Drapal N., Böck A. (2004) Analysis of the transcarbamoylation-dehydration reaction catalysed by the hydrogenase maturation proteins HypF and HypE. *Eur. J. Biochem.* 271: 3428-3436
- Spieß C., Meyer S.A., Reissmann S. and Frydman J. (2004) Mechanism

of the eukaryotic chaperonin: protein folding in the chamber of secrets.
Trends Cell Biol. 2004 Nov;14(11):598-604.

Reissmann S., Parnot C., Booth CR, Chiu W. and Frydman J. (2007)
Essential function of the built-in lid in the allosteric regulation of
eukaryotic and archaeal chaperonins. *Nat. Struct. Mol. Biol.*
May;14(5):432-440.

Conferences:

"Selenium 2000" in Venice, Italy, October 1 - October 5, 2000

"COST Action 841" Hydrogenase workshop 2002 in Cercedilla
(Madrid), Spain, poster presentation

EMBO-FEBS Workshop on Biology of Molecular Chaperones in
Zakopane, Poland, 28 May – 2 June, 2005, poster presentation

FASEB Summer Research Conference on Protein Folding in the cell
In Vermont, U.S.A., 29 July – 3 August 2006, poster presentation